Examining the sequence and function of HIV Gag-specific T cell receptors restricted by HLA-B*57 and HLA-E

by

Hua-Shiuan (Amy) Hsieh

B.Sc., University of Washington, 2018

Thesis Submitted in Partial Fulfillment of the
Requirements for the Degree of
Master of Science

in the
Department of Molecular Biology and Biochemistry
Faculty of Science

SIMON FRASER UNIVERSITY
Fall 2023

Declaration of Committee

Name:	**Hua-Shiuan (Amy) Hsieh**
Degree:	**Master of Science**
Title:	**Examining the sequence and function of HIV Gag-specific T cell receptors restricted by HLA-B*57 and HLA-E**
Committee:	**Chair: Mark Paetzel** Professor, Molecular Biology and Biochemistry
	Mark Brockman Supervisor Professor, Heath Sciences and Molecular Biology and Biochemistry
	Lisa Craig Committee Member Professor, Molecular Biology and Biochemistry
	Jonathan Choy Committee Member Professor, Molecular Biology and Biochemistry
	Mani Larijani Examiner Professor, Molecular Biology and Biochemistry

Abstract

Antiretroviral therapy suppresses HIV viremia, but no vaccine or cure exists. Rare individuals who spontaneously control infection mount robust antiviral CD8 T cell responses, indicating that these cells are crucial. T cell receptors (TCR) recognize viral peptides presented on infected cells by HLA. HLA are diverse, but only classical HLA-A,-B, and -C alleles were thought to contribute to the HIV response. Recent studies identified T cells that recognize HIV Gag KF11 (KAFSPEVIPMF) presented by non-classical HLA-E, providing a new mechanism for control. My thesis examined the sequence and function of KF11-specific TCR in the context of HLA-B*57 and HLA-E. I identified seven highly functional TCR, including one likely dual HLA-restricted clone. These TCR displayed substantial sequence similarity and all required KF11 position 6 (E) for recognition. My results highlight features of KF11-specific TCR that may support efforts to develop a more effective vaccine to prevent HIV infection.

Keywords: HIV; CD8 T cell response; T cell receptor (TCR); HLA-B*57; HLA-E and KF11-specific TCR

Dedication

To every individual whose life has been affected by HIV, and I hope that this research has made a meaningful contribution to find HIV cure.

I want to extend my heartfelt gratitude to my friends, family, community, supervisors, committee members, and loved ones who have provided unwavering support, inspiration, and guidance throughout my academic journey. Your encouragement has made you my greatest cheerleaders throughout my studies.

Finally, I would like to express my gratitude to the underrepresented groups in the field of science, particularly women of color and the LGBTQIA2S+ community It has been an honor and a privilege to build upon the foundation you have laid and pursue my own dreams.

Acknowledgements

The work presented in this thesis is a result of the incredible support from many. I would not be able to complete my thesis without such collective support. I am deeply grateful for the encouragement I received throughout my academic career, especially during the second year of my graduate study. This includes individuals who provided academic guidance, cheered me on, and believed in my ability to achieve my academic goals. To everyone, thank you !

First of all, I will like to express my deepest gratitude to my senior supervisor Dr. Mark Brockman. Dr. Mark Brockman has been an incredible supervisor with his constant mentorship and guidance during my graduate study. He has been an exceptional mentor and always taking the time to provide constructive feedback. He consistently encouraged me to think critically during experimental design. Whenever challenges occur in my experiments, he was always there, motivating me to explore alternative approaches. Following his guidance, I have become a better scientist and learned many valuable lessons during my journey here at SFU. Thank you Mark ! I would also like to thank Dr. Zabrina Brumme. As a role model for women in science, she provided valuable feedback and showed great interest in my project. In addition, I will also like thank my committee members, Dr. Lisa Craig and Dr. Jonathan Choy, who encouraged me to delve deeper into science and offered me valuable insights for my projects.

I would like to thank all the members from BB lab and Choy lab including Dr.Gisele Umviligihozo, Dr. Francis Mwimanzi, Dr. Yurou Sang, Dr. Sneha Goswami, Dr. Rebecca Kalikawe, Rachel Waterworth, Maggie Duncan, Hanwei Sudderuddin, Dr. Peter Cheung, Sarah Speckmaier, Anna Appah, Fatima Yasen, Precious Akindele, Harrison Omondi, Cristina Dalmaestro and Zerufael Derza, Franklin Tam, Winne Ennis, Javeria Rahim, Kevin Luong, Jenice Dumlao, and Kennedy Ahoven. Each of you has given me valuable advice on experiments and navigating graduate school life, which has been instrumental during my time at SFU. You are all outstanding colleagues who have cultivated an encouraging learning environment that has enabled my growth and learning. Special thanks to Dr. Gisele Umviligihozo for her assistance with my experiments and for sharing invaluable feedback from her academic journey. She has truly been an inspiring role model, motivating me to become a better scientist.

I would like to extend my gratitude to my community in both Seattle and Vancouver. My gratitude goes out to Dr. Kyle Lakatos, Kellen Thomas, Cindy Nguyen, Danielle and Tim McLean, Tony Pu, Susan Casey, Olivia Scholes, Jackie Ho, Ash Carter. Many of you have been a part of my life for over a decade, and I'm profoundly grateful for your support throughout my academic journey. My heartfelt thanks go out to each one of you for your meaningful contributions to my journey.

I'd like to give special shoutout to Angela Leong for guiding me in finding self-confidence and bringing out the best of me. Amanda Goll, thank you for cheering me up throughout my academic journey especially your weekend call has always makes me smile. Jesse Kaufman and Sophie Roth, both of you have been amazing friends and guide me to make healthier life choices. Anna Bruns, thank you for your constant care and listening. Michelle Toop, your kindness, sincere support, and encouragement were invaluable during some of my toughest times in graduate school. Michelle Lu, I'm grateful for those late-night calls you've always been there for, continuing to cheer me up throughout my studies. Samantha Clark, thank for your unconditional love, understanding and support throughout the whole process. Sarah Krischkowski, thank you for always being there for me and your unconditional support. Lisa and Ela , thank you for your support, care and love over past 14 years especially your facetime call has always bring joy to my life.

I want to thank my family especially my mom and dad who have been supporting me unconditionally throughout my life. You have been my biggest cheer leaders since day one and always encourage to pursue my dream. Thank you to my siblings who have always been my anchor and believing in me even when I doubted myself. Special thanks to my sister, Cassie Hsieh, who has always bring me late night dinners and stayed with me in lab till late night. You have always make sure I am healthy and making me to be able finish my study. I love you all !

Finally, I will like to acknowledge the support from Dr. Paul Goepfert's lab in University of Alabama-Bellingham, BC Centre for Excellence in HIV/AIDS (BC-CfE) in Vancouver, collaborators and all of the study participates without whom this research will not be possible.

Table of Contents

List of Figures

List of Acronyms

Ags	Antigen Sensitivity
AP-1	Activator Protein
ART	Antiretroviral Therapy
C	Constant
CCR5	CC-Chemokine Receptor Type 5
CD4+	T Helper Cells or Th cells
CD8+	Cytotoxic T Cells or Cytotoxic T Lymphocyte or CTL
CDR	Complementarity-Determining Regions
CMV	Cytomegalovirus
D	Diversity
DC	Dendritic Cells
DMSO	Dimethyl Sulfoxide
EBV	Epstein-Barr Virus
ER	Endoplasmic Reticulum
ERAPs	ER Resident Aminopeptidases
FACS	Fluorescence-Activated Cell Sorting
FK10	HLA-A*02 Restricted Gag Epitope
gp160	Glycoprotein 160
HCV	Hepatitis C virus
HIV	Human Immunodeficiency Cirus
IFNs	Interferon
IP3	Inositol-1,4,5-Trisphosphate
J	Joining
KF11	B57 Restricted Gag Epitope (KAFSPEVIMF)
LTR	Long Terminal Repeat
M.tb	Mycobacterium Tuberculosis
MHC	Major Histocompatibility Complex
NFAT	Nuclear Factor of Activated T cells
NF-κb	Nuclear Factor Kappa B

NK	Natural Killer Cells
P. carinii	Pneumocystis carinii
PAMPs	Pathogen-Associated Molecular Patterns
PBMC	Peripheral Blood Mononuclear Cells
PLC	Phospholipase C
PLCs	Peptide-loading Complex
PRRs	Pathogen Recognition Receptors
pTEFb	Positive Transcription Elongation Complex
RhCMV	Rhesus Cytomegalovirus Vector
S. Typhi	Salmonella enterica
SIV	Simian Immunodeficiency virus
TAR	Trans-Acting Response Element
TCR	T cell Receptors
TLRs	Toll-Light Receptors
TNF-α	Tumor Necrosis Factor α
TRAV	T Cell Receptor Alpha Gene
TRBV	T Cell Receptor Beta Gene
V	Variable
VNPs	Viraemic Non-Progressors
ZAP70	Cytoplasmic Protein Tyrosine Kinase

Chapter 1.

Introduction to HIV and the host immune response: understanding the role of T cells, T cell receptors, and HLA

1.1. Overview of HIV

1.1.1. Epidemiology of HIV and AIDS

As of 2022, there were approximately 39 million people living with Human Immunodeficiency virus (HIV) (UNAIDS, 2023). HIV is an enveloped retrovirus that has two subtypes: HIV-1 and HIV-2. HIV-1 and HIV-2 share similar transmission routes and can lead to AIDS if untreated (Sharp and Hahn, 2010). HIV-1 is the predominant subtype circulating globally, while HIV-2 is primarily found in West Africa (Esbjörnsson et al., 2019). If HIV is untreated, it can lead to Acquired Immune Deficiency Syndrome (AIDS). AIDS was first diagnosed in a young homosexual man in Los Angeles in 1981, who presented with Pneumocystis carinii (*P. carinii*) pneumonia symptoms (Greene, 2007). Soon after, other AIDS patients were identified, displaying similar symptoms, including signs of opportunistic infections like Kaposi's sarcoma, oral candidiasis, cytomegalovirus (CMV), and *P. carinii* pneumonia (CDC, 1996). Currently, 76.4% of HIV-infected individuals have access to safe and highly effective combination antiretroviral therapy (cART). The availability of cART has significantly reduced the number of AIDS-related deaths, but there is still no vaccine or cure available for HIV. Thus, HIV continues to be one of the most prominent health issues in the world (UNAIDS, 2023).

1.1.2. The HIV genome

The HIV-1 genome consists of two positive sense single-stranded RNAs (~9.8 kb) that encodes nine genes and fifteen viral proteins (Figure 1.1 and Li et al., 2015). These nine viral genes are Gag, Pol, Env, Tat, Rev, Vif, Vpr, Vpu and Nef. These viral genes encode different proteins needed for viral replication and assembly of new virions in infected host cells (van Heuvel et al., 2022). The Gag gene encodes four proteins - matrix, capsid, nucleocapsid and p6, which play important structural roles during viral

assembly, release and maturation (Waheed et al., 2012). Matrix forms an inner shell that interacts with the viral lipid membrane and facilitates the recruitment of Env glycoproteins into assembled viral particles (Tedburt et al., 2015). Capsid forms a conical protein core that harbors the RNA genome (Campbell et al.,2015). Nucleocapsid protein plays an important role in viral replication by protecting the RNA genome and by mediating reverse transcription (Levin et al., 2010). The Pol gene encodes the major enzymatic proteins that are essential for viral replication, including protease, reverse transcriptase, and integrase (Yu et al., 2020). Protease plays a crucial role in producing viral enzymes and structural proteins by cleaving viral polyproteins into subunits (Ghosh et al., 2016). Reverse transcriptase is responsible for converting viral RNA to DNA, which is achieved through RNA and DNA dependent polymerase activities (Hu and Hughes, 2012). After viral DNA is produced, integrase facilitates insertion of viral DNA into host chromosomal DNA (Chiu and Davies, 2004).

The Env gene expresses the only viral surface protein, Glycoprotein 160 (gp160), which is cleaved to produce a trimer of gp120/gp41 heterodimers (Kesavardhana and Varadarajan, 2014). Gp120 is a surface glycoprotein that determines viral tropism by binding to CD4 and co-receptors CC-chemokine receptor type 5 (CCR5) or C-X-C chemokine receptor type 4 (CXCR4) on target cells, whereas gp41 facilitates the fusion between viral and cellular lipid membranes (Hung et al., 1999). Tat and Rev are two viral regulatory proteins that direct viral transcription and the transport of viral RNAs within cells (Karn and Stoltzfus, 2012). Vif, Vpr, Vpu, and Nef are HIV accessory proteins that do not display enzymatic activities but are crucial for HIV pathogenesis in vivo. HIV accessory proteins play important roles in viral transmission and replication by modifying the host and cellular environment to ensure persistent viral infection (Malim and Emerman, 2008).

1.1.3. The HIV replication cycle

HIV predominantly targets CD4+T cells and utilizes gp120 to bind to CD4 and the chemokine receptors CCR5 or CXCR4 on these cells. When virus attaches to the host cell, gp41 undergoes a structural transformation to form a helical bundle. This structure brings the viral and host cell membranes close together, allowing the viral lipid membrane to merge with the host cell membrane and release the viral capsid containing the viral RNA genome inside. Following entry, the viral RNA is converted into double-

stranded DNA through the process of reverse transcription. The protective shell of the virus is uncoated, enabling the viral DNA to enter the nucleus and integrate into the host cellular DNA. This integrated viral genome is termed a "provirus".

Viral transcription from the provirus begins at the 5' long terminal repeat (LTR), with the help of the Tat protein, which boosts the efficiency of RNA polymerase II. This action requires Tat to bind to the trans-acting response (TAR) element, which is heavily reliant on cellular components, mainly the positive transcription elongation factor b complex (pTEFb). While Tat ensures the initiation of HIV transcription, the process results in varied mRNA transcripts due to alternative splicing. For instance, an unspliced RNA transcript produces Gag and Gag-Pol precursors and new RNA genomes, singly spliced RNAs code for Vif, Vpr, Vpu, and Env, and a multiply spliced RNA transcript produces Tat, Rev, and Nef. The Rev protein directs the transport of unspliced or partially spliced mRNA from the nucleus to the cytoplasm. Gag and Gag-Pol precursors undergo further processing to form the structural or enzymatic proteins, while singly spliced RNA is processed to produce the Vif, Vpr, Vpu, and Env proteins. Once the virus has completed its transcription and translation phases, it assembles new virion particles and exits the host cell in a process known as budding. After budding, maturation of the virus continues as the viral protease enzyme processes any remaining uncleaved proteins, resulting in an infectious virion (Freed et al., 2015).

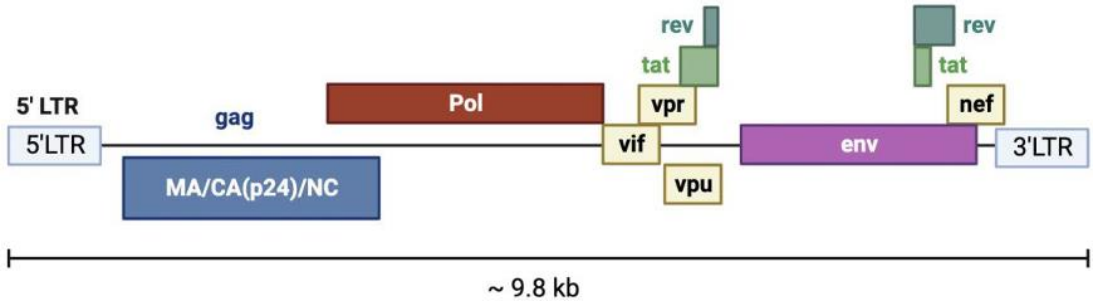

Figure 1.1. HIV genome
HIV-1 contained 9 genes: Gag, Pol, Env, Rev, Tat, Vpr, Vpu, Vif and Nef. The complete HIV-1 genome is approximately 9.8 kb in length. Data was obtained from the Los Alamos National Laboratory, available at (https://www.hiv.lanl.gov/content/sequence/HIV/MAP/landmark.html) This image was created with BioRender (https://www.biorender.com/).

1.2. HIV and the host immune response

1.2.1. HIV and the innate immune response

The innate immune system acts as the primary defense mechanism to combat pathogens before the induction of the adaptive immune response. This response utilizes Pathogen-Associated Molecular Patterns (PAMPs) to detect pathogens. Examples of PAMPs include peptidoglycan, lipopolysaccharide, viral RNA, and polyinosinic-polycytidylic acid. These PAMPs are identified by specific receptors called pathogen recognition receptors (PRRs) (Asiamah et al., 2019). In addition, a number of host-encoded proteins, including apolipoprotein B mRNA editing enzyme catalytic subunit 3G (APOBEC3G), tripartite motif-containing protein 5 alpha (TRIM5a), and tetherin can suppress HIV viral replication. These cellular “restriction” factors serve as a first line of defense against viral infection and also contribute to the tropism of HIV and other retroviruses for their respective host species (Malim and Bieniasz, 2012). Indeed, HIV accessory proteins have evolved to counteract the antiviral activities of these cellular factors.

During the acute phase of HIV infection, macrophages encounter viruses and virus- infected cells and help to orchestrate the adaptive immune response (Koppensteiner et al., 2012). HIV infection also activates dendritic cells (DC), which are triggered by toll-like receptors (TLR) and cytokines produced by other cells to secrete two main cytokines: type 1 interferons (IFNs) and tumor necrosis factor α (TNF-α) that further activate the adaptive immune response (Ahmed et al., 2015). DC serve as the primary antigen-presenting cells for viruses, since they are capable of processing peptide antigens on both Major Histocompatibility Complex (MHC) class I and II, subsequently presenting them to CD4 and CD8 T cells. This pivotal role activates the adaptive immune response (Ahmed et al., 2015; Carrington and Alter, 2012). Natural killer (NK) cells play a crucial role during acute HIV infection by eliminating virus-infected cells. NK cells also detect cytokines like IL-12, IL-18, and type I IFNs released by DC. This leads to the activation of their cytotoxic abilities. Furthermore, the production of IFN-γ by NK cells influences the maturation of DC, highlighting their multifaceted role in combating infection (Flórez-Álvarez et al., 2018).

1.2.2. HIV and the adaptive immune response

The adaptive immune response, consisting of B cells and T cells, provides specific and long-lasting protection against HIV. There are two types of T cells, CD4+ cells (also called T helper cells or Th cells) and CD8+ cells (also called cytotoxic T cells or CTL) which recognize diverse peptide antigens utilizing T cell receptors (TCR) (Kumar et al., 2018). T cells are activated when they encounter an antigen-MHC complex, but they perform distinct functions upon activation. CD4+ T cells orchestrate the adaptive immune response based on the surrounding cytokine environment (Luckheeram et al., 2012). Once activated, CD4+ T cells can differentiate into various T helper (Th) cells subtypes with specialized functions. Many CD4+ T cells evolve into Th1 cells, which further stimulate CD8+ T cells, macrophages, NK cells, and B cells during HIV infection (Lee et al., 2017; Eagar and Miller, 2023). However, HIV predominantly targets CD4+ T cells, which results in a gradual loss of these cells and a decline in immune function in the absence of cART (Aavani and Allen, 2019). CD8+ T cells are crucial for HIV clearance. They are activated upon recognizing antigens presented by MHC-I on infected cells. Upon activation, CD8+ T cells display cytotoxic behaviors, discharging lytic granules that contain perforin and granzymes to eliminate infected cells (Gulzar and Copeland, 2004).

1.2.3. Spontaneous control of HIV infection

While HIV attacks CD4+ T cells and progresses to AIDS in most individuals without cART, a rare subset of HIV infected individuals (0.5% or less) are able to control viral replication spontaneously without treatment. These individuals are called “HIV controllers” or “elite controllers” and often have low to undetectable viremia in the blood (Saez-Cirion et al., 2013).

HIV controllers typically mount robust CD8+ T cell responses against highly conserved elements of the HIV genome, such as structurally constrained epitopes in the Gag protein (Walker and Yu, 2013). This suggests that an active, immune-mediated mechanism contributes to viral control in these individuals. On the other hand, another group of controllers, known as viremic non-progressors (VNPs), maintain high CD4+ T cell counts and appear to suppress HIV- associated disease despite having detectable viremia. It is believed that VNPs have a mechanism that shields them from the CD4+ T

cell loss induced by HIV infection (Saez-Cirion et al., 2014). A strong and specific CD8+ T cell response is often observed in HIV controllers and is associated with certain genetic traits seen frequently in these individuals. Gaining insights into these genetic traits that generate robust the CD8+ T cell responses could help in the development of HIV vaccines and treatments (Ndhlovu et al., 2012).

Some HIV elite controllers generate antibody responses that block infection by diverse HIV strains, which are often referred to as broadly neutralizing antibodies (or bNAbs), or display elevated levels of antibody-dependent cellular cytotoxicity (ADCC), highlighting the potential involvement of the B cell response in suppressing HIV infection (Hartana and Yu, 2022). However, bNAbs and heightened ADCC activity have also been found in individuals who do not control infection.

1.2.4. Classical HLA class I (HLA-I)

The MHC complex, referred to in humans as Human Leukocyte Antigen (HLA), is encoded on the short arm of chromosome 6 in the human genome. Based on the structure and function of these diverse genes, HLAs are categorized into three classes: HLA class I, class II, and class III. HLA class I presents endogenous peptides to CD8+ T cells, while HLA class II presents exogenous peptides to CD4+ T cells. The main function of HLA class III is to regulate immune responses (Janeway et al., 2001 and Cruz-Tapias et al., 2013).HLA class I is composed of two polypeptide chains that are non-covalently linked: the HLA-encoded α chain (44-47 kD) and the non-HLA-encoded β2 microglobulin (12 kD). The α chain of HLA class I is made up of α1, α2, and α3 domains. The α1 and α2 domains contain a heterodimer where the peptide-binding groove is located, and it is highly polymorphic. The α3 domain, containing hydrophobic amino acids, anchors the HLA structure to the plasma membrane and is notably conserved (Figure 1.2 and Cruz-Tapias et al., 2013). The α3 region is known for its ability to bind with the CD8 co-receptor, which facilitates the stable interaction between cytotoxic T cells and HLA. This binding allows the T cell receptor to engage with the peptide-binding groove found in the α1 and α2 domains (Wesley et al., 1993). “Classical” HLA class I alleles, also known as HLA class Ia, including HLA-A, HLA-B, and HLA-C, are crucial for presenting pathogen-derived peptide epitopes to CD8+ T cells (Crux and Elahi, 2017). Certain HLA class I alleles are linked to a slower progression of HIV disease. These alleles, namely HLA-B*57, HLA-B*27, HLA-B*81, and HLA-B*51, are

often referred to as "protective alleles" (Kiepiela et al., 2004; Naruto et al., 2012; Lobas et al., 2022). While these alleles are relatively uncommon in the general population, they are highly over-represented among elite controllers. For instance, while HLA-B*57 appears in less than 1% of the general population, it is found in 40% to 60% of elite controllers (Lobas et al., 2022). These protective alleles often mount superior CD8+ T cell responses that target highly conserved HIV epitopes (Lobas et al., 2022). Studying the relationship between TCR and protective HLA alleles may offer a deeper understanding of mechanism of HIV control that can assist with the design of new HIV vaccine or therapeutic strategies.

1.2.5. Non-classical HLA class Ib (HLA-Ib)

“Non-classical” HLA class Ib (or HLA-Ib) alleles includes HLA-E, HLA-F, HLA-G and HFE or HLA-H, which are distinguished from HLA-I due to their limited polymorphism and low surface expression on cells (Braud et al.,1999). HLA-Ib plays an important immune regulatory role, primarily interacting with NK receptors to exert inhibitory effects (Wyatt et al., 2019).

HLA-E is expressed on all nucleated cells, with highest expression levels observed on leukocytes, endothelial cells and trophoblast cells (Kanevskiy et al., 2019). HLA-E is essentially non-polymorphic, with only two functional alleles observed in the human population – HLA- E*01:01 and HLA-E*01:03 – that are equally distributed (Petersdorf and Socié, 2019). HLA-E*01:01 and HLA-E*01:03 differ by one amino acid at position 107, which is located outside of peptide binding groove, where E*01:01 encodes arginine and E*01:03 encodes glycine. Both HLA-E alleles share similar structural features, but E*01:03 exhibits a higher level of surface expression and a higher peptide affinity. This might be related to the fact that E*01:03 has higher thermal stability (Strong et al., 2003). Peptide loads onto HLA-E via TAP dependent or independent manner, and HLA-E normally binds to leader sequence VL9 via TAP during homeostatic conditions (Bansal et al., 2021). The main role of HLA-E is to present VL9 leader sequences, a self-peptide, (VMAPRT(L/V)(V/L/I/F)L) derived from HLA-A, B, C and G and to engage with NKG2A/CD94 receptor, which inhibits the activation of natural killer cells. Thus, the HLA-E-VL9 complex serves an important role in mediating NK cell cytotoxic activity (Li et al., 2022). Recent studies have shown that the presentation of pathogen-derived sequences by HLA-E is capable of inducing CD8+ T cell responses. For example, HLA-E

recognizes peptides derived from Mycobacterium tuberculosis (*M. tb*), Salmonella enterica (*S. typhi*), Hepatitis C virus (HCV), Epstein-Barr virus (EBV) and HIV via TCR on CD8+ T cells (Hannoun et al., 2018 and Yang et al., 2021). On the other hand, certain viral or tumor peptides can be loaded on to HLA-E via TAP dependent manner. However, there are several proposed TAP independent alternative pathway, such as, SPase/SPPase-mediated, furin-mediated, and autophagy-mediated pathways, these pathways required to be further verified (Voogd et al.,2022).

While classical and non-classical HLA proteins share some similarities, such as having a similar structure and being able to present foreign antigens to T cells, there are many differences between the two groups. The structure of classical and non-classical HLAs is similar in that both consist of an α chain and β2 microglobulin, but they display different peptide affinities and peptide binding repertoires (Figure 1.2 and Wyatt et al., 2019). Classical HLA molecules are highly polymorphic, with thousands of alleles, while HLA-E is poorly polymorphic, with only two functional alleles observed in the human population (Strong et al., 2003). While the main function of classical HLAs is to present endogenous antigens to CD8 T cells, the function of non-classical HLAs is to modulate the NK cell response (Cruz-Tapias et al., 2013). In addition, while peptide loading on classical HLAs is typically dependent on the TAP complex, non-classical HLAs appear to use both TAP-dependent and TAP-independent pathways (Voogd et al., 2022).

1.2.6. Essential role to study HLA-E

It is known that HIV-1 accessory protein Nef downregulates MHC-I by modulating host trafficking pathway in two models. First, Nef binds to the cytoplasmic tail of MHC-I, disrupting MHC-I trafficking, which further leads MHC-I to enter endosomes for degradation (Dirk et al., 2016). Second, Nef binds to newly synthesized MHC-I in the trans-Golgi network by engaging with membrane adapter protein-1 (AP-1). The Nef-AP-1-MHC-I complex is then transported to lysosomes for degradation (Tavares et al., 2020). Initial studies indicated that the HIV-1 accessory protein, Nef, did not impact HLA-C or non-classical proteins like HLA-E, suggesting that T cells restricted by HLA-C or HLA-E might maintain a greater ability to suppress HIV infection (Swann et al., 2001). More recent studies have shown that primary HIV isolates can downregulate HLA-C and HLA-E (van Stigt Thans et al., 2019, and Apps et al., 2016), but the degree of

downregulation of these molecules appears to be modest compared to that of HLA-A and HLA-B.

Several SIV epitopes have been identified that are capable of triggering HLA-E specific CD8 T cell responses in non-human primates, but the HLA-E restricted T cell response to HIV appears to be highly constrained in humans. The Goepfert lab (Univ of Alabama-Birmingham) has identified CD8 T cell responses in individuals living with HIV that target Gag KF11 (KAFSPEVIPMF, aa30-40), which may be restricted by HLA-B*57:01 and/or HLA-E*01:01 (Bansal et al., 2021). To our knowledge, this represents the first evidence that HLA-E restricted CD8 T cells can be elicited in humans during natural HIV infection, complementing studies by Yang et al. (Yang et al., 2021). A couple of HIV epitopes (Gag RL9 and KF11) were able to elicit HLA-E restricted T cell responses and circumvent downregulation by Nef. This has raised a great interest to use of HLA-E-restricted CD8 T cells as an alternative strategy for eliciting cytotoxic T cell responses against HIV. HLA-E is almost monomorphic, with only two alleles, HLA-E*01:01 and HLA-E*01:03, available within human population. In addition, these two alleles share similar structural features and peptide repertoires in which making them attractive targets for developing universal vaccines (Grant et al., 2020). Overall, the potential use of HLA-E-restricted CD8 T cells as an alternative strategy for eliciting cytotoxic T cell responses against HIV could further be developed into HIV universal vaccines or therapeutics.

1.2.7. Antigen processing and presentation

MHC-I molecules usually present the products of cytosolic proteolysis, which typically are proteins generated by ubiquitin-proteasome system in cytosol. Viral replication can occur in any nucleated cells. When translation errors lead to defective peptides, they are broken down by the proteasome into peptides which are then transported to the endoplasmic reticulum (ER). This transportation is facilitated by transporter associated with antigen processing (TAP).

Peptide fragments undergo further trimming of their N-terminal extension in the ER by ER resident aminopeptidases (ERAPs) resulting mainly in peptides of 8-9 residues. While the ERAP determines the N-terminus of the peptide, the proteasome cleavage defines its C-terminus (Pishesha et al., 2022; Mpakali et al., 2018). Peptide-

loading complex (PLC) assists in peptide loading onto MHC-I. Once peptide is loaded on MHC-I, the MHC-I complex travels to the cell surface through the Golgi apparatus. The human version of MHC-I, known as HLA-I, is highly polymorphic, leading to extensive variation in the peptide repertoires that are presented by an individual's HLA alleles.

Each HLA-I allele displays a distinct preference of certain peptides (Sidney et al., 2020). The interaction of peptides with HLA-I typically involves binding to the B and F pockets of the HLA. Notably, the B pocket often accommodates position 2 of a 9-mer peptide, while the F pocket usually binds the C-terminal residue, as shown in Figure 1.3 (Nguyen et al., 2021). Although HLA-E has similar binding anchors, its E pocket, which is usually occupied by position 7 in a 9-mer peptide, plays an enhanced role in peptide presentation (Figure 1.3; O'Callaghan et al., 1998). In addition, once the HLA class I presents a peptide on the cell surface, it is identified by the TCR on the CD8+ T cell (Pishesha et al., 2022).

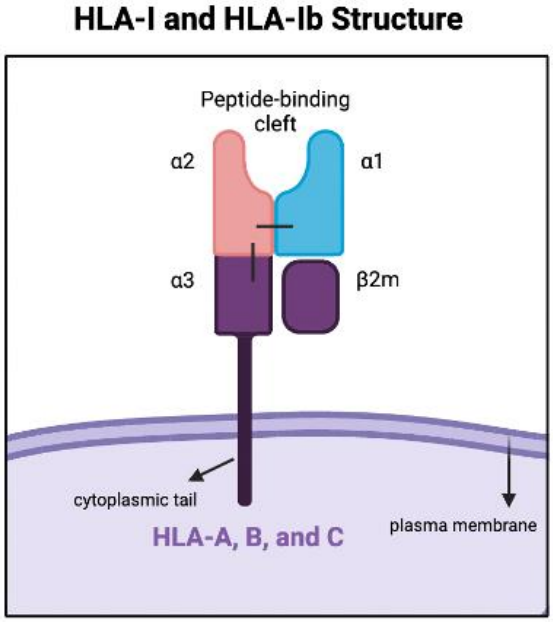

Figure 1.2. The structure of HLA-I and HLA-Ib
Both HLA-I (HLA-A, B, C) and HLA-Ib (HLA-E, F, G, H) have similar structures. The α chain consists of α1, α2, and α3 domains. The peptide-binding groove is situated between the α1 and α2 domains. The α3 domain features a cytoplasmic tail that extends through the transmembrane region, ending at the C-terminus. The information in this graph was obtained from Janeway et al., 2001, available at (http://www/ncbi.nlm.nih.gov/books/NBK27156). This image was created with BioRender (https://www.biorender.com/).

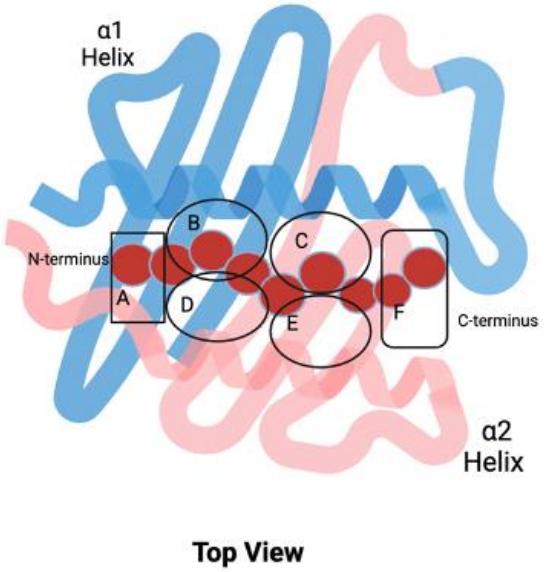

Figure 1.3. Schematic view of the peptide binding pockets in HLA-I and HLA-Ib
HLA-I and HLA-Ib have six peptide binding pockets within the peptide binding groove and defined as pocket A-F. Typically, pocket A binds to the peptide's N-terminus, while pocket F engages with the C-terminus. Pockets B and F are the primary sites where anchor residues attached. In HLA-E, residues in pocket E plays a crucial role in stabilizing peptide presentation. For 9-mer peptides, the residue at position 2 often fills pocket B, position 7 fills pocket E, and the C-terminus resides in pocket F. The information in this graph was obtained from O'Callaghan et al., 1998 available at: https://doi.org/10.1016/S1097-2765(00)80053-2. This image was generated using BioRender (https://www.biorender.com/).

1.3. TCR recognition of peptide/HLA

1.3.1. TCR development and structure

T lymphocytes originate from bone marrow and are derived from hematopoietic progenitor cells. Progenitor cells migrate to the thymus and develop into thymocytes (Trowbridge et al., 1985). Thymocytes then further go through negative and positive selection, becoming a mature naïve T cell. Each naïve T cell contains a unique TCR pair as well as CD4 or CD8 co-receptors on the cell surface (Gameiro et al.,2010). Naïve CD8+ T cells travel through the bloodstream and receive antigenic signals from antigen presenting cells via their TCR, and subsequently proliferate and become an effector or memory CD8+ T cells (Nolz et al., 2011).

A TCR is made up of α and β chains that form a heterodimer that shares structural similarities with immunoglobulins. TCR are highly diverse, with a potential for

approximately 10^{15} distinct versions as the result of genomic rearrangements in the TCR α and β loci during development (Bosselut, 2019). The genomic rearrangement process takes place in the thymus involving the Variable (V), Diversity (D), and Joining (J) segments. The TCR α chain consists of one V gene (with 47 possible gene segments), one J gene (with 61 possible gene segments), and one C gene. The TCR β chain includes one V gene (with 54 possible gene segments), one D gene (with 2 possible gene segments), one J gene (with 14 possible gene segments), and one C gene (with 2 possible gene segments) (La Gruta et al., 2018). The nomenclature for these gene segments are defined by The International Immunogenetics Information System (IMGT). The TCRα segments are denoted as TRAV for the V gene, TRAJ for the J gene, and TRAC for the C gene. The TCRβ segments are labeled as TRBV for the V gene, TRBD for the D gene, TRBJ for the J gene, and TRBC for the C gene (Figure 1.4).

TCR α and β chains each possess V(D)J genes and further form into three hypervariable regions defined as complementarity-determining regions (CDR) named as CDR1, CDR2, and CDR3. CDR1 and CDR2 motifs are encoded by the V gene, and the CDR3 motif is formed at the junction between V, (D), and J genes. As a result, the CDR3s are the most variable domains of a TCR and is typically where TCR interacts with the peptide presented by HLAs(Figure 1.5).

1.3.2. Elements of TCR that influence CD8 T cell responses against HIV

Research has shown that specific features of TCR, HIV epitopes, and the nature of viremia can contribute to enhanced CTL responses. Notably, HIV epitopes derived from the Gag region, such as Gag KF11 (KAFSPEVIPMF) and Gag KK10 (KRWIILGLNK), are associated with more robust CTL responses, especially in HIV controllers (Jia et al., 2012). Two main reasons why Gag-derived epitopes might be more effective against HIV are: 1) Virion associated Gag can be processed at early stages of infection, potentially allowing CTL to eliminate HIV before Nef downregulates HLA-I (Sacha et al., 2007); 2) Mutations in certain Gag epitopes are limited since mutations result in a significant fitness cost to the virus (Tenzer et al., 2009; van Baalen et al., 2002).

CTL responses rely heavily on TCR recognition. However, few studies have delved into how variability in TCR affects T cell reactions. Some research indicates that specific genetic characteristics of TCR correlate with a stronger CTL response, but in-depth mechanistic studies are limited (Iglesias et al., 2011; Mendoza et al., 2020). The term "TCR repertoire" denotes the complete set of TCR within an individual. Every individual possesses a unique and varied TCR repertoire (Gutierrez et al., 2020). Generally, an individual employs multiple TCRs to identify antigenic epitopes, leading to a vast and distinct TCR repertoire. On the other hand, "public TCR sequences" are sequences identified across many unrelated individuals when responding to the same epitope. Public T cell clones have been observed to produce a similar CD8 T cell response. This suggests that beneficial biological outcomes may be driven in part by the TCR (Li et al., 2012). These TCRs are notable in their role as public clones, using comparable TCR sequences in eliciting CTL reactions to epitopes like KF11 (KAFSPEVIPMF) and KK10 (KRWIILGLNK) (Iglesias et al., 2011; Mendoza et al., 2020). There are several factors contributing to TCR clones generating more robust CTL responses in controlling HIV. 1) T cell antigen sensitivity is determined in part by TCR avidity for peptide and MHC; and 2) The ability of a TCR to recognize HIV mutants will determine if a T cell can continue to respond to an evolving pathogen (Lissina et al., 2016; Iglesias et al., 2011).

TCR antigen sensitivity (AgS) or functional avidity is defined as the antigen concentration needed to activate a T cell response. There are several factors that can impact AgS, such as the level of TCR expression, the quality and quantity of the epitope present, and the presence of co-stimulatory or co-inhibitory receptors. Studies indicate that TCR avidity, the interaction of individual TCR with the HLA-peptide complex, plays a significant role in AgS and affecting CTL responses (Lissina et al., 2016). A diverse TCR repertoire can lead to variation in TCR avidity, resulting in highly effective oligoclonal CTL responses. Public clonotypes TRBV4-3/ TRBJ1-3, isolated from different individuals, have been shown to generate high avidity responses against HIV Gag KK10. Similarly, the public TCR clone AGA is associated with a robust CTL response to Gag KF11 (Iglesias et al., 2011; Mendoza et al., 2020). Furthermore, public TCR with high AgS have been linked with superior CTL responses with enhanced cytotoxic activity in HIV (Iglesias et al., 2011). Public clones are considered to be rare events, thus their

presence suggests that they have advantageous genetic characteristics that are selected in the setting of infection.

While HIV-1 constantly mutates, the CTL response must be able to recognize these mutants. TCRs that cross-recognize HIV variants are associated with delayed disease progression Lissina et al., 2016). Public TCR clones that encode the TRBV4-3/TRBK1-3 genes show high avidity towards WT KK10 but cannot recognize the KK10 L268-M- mutant. In contrast, cross-reactive TCRs encoding TRBV6-5/TRBJ1-1 can identify KK10 mutants and continue to generate robust CTL responses. Individuals with these cross-reactive TCR consistently generate a strong CTL response that is more effective at suppressing HIV replication (Lissina et al., 2016).

In summary, a diverse TCR repertoire plays an important role in mediating an effective CD8 T cell response. More comprehensive studies of the relationship between TCR sequences and functional variation may reveal the characteristics required to generate robust CTL response that contributes to HIV control.

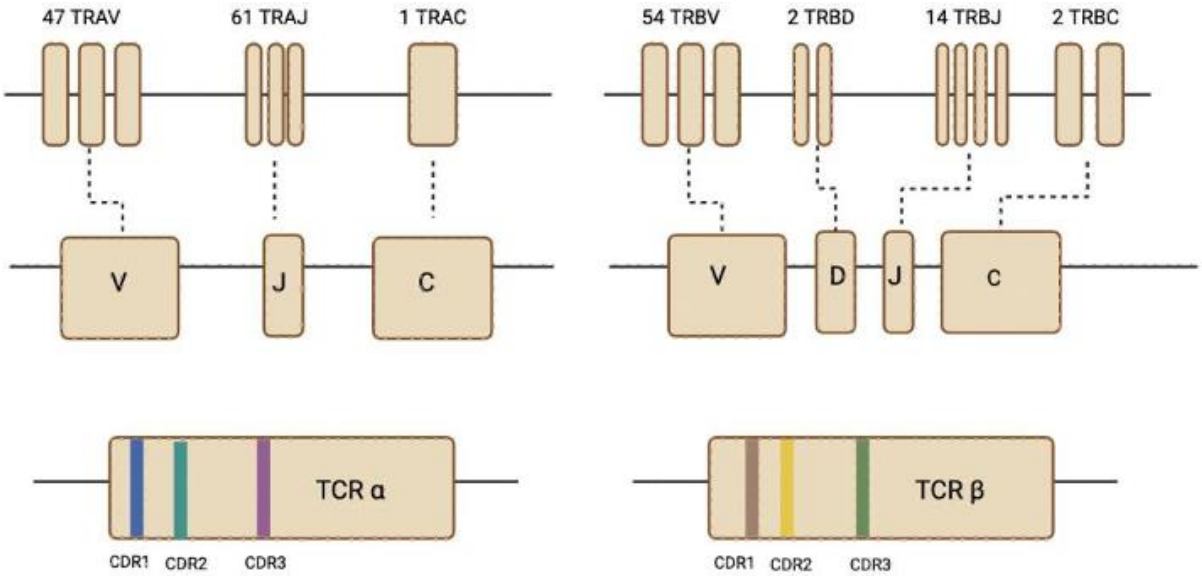

Figure 1.4. Gene rearrangement of TCR genes
This graph represents genetic V(D)J recombination in TCR alpha and beta. CDR1, 2 and 3 are shown in blue, green and purple respectively. CDR1,2 and 3 are shown in brown, yellow, and dark green respectively. This graph is generated from BioRender (https://www.biorender.com/). The information in generating this graph is obtained from La Gruta et al., 2018 available at https://www.nature.com/articles/s41577-018-0007-5#Fig2

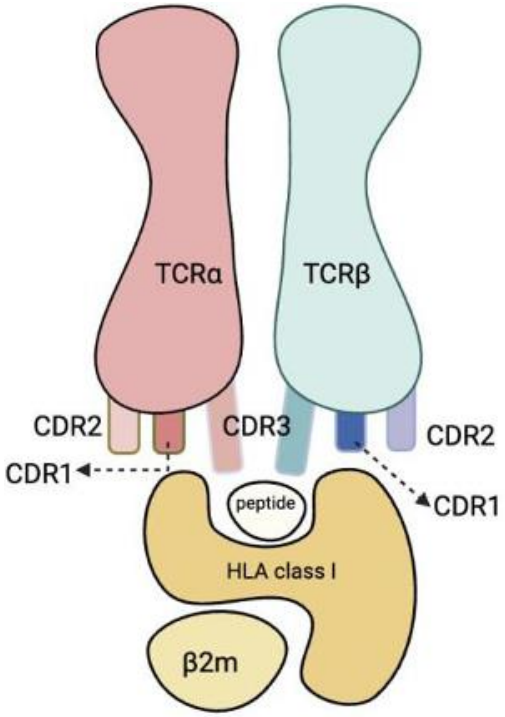

Figure 1.5. TCR interaction with HLA-1 and peptide
TCR α and TCRβ form heterodimer and interacts with HLA-peptide complex with CDR loops. CDR3 regions are known to interacts with peptide directly while CDR1 and 2 interact with HLA molecules. This graph is generated from BioRender (https://www.biorender.com/). The information in generating this graph is obtained from La Gruta et al., 2018 available at https://www.nature.com/articles/s41577-018-0007-5#Fig2.

1.3.3. Analyzing TCR sequence diversity using bioinformatics tools

TCR repertoires are diverse, but TCR that respond to the same epitope often share similar genetic features. This suggests that it may be possible to predict TCR-epitope specificity based on distinct genetic features of TCR. Dash et al., developed an analytical tool, called TCRdist, to characterize epitope specific TCR repertories focusing on the highly diverse CDR regions that determine HLA-peptide contact sites (La Gruta et al., 2018; Dash et al., 2017).

TCRdist calculates a similarity-weighted distance between pairs of amino acid sequences in theCDR1, CDR2, CDR2.5, and CDR3 loop motifs based on Blossum62 scoring (Figure 1.6). A smaller value calculated between two TCRs pairs indicates that they are similar in sequence, and thus more likely to share important genetic features and to have similar epitope specificity (Dash et al., 2017). TCRdist generates a matrix of pair-wise distances between all studied TCR samples, which can be visualized as a

network graph using various softwares, such as Cytoscape. In the network graph, each TCR clone is represented by a node and TCR clones with similar genetic features (i.e. low TCRdist values) can be linked by edges. By applying different Hamming distance thresholds (Shannon et al., 2003), TCR clusters can be viewed across a range of similarity scores (from conservative to liberal). For this thesis, our collaborator collected TCR sequences from single cell sequencing and Dr. Brockman generated an initial network graph based on TCRdist values to visualize the results (Figure 2.1). We analyzed the sequence differences in this graph and selected more than 50 TCR clones for further studies.

Sequence-based clustering may be able to predict a TCR's epitope specificity based on its genetic features, but functional characteristics that may contribute to CTL responses remain unknown. Therefore, further assessment of TCR function will be useful to verify the results.

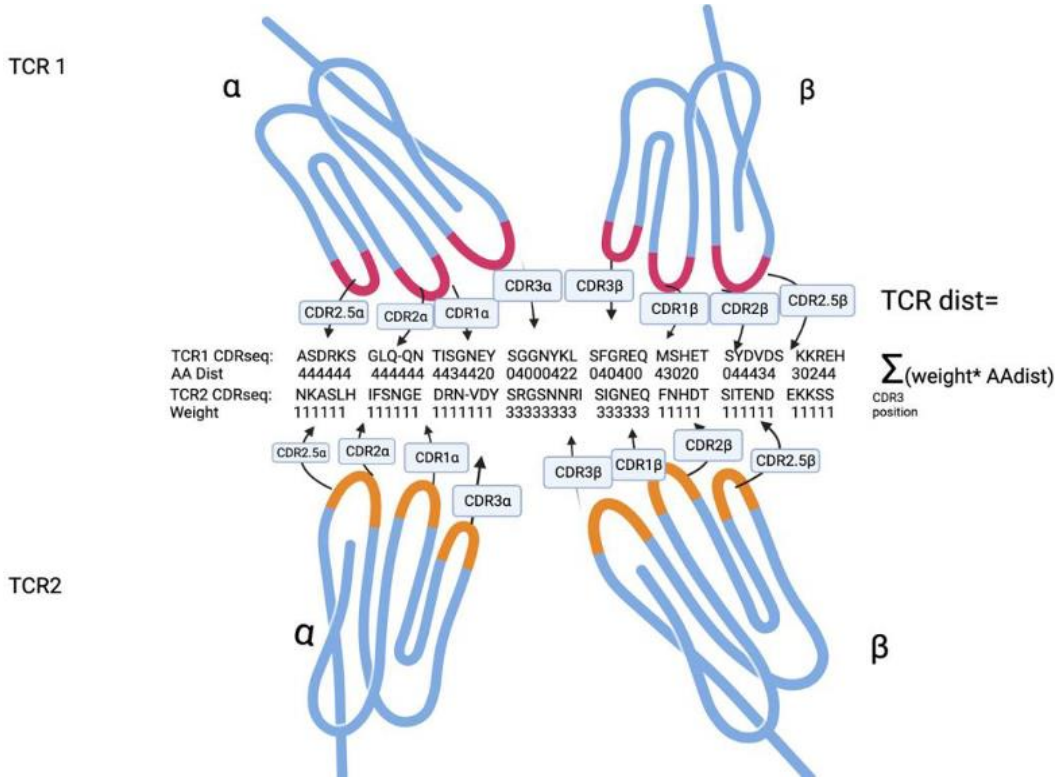

Figure 1.6. Overview of TCRdist calculation
Two TCRs are first mapped to the amino acids within CDR loops. CDR loops are colored in red and orange. The CDR3 sequences are aligned and assigned with AA dist, which is calculated by Blossum62 similarity matrix scoring system. The AA dist scores are weighted in different CDR regions based on their significance during peptide and TCR recognition. Finally, the sum between

weight and AAdist produces TCRdist. The information in generating this graph is obtained from Dash et al., 2017 available at https://www.ncbi.nlm.nih.gov/pmc/articles/PMC5616171/.

1.3.4. CD8+ T cell activation and function

Robust CTL response has been observed frequently in HIV controllers which played a pivotal role to suppress HIV replication (Benito et al., 2004). As mentioned previously, some studies have linked TCR genetic characteristics with stronger CTL responses. However, there are limited studies focusing on this topic.

There are two widely used methods to capture CTL response when activated by TCR- peptide recognition. 1) Measurement of cytokine production or other activation induced markers 2) Peptide-HLA-tetramer staining. When CD8+ T cells become activated by engaging cognate antigen presented by HLA-I, they secrete cytokines and upregulate surface markers. IFNγ is a common cytokine secreted by CD8+ T cells upon activation, and it can be readily detected by flow cytometry (Ghanekar et al., 2001). Certain T-cell subsets, however, may not secrete IFNγ. As a result, measuring cytokine production might not always be a reliable method to measure T cells function (Vukmanovic-Stejic et al., 2000). As an alternative, stimulated CD8+ T cells also upregulate expression of CD69, CD107, CD137 and other activation-induced surface markers that can be detected by flow cytometry (Altosole et al., 2023). Peptide-HLA tetramers with fluorochromes are frequently employed to detect CD8+ T cells via binding to TCR, and can also be analyzed by flow cytometry. However, tetramer binding can be affected by CD8, possibly leading to a false positive or false negative outcomes (Choi et al., 2003).

To complement these strategies to study CTL responses, we have implemented a versatile reporter cell-based assay to evaluate the in vitro function of TCR clones (Anmole et al., 2015) (Figure 1.8). Upon T cell activation, AP-1, NFAT, and NF-κB transcription factors are translocated into the nucleus to promote gene expression associated with T cell proliferation, differentiation and survival (Barnes et al., 2015). Our reporter assay utilizes nuclear factor of activated T cells (NFAT)-dependent gene expression to quantify TCR antigen recognition (Figure 1.7). Briefly, when T cells are activated via TCR-peptide/HLA recognition, this leads to the activation of phospholipase C (PLC) binding to receptor tyrosine kinase, immunoreceptors and G-protein-coupled receptors. This reaction results in the production of inositol-1,4,5- trisphosphate (IP3),

which triggers Ca2+ flux from the ER to cytoplasm. Ca2+ in the cytoplasm binds to calmodulin and triggers calcineurin to activate NFAT through dephosphorylation (Muller et al., 2010). During our reporter assay, TCR alpha/beta proteins are transiently expressed in immortalized Jurkat T cells along with CD8α and an NFAT-driven luciferase reporter (Figure 1.8). Following co-culture with peptide/HLA target cells, activated T cells will produce luciferase enzyme, that can be quantified by luminescence.

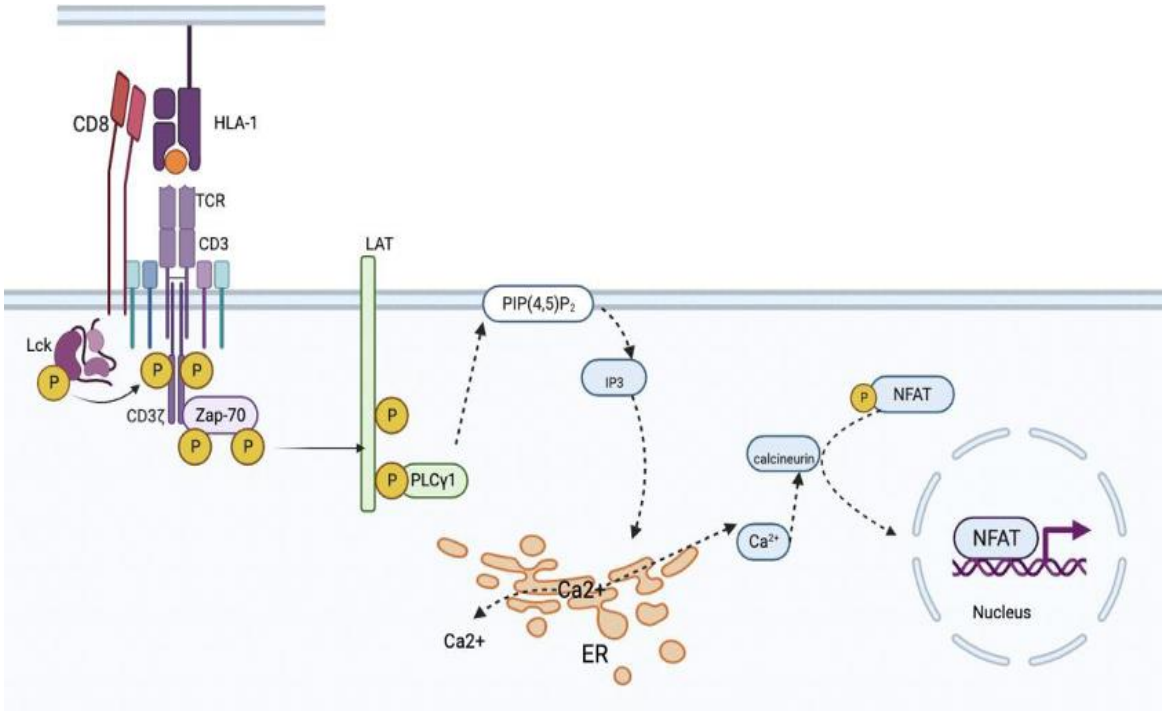

Figure 1.7. T cell activation and NFAT signaling
Upon T cell activation, CD8 recruits Lck 70 to phosphorylates ITAMs. Doubled phosphorylated ITAMs recruit Zap-70 and phosphorylated Lck for fully activation. Then, Zap-70 activates Lat and further activates PLC and converts PIP(4.5)P2 to IP3. IP3. Induces calcium flux from the ER to cytosol. Released calcium binds to calmodulin and activates calcineurin which dephosphorylates NFAT. This leads NFAT translocates into nuclease resulting expression of gene. This graph is generated from BioRender (https://www.biorender.com/). The information in generating this graph is obtained from Macian,2005 and Yan et al., 2013 available at https://pubmed.ncbi.nlm.nih.gov/15928679/ and https://www.ncbi.nlm.nih.gov/pmc/articles/PMC3648074/#:~:text=Phosphorylation%20of%20ZAP%2D70%20is,chains%20of%20the%20TCR%20complex.

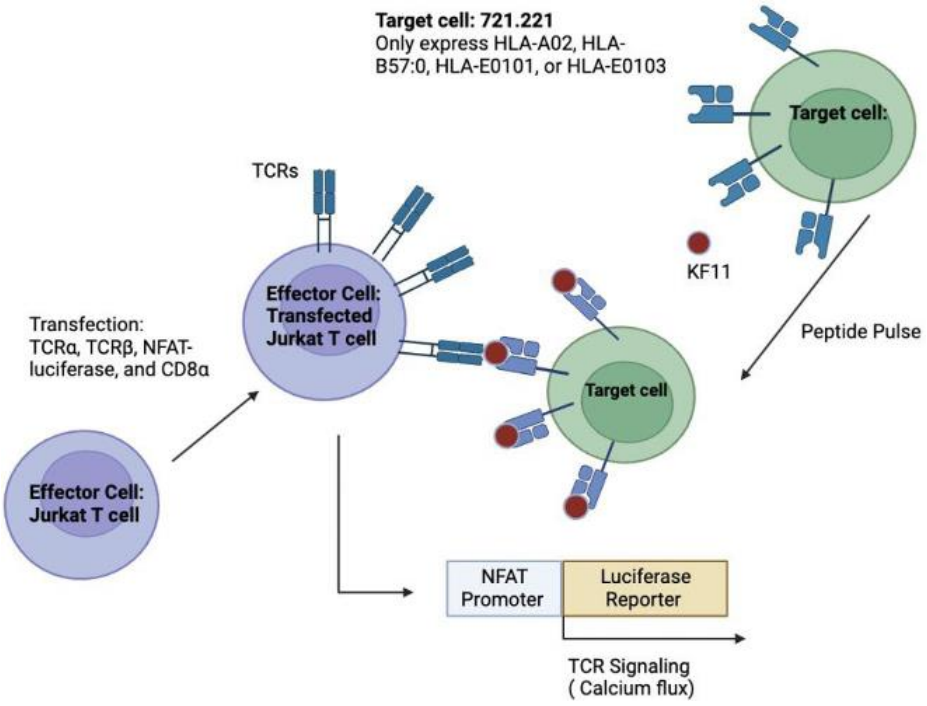

Figure 1.8. Overview of TCR reporter assay
Effector jurakt cells are transfected with TCR plasmids, CD8 and NFAT-luciferase. Following transfection, peptide pulsed target cells are co-cultured with effector cells. When TCR recognizes peptide/HLA complex, it activates downstream NFAT promoter gene, resulting quantifiable luminescence signals. 21.221 cell lines are used as target cell lines in our assay and described in chapter 2 figure 2.5. This graph is generated from BioRender (https://www.biorender.com/). The information in generating this graph is obtained from Anmole et al., 2015 available at https://pubmed.ncbi.nlm.nih.gov/26319395/.

1.4. Thesis Objectives

The objective of this thesis is to study the in vitro function of Gag KF11-specific TCR clones in the context of the protective HLA-B*57 allele and the non-classical HLA-E allele. We hypothesize that intrinsic features of each TCR clone will contribute to its antigen specificity and potential antiviral function. Specifically, we anticipate that TCR clones capable of generating robust Gag KF11 responses will display similar sequence and/or functional characteristics, which can be identified through careful analysis of TCR/peptide/HLA interactions. A better understating of KF11-specific TCR, including the discovery and validation of high affinity HLA- B*57- and/or HLA-E restricted TCR clones, may support efforts to design new vaccines or therapeutics to prevent or treat HIV.

In chapter 2, we screen TCR clones for activity against B*57-KF11 using our reporter cell assay, and identify seven functional TCR that can generate robust

responses. We further examined the antigen sensitivity of these TCR as well as their ability to recognize KF11 alanine variants. We found that our functional TCR clones shared genetic similarities with a “public” KF11-specific clone AGA, for which a crystal structure is available – allowing us to explore potential structural features of this TCR response. In chapter 3, we used the TCR reporter assay to screen TCR clones for activity against KF11 presented by HLA-E. We identified five clones with weak functional activity, but noted that signal intensity for the assay on HLA-E targets was low. As a result, this chapter also describes our efforts to adapt the TCR reporter assay to make it more sensitive and suitable for studying HLA-E responses. In chapter 4, I summarize the results of this research and discuss the broader implications of this thesis.

1.5. Reference

Aavani, P., Allen, L. J.S.,The role of CD4 T cells in immune system activation and viral reproduction in a simple model for HIV infection, *Applied Mathematical Modelling*,Volume 75,2019,Pages 210-222,ISSN 0307-904X,https://doi.org/10.1016/j.apm.2019.05.028.

Ahmed, Z., Kawamura, T., Shimada, S., & Piguet, V. (2015). The role of human dendritic cells in HIV-1 infection. *The Journal of investigative dermatology*, 135(5), 1225–1233. https://doi.org/10.1038/jid.2014.490

Altosole, T., Rotta, G., Uras, C. R. M., Bornheimer, S. J., & Fenoglio, D. (2023). An optimized flow cytometry protocol for simultaneous detection of T cell activation induced markers and intracellular cytokines: Application to SARS-CoV-2 immune individuals. *Journal of immunological methods*, 515, 113443. https://doi.org/10.1016/j.jim.2023.113443

Anmole, G., Kuang, X. T., Toyoda, M., Martin, E., Shahid, A., Le, A. Q., Markle, T., Baraki, B., Jones, R. B., Ostrowski, M. A., Ueno, T., Brumme, Z. L., & Brockman, M. A. (2015). A robust and scalable TCR-based reporter cell assay to measure HIV-1 Nef-mediated T cell immune evasion. *Journal of immunological methods*, 426, 104–113. https://doi.org/10.1016/j.jim.2015.08.010

Apps, R., Del Prete, G. Q., Chatterjee, P., Lara, A., Brumme, Z. L., Brockman, M. A., Neil, S., Pickering, S., Schneider, D. K., Piechocka-Trocha, A., Walker, B. D., Thomas, R., Shaw, G. M., Hahn, B. H., Keele, B. F., Lifson, J. D., & Carrington, M. (2016). HIV-1 Vpu Mediates HLA-C Downregulation. *Cell host & microbe*, 19(5), 686–695. https://doi.org/10.1016/j.chom.2016.04.005

Asiamah, E. K., Ekwemalor, K., Adjei-Fremah, S., Osei, B., Newman, R., & Worku, M. (2019). Natural and synthetic pathogen associated molecular patterns modulate galectin expression in cow blood. *Journal of animal science and technology*, 61(5), 245–253. https://doi.org/10.5187/jast.2019.61.5.245

Bansal, A., Gehre, M. N., Qin, K., Sterrett, S., Ali, A., Dang, Y., Abraham, S., Costanzo, M. C., Venegas, L. A., Tang, J., Manjunath, N., Brockman, M. A., Yang, O. O., Kan-Mitchell, J., & Goepfert, P. A. (2021). HLA-E-restricted HIV-1-specific CD8+ T cell responses in natural infection. *The Journal of clinical investigation*, 131(16), e148979. https://doi.org/10.1172/JCI148979

Barnes, S. E., Wang, Y., Chen, L., Molinero, L. L., Gajewski, T. F., Evaristo, C., & Alegre, M. L. (2015). T cell-NF-κB activation is required for tumor control in vivo. *Journal for immunotherapy of cancer*, 3(1), 1. https://doi.org/10.1186/s40425-014-0045-x

Benito, J. M., López, M., & Soriano, V. (2004). The role of CD8+ T-cell response in HIV infection. *AIDS Reviews*, 6(2), 79–88.

Bosselut R. (2019). T cell antigen recognition: Evolution-driven affinities. *Proceedings of the National Academy of Sciences of the United States of America*, 116(44), 21969–21971. https://doi.org/10.1073/pnas.1916129116

Braud, V. M., Allan, D. S., & McMichael, A. J. (1999). Functions of nonclassical MHC and non- MHC-encoded class I molecules. *Current opinion in immunology*, 11(1), 100–108. https://doi.org/10.1016/s0952-7915(99)80018-1

Campbell, E. M., & Hope, T. J. (2015). HIV-1 capsid: the multifaceted key player in HIV-1 infection. *Nature reviews. Microbiology*, 13(8), 471–483. https://doi.org/10.1038/nrmicro3503

Carrington, M., & Alter, G. (2012). Innate immune control of HIV. *Cold Spring Harbor perspectives in medicine*, 2(7), a007070. https://doi.org/10.1101/cshperspect.a007070

Centers for Disease Control and Prevention (CDC) (1996). Pneumocystis pneumonia--Los Angeles. 1981. *MMWR. Morbidity and mortality weekly report*, 45(34), 729–733.

Chiu, T. K., & Davies, D. R. (2004). Structure and function of HIV-1 integrase. *Current topics in medicinal chemistry*, 4(9), 965–977. https://doi.org/10.2174/1568026043388547

Choi, E. M., Chen, J. L., Wooldridge, L., Salio, M., Lissina, A., Lissin, N., Hermans, I. F., Silk, J. D., Mirza, F., Palmowski, M. J., Dunbar, P. R., Jakobsen, B. K., Sewell, A. K., & Cerundolo, V. (2003). High avidity antigen-specific CTL identified by CD8-independent tetramer staining. *Journal of immunology* (Baltimore, Md. : 1950), 171(10), 5116–5123. https://doi.org/10.4049/jimmunol.171.10.5116

Crux, N. B., & Elahi, S. (2017). Human Leukocyte Antigen (HLA) and Immune Regulation: How Do Classical and Non-Classical HLA Alleles Modulate Immune Response to Human Immunodeficiency Virus and Hepatitis C Virus Infections?. *Frontiers in immunology*, 8, 832. https://doi.org/10.3389/fimmu.2017.00832

Cruz-Tapias P, Castiblanco J, Anaya JM. Major histocompatibility complex: Antigen processing and presentation. In: Anaya JM, Shoenfeld Y, Rojas-Villarraga A, et al., editors. Autoimmunity: From Bench to Bedside [Internet]. Bogota (Colombia): El Rosario University Press; 2013 Jul 18. Chapter 10. Available from: https://www.ncbi.nlm.nih.gov/books/NBK459467/

Dash, P., Fiore-Gartland, A. J., Hertz, T., Wang, G. C., Sharma, S., Souquette, A., Crawford, J. C., Clemens, E. B., Nguyen, T. H. O., Kedzierska, K., La Gruta, N. L., Bradley, P., & Thomas, P.G. (2017). Quantifiable predictive features define epitope-specific T cell receptor repertoires. *Nature*, 547(7661), 89–93. https://doi.org/10.1038/nature22383

Dirk, B. S., Pawlak, E. N., Johnson, A. L., Van Nynatten, L. R., Jacob, R. A., Heit, B., & Dikeakos, J. D. (2016). HIV-1 Nef sequesters MHC-I intracellularly by targeting early stages of endocytosis and recycling. *Scientific reports*, 6, 37021. https://doi.org/10.1038/srep37021

Eagar,T. N., Miller, S. D., 11 - Helper T-Cell Subsets and Control of the Inflammatory Response,Editor(s): Robert R. Rich, Thomas A. Fleisher, Harry W. Schroeder, Cornelia M. Weyand, David B. Corry, Jennifer M. Puck,Clinical Immunology (SixthEdition),*Elsevier*,2023,Pages 151-161,I SBN 9780702081651,https://doi.org/10.1016/B978-0-7020-8165-1.00011-3.

Esbjörnsson, J., Jansson, M., Jespersen, S., Månsson, F., Hønge, B. L., Lindman, J., Medina, C., da Silva, Z. J., Norrgren, H., Medstrand, P., Rowland-Jones, S. L., & Wejse, C. (2019). HIV- 2 as a model to identify a functional HIV cure. *AIDS research and therapy*, *16*(1), 24. https://doi.org/10.1186/s12981-019-0239-x

Flórez-Álvarez, L., Hernandez, J. C., & Zapata, W. (2018). NK Cells in HIV-1 Infection: From Basic Science to Vaccine Strategies. *Frontiers in immunology*, 9, 2290. https://doi.org/10.3389/fimmu.2018.02290

Freed E. O. (2015). HIV-1 assembly, release and maturation. *Nature reviews. Microbiology*, 13(8), 484–496. https://doi.org/10.1038/nrmicro3490

Gameiro, J., Nagib, P., & Verinaud, L. (2010). The thymus microenvironment in regulating thymocyte differentiation. *Cell adhesion & migration*, 4(3), 382–390. https://doi.org/10.4161/cam.4.3.11789

Ghanekar, S. A., Nomura, L. E., Suni, M. A., Picker, L. J., Maecker, H. T., & Maino, V. C. (2001). Gamma interferon expression in CD8(+) T cells is a marker for circulating cytotoxic T lymphocytes that recognize an HLA A2-restricted epitope of human cytomegalovirus phosphoprotein pp65. *Clinical and diagnostic laboratory immunology*, 8(3), 628–631. https://doi.org/10.1128/CDLI.8.3.628-631.2001

Ghosh, A. K., Osswald, H. L., & Prato, G. (2016). Recent Progress in the Development of HIV-1 Protease Inhibitors for the Treatment of HIV/AIDS. *Journal of medicinal chemistry*, 59(11), 5172–5208. https://doi.org/10.1021/acs.jmedchem.5b01697

Grant, E. J., Nguyen, A. T., Lobos, C. A., Szeto, C., Chatzileontiadou, D. S. M., & Gras, S. (2020). The unconventional role of HLA-E: The road less traveled. *Molecular immunology*, 120, 101–112. https://doi.org/10.1016/j.molimm.2020.02.011

Greene W. C. (2007). A history of AIDS: looking back to see ahead. *European journal of immunology*, 37 Suppl 1, S94–S102. https://doi.org/10.1002/eji.200737441

Gutierrez, L., Beckford, J., & Alachkar, H. (2020). Deciphering the TCR Repertoire to Solve the COVID-19 Mystery. *Trends in pharmacological sciences*, 41(8), 518–530. https://doi.org/10.1016/j.tips.2020.06.001

Gulzar, N., & Copeland, K. F. (2004). CD8+ T-cells: function and response to HIV infection. *Current HIV research*, 2(1), 23–37. https://doi.org/10.2174/1570162043485077

Hannoun, Z., Lin Z., Brackenridge, S., Kuse, N., Akahoshi, T., Borthwick, N., McMichael, A., Murakoshi, H., Takiguchi,M., Hanke, T. Identification of novel HIV-1-derived HLA-E-binding peptides,*Immunology letters*,Volume 202,2018,Pages 65-72,ISSN 0165-2478

Hartana, C. A., & Yu, X. G. (2021). Immunological effector mechanisms in HIV-1 elite controllers. *Current opinion in HIV and AIDS*, 16(5), 243–248. https://doi.org/10.1097/COH.0000000000000693

Hu, W. S., & Hughes, S. H. (2012). HIV-1 reverse transcription. *Cold Spring Harbor perspectives in medicine*, 2(10), a006882. https://doi.org/10.1101/cshperspect.a006882

Hung, C. S., Vander Heyden, N., & Ratner, L. (1999). Analysis of the critical domain in the V3 loop of human immunodeficiency virus type 1 gp120 involved in CCR5 utilization. *Journal of virology*, 73(10), 8216–8226. https://doi.org/10.1128/JVI.73.10.8216-8226.1999

Iglesias, M. C., Almeida, J. R., Fastenackels, S., van Bockel, D. J., Hashimoto, M., Venturi, V., Gostick, E., Urrutia, A., Wooldridge, L., Clement, M., Gras, S., Wilmann, P. G., Autran, B., Moris, A., Rossjohn, J., Davenport, M. P., Takiguchi, M., Brander, C., Douek, D. C., Kelleher, A. D., … Appay, V. (2011). Escape from highly effective public CD8+ T-cell clonotypes by HIV. *Blood*, 118(8), 2138–2149. https://doi.org/10.1182/blood-2011-01-328781

Janeway CA Jr, Travers P, Walport M, et al. Immunobiology: The Immune System in Health and Disease. 5th edition. New York: Garland Science; 2001. The major histocompatibility complex and its functions. Available from: https://www.ncbi.nlm.nih.gov/books/NBK27156/

Jia, M., Hong, K., Chen, J., Ruan, Y., Wang, Z., Su, B., Ren, G., Zhang, X., Liu, Z., Zhao, Q., Li, D., Peng, H., Altfeld, M., Walker, B. D., Yu, X. G., & Shao, Y. (2012). Preferential CTL targeting of Gag is associated with relative viral control in long-term surviving HIV-1 infected former plasma donors from China. *Cell research*, 22(5), 903–914. https://doi.org/10.1038/cr.2012.19

Kanevskiy, L., Erokhina, S., Kobyzeva, P., Streltsova, M., Sapozhnikov, A., & Kovalenko, E. (2019). Dimorphism of HLA-E and its Disease Association. *International journal of molecular sciences*, 20(21), 5496. https://doi.org/10.3390/ijms20215496

Karn, J., & Stoltzfus, C. M. (2012). Transcriptional and posttranscriptional regulation of HIV-1 gene expression. *Cold Spring Harbor perspectives in medicine*, 2(2), a006916. https://doi.org/10.1101/cshperspect.a006916

Kesavardhana, S., & Varadarajan, R. (2014). Stabilizing the native trimer of HIV-1 Env by destabilizing the heterodimeric interface of the gp41 post fusion six-helix bundle. *Journal of virology*, 88(17), 9590–9604. https://doi.org/10.1128/JVI.00494-14

Kiepiela, P., Leslie, A., Honeyborne, I. et al. Dominant influence of HLA-B in mediating the potential co-evolution of HIV and HLA. *Nature* 432, 769–775 (2004). https://doi.org/10.1038/nature03113

Koppensteiner, H., Brack-Werner, R., & Schindler, M. (2012). Macrophages and their relevance in Human Immunodeficiency Virus Type I infection. *Retrovirology*, 9, 82. https://doi.org/10.1186/1742-4690-9-82

Kumar, B. V., Connors, T. J., & Farber, D. L. (2018). Human T Cell Development, Localization, and Function throughout Life. *Immunity*, 48(2), 202–213. https://doi.org/10.1016/j.immuni.2018.01.007

La Gruta, N. L., Gras, S., Daley, S. R., Thomas, P. G., & Rossjohn, J. (2018). Understanding the drivers of MHC restriction of T cell receptors. *Nature reviews. Immunology*, 18(7), 467–478. https://doi.org/10.1038/s41577-018-0007-5

Lee, G. Q., Orlova-Fink, N., Einkauf, K., Chowdhury, F. Z., Sun, X., Harrington, S., Kuo, H. H.,Hua, S., Chen, H. R., Ouyang, Z., Reddy, K., Dong, K., Ndung'u, T., Walker, B. D., Rosenberg,E. S., Yu, X. G., & Lichterfeld, M. (2017). Clonal expansion of genome-intact HIV-1 in functionally polarized Th1 CD4+ T cells. *The Journal of clinical investigation*, 127(7), 2689– 2696. https://doi.org/10.1172/JCI93289

Levin, J. G., Mitra, M., Mascarenhas, A., & Musier-Forsyth, K. (2010). Role of HIV-1 nucleocapsid protein in HIV-1 reverse transcription. *RNA biology*, 7(6), 754–774. https://doi.org/10.4161/rna.7.6.14115

Li, D., Brackenridge, S., Walters, L. C., Swanson, O., Harlos, K., Rozbesky, D., Cain, D. W., Wiehe, K., Scearce, R. M., Barr, M., Mu, Z., Parks, R., Quastel, M., Edwards, R. J., Wang, Y., Rountree, W., Saunders, K. O., Ferrari, G., Borrow, P., Jones, E. Y., … Haynes, B. F. (2022). Mouse and human antibodies bind HLA-E-leader peptide complexes and enhance NK cell cytotoxicity. *Communications biology*, 5(1), 271. https://doi.org/10.1038/s42003-022-03183-5

Li, G., Piampongsant, S., Faria, N. R., Voet, A., Pineda-Peña, A. C., Khouri, R., Lemey, P., Vandamme, A. M., & Theys, K. (2015). An integrated map of HIV genome-wide variation from a population perspective. *Retrovirology*, 12, 18. https://doi.org/10.1186/s12977-015-0148-6

Li, H., Ye, C., Ji, G., & Han, J. (2012). Determinants of public T cell responses. *Cell research*, 22(1), 33–42. https://doi.org/10.1038/cr.2012.1

Lissina, A., Chakrabarti, L. A., Takiguchi, M., Appay, V. TCR clonotypes: molecular determinants of T-cell efficacy against HIV, *Current opinion in Virology,* Volume 16,2016,Pages 77-85,ISSN 1879-6257, https://doi.org/10.1016/j.coviro.2016.01.017.

Liu, R. D., Wu, J., Shao, R., & Xue, Y. H. (2014). Mechanism and factors that control HIV-1 transcription and latency activation. *Journal of Zhejiang University. Science*. B, 15(5), 455–465. https://doi.org/10.1631/jzus.B1400059

Lobos, C. A., Downing, J., D'Orsogna, L. J., Chatzileontiadou, D. S. M., & Gras, S. (2022). Protective HLA-B*57: T cell and natural killer cell recognition in HIV infection. *Biochemical Society transactions*, 50(5), 1329–1339. https://doi.org/10.1042/BST20220244

Los Alamos, H. s. d. (2022). HIV Sequence Database https://www.hiv.lanl.gov/content/sequence/HIV/MAP/landmark.html

Luckheeram, R. V., Zhou, R., Verma, A. D., & Xia, B. (2012). $CD4^+$T cells: differentiation and functions. *Clinical & developmental immunology*, 2012, 925135. https://doi.org/10.1155/2012/925135

Macian F. (2005). NFAT proteins: key regulators of T-cell development and function. *Nature reviews. Immunology*, 5(6), 472–484. https://doi.org/10.1038/nri1632

Malim, M. H., & Bieniasz, P. D. (2012). HIV Restriction Factors and Mechanisms of Evasion. *Cold Spring Harbor perspectives in medicine*, 2(5), a006940. https://doi.org/10.1101/cshperspect.a006940

Malim, M. H., & Emerman, M. (2008). HIV-1 accessory proteins--ensuring viral survival in a hostile environment. *Cell host & microbe*, 3(6), 388–398. https://doi.org/10.1016/j.chom.2008.04.008

Mendoza, J. L., Fischer, S., Gee, M. H., Lam, L. H., Brackenridge, S., Powrie, F. M., Birnbaum, M., McMichael, A. J., Garcia, K. C., & Gillespie, G. M. (2020). Interrogating the recognition landscape of a conserved HIV-specific TCR reveals distinct bacterial peptide cross-reactivity. *eLife*, 9, e58128. https://doi.org/10.7554/eLife.58128

Mpakali, A., Maben, Z., Stern, L. J., & Stratikos, E. (2019). Molecular pathways for antigenic peptide generation by ER aminopeptidase 1. *Molecular immunology*, 113, 50–57. https://doi.org/10.1016/j.molimm.2018.03.026

Müller, M. R., & Rao, A. (2010). NFAT, immunity and cancer: a transcription factor comes of age. *Nature reviews*. *Immunology*, 10(9), 645–656. https://doi.org/10.1038/nri2818

Naruto, T., Gatanaga, H., Nelson, G., Sakai, K., Carrington, M., Oka, S., & Takiguchi, M. (2012). HLA class I-mediated control of HIV-1 in the Japanese population, in which the protective HLA- B*57 and HLA-B*27 alleles are absent. *Journal of virology,* 86(19), 10870–10872. https://doi.org/10.1128/JVI.00689-12

Ndhlovu, Z. M., Proudfoot, J., Cesa, K., Alvino, D. M., McMullen, A., Vine, S., Stampouloglou, E., Piechocka-Trocha, A., Walker, B. D., & Pereyra, F. (2012). Elite controllers with low to absent effector CD8+ T cell responses maintain highly functional, broadly directed central memory responses. *Journal of virology*, 86(12), 6959–6969. https://doi.org/10.1128/JVI.00531- 12

Nguyen, A. T., Szeto, C., & Gras, S. (2021). The pockets guide to HLA class I molecules. *Biochemical Society transactions*, 49(5), 2319–2331. https://doi.org/10.1042/BST20210410

Nolz, J. C., Starbeck-Miller, G. R., & Harty, J. T. (2011). Naive, effector and memory CD8 T-cell trafficking: parallels and distinctions. *Immunotherapy*, 3(10), 1223–1233. https://doi.org/10.2217/imt.11.100

O'Callaghan, C. A., Tormo, J., Willcox, B. E., Braud, V. M., Jakobsen, B. K., Stuart, D. I., McMichael, A. J., Bell, J. I., & Jones, E. Y. (1998). Structural features impose tight peptide binding specificity in the nonclassical MHC molecule HLA-E. *Molecular cell*, *1*(4), 531–541. https://doi.org/10.1016/s1097-2765(00)80053-2

Petersdorf, E., Socié, G. Chapter 2 - The HLA System in Hematopoietic Stem Cell Transplantation,Editor(s): Gérard Socié, Robert Zeiser, Bruce R. Blazar,Immune Biology of Allogeneic Hematopoietic Stem Cell Transplantation (Second Edition), Academic Press,2019,Pages 15-32,ISBN 9780128126301,https://doi.org/10.1016/B978-0-12- 812630-1.00002-5.

Pishesha, N., Harmand, T. J., & Ploegh, H. L. (2022). A guide to antigen processing and presentation. *Nature reviews. Immunology*, 22(12), 751–764. https://doi.org/10.1038/s41577- 022-00707-2

Sacha, J. B., Chung, C., Rakasz, E. G., Spencer, S. P., Jonas, A. K., Bean, A. T., Lee, W.,Burwitz, B. J., Stephany, J. J., Loffredo, J. T., Allison, D. B., Adnan, S., Hoji, A., Wilson, N. A., Friedrich, T. C., Lifson, J. D., Yang, O. O., & Watkins, D. I. (2007). Gag-specific CD8+ T lymphocytes recognize infected cells before AIDS-virus integration and viral protein expression. *Journal of immunology* (Baltimore, Md. : 1950), 178(5), 2746–2754. https://doi.org/10.4049/jimmunol.178.5.2746

Saez-Cirion, A., Jacquelin, B., Barré-Sinoussi, F., & Müller-Trutwin, M. (2014). Immune responses during spontaneous control of HIV and AIDS: what is the hope for acure?. Philosophical transactions of the Royal Society of London. Series B, *Biological sciences*, 369(1645), 20130436. https://doi.org/10.1098/rstb.2013.0436

Sáez-Cirión, A., & Pancino, G. (2013). HIV controllers: a genetically determined or inducible phenotype?. *Immunological reviews*, 254(1), 281–294. https://doi.org/10.1111/imr

Shannon, P., Markiel, A., Ozier, O., Baliga, N. S., Wang, J. T., Ramage, D., Amin, N., Schwikowski, B., & Ideker, T. (2003). Cytoscape: a software environment for integrated models of biomolecular interaction networks. *Genome research*, *13*(11), 2498–2504. https://doi.org/10.1101/gr.1239303

Sharp, P. M., & Hahn, B. H. (2010). The evolution of HIV-1 and the origin of AIDS. Philosophical transactions of the Royal Society of London. Series B, *Biological sciences*, 365(1552), 2487– 2494. https://doi.org/10.1098/rstb.2010.0031

Sidney, J., Peters, B., & Sette, A. (2020). Epitope prediction and identification- adaptive T cell responses in humans. *Seminars in immunology*, 50, 101418. https://doi.org/10.1016/j.smim.2020.101418.12076

Strong, R. K., Holmes, M. A., Li, P., Braun, L., Lee, N., & Geraghty, D. E. (2003). HLA-E allelic variants. Correlating differential expression, peptide affinities, crystal structures, and thermal stabilities. *The Journal of biological chemistry*, 278(7), 5082–5090. https://doi.org/10.1074/jbc.M208268200

Swann, S. A., Williams, M., Story, C. M., Bobbitt, K. R., Fleis, R., & Collins, K. L. (2001). HIV-1 Nef blocks transport of MHC class I molecules to the cell surface via a PI 3-kinase- dependentpathway. *Virology,* 282(2), 267–277. https://doi.org/10.1006/viro.2000.081

Tavares, L. A., de Carvalho, J. V., Costa, C. S., Silveira, R. M., de Carvalho, A. N., Donadi, E. A., & daSilva, L. L. P. (2020). Two Functional Variants of AP-1 Complexes Composed of either γ2 or γ1 Subunits Are Independently Required for Major Histocompatibility Complex Class I Downregulation by HIV-1 Nef. *Journal of virology*, 94(7), e02039-19. https://doi.org/10.1128/JVI.02039-19

Tedbury, P. R., Novikova, M., Ablan, S. D., & Freed, E. O. (2016). Biochemical evidence of a role for matrix trimerization in HIV-1 envelope glycoprotein incorporation. *Proceedings of the National Academy of Sciences of the United States of America*, 113(2), E182–E190. https://doi.org/10.1073/pnas.1516618113

Tenzer, S., Wee, E., Burgevin, A., Stewart-Jones, G., Friis, L., Lamberth, K., Chang, C. H., Harndahl, M., Weimershaus, M., Gerstoft, J., Akkad, N., Klenerman, P., Fugger, L., Jones, E. Y., McMichael, A. J., Buus, S., Schild, H., van Endert, P., & Iversen, A. K. (2009). Antigen processing influences HIV-specific cytotoxic T lymphocyte immunodominance. *Nature immunology*, 10(6), 636–646. https://doi.org/10.1038/ni.1728

Trowbridge, I. S., Lesley, J., Trotter, J., & Hyman, R. (1985). Thymocyte subpopulation enriched for progenitors with an unrearranged T-cell receptor beta-chain gene. *Nature*, 315(6021), 666– 669. https://doi.org/10.1038/315666a0

UNAIDS. (n.d.). Global HIV & AIDS statistics - fact sheet. UNAIDS. Retrieved October 16, 2022, from https://www.unaids.org/en/resources/fact-sheet

van Baalen, C. A., Guillon, C., van Baalen, M., Verschuren, E. J., Boers, P. H., Osterhaus, A. D., & Gruters, R. A. (2002). Impact of antigen expression kinetics on the effectiveness of HIV- specific cytotoxic T lymphocytes. *European journal of immunology*, 32(9), 2644–2652. https://doi.org/10.1002/1521-4141(200209)32:9<2644::AID-IMMU2644>3.0.CO;2-R

van Heuvel, Y., Schatz, S., Rosengarten, J. F., & Stitz, J. (2022). Infectious RNA: Human Immunodeficiency Virus (HIV) Biology, Therapeutic Intervention, and the Quest for a Vaccine. *Toxins*, 14(2), 138. https://doi.org/10.3390/toxins14020138

van Stigt Thans, T., Akko, J. I., Niehrs, A., Garcia-Beltran, W. F., Richert, L., Stürzel, C. M., Ford, C. T., Li, H., Ochsenbauer, C., Kappes, J. C., Hahn, B. H., Kirchhoff, F., Martrus, G., Sauter, D., Altfeld, M., & Hölzemer, A. (2019). Primary HIV-1 Strains Use Nef To Downmodulate HLA-E Surface Expression. *Journal of virology*, 93(20), e00719-19.

Voogd, L., Ruibal, P., Ottenhoff, T. H. M., & Joosten, S. A. (2022). Antigen presentation by MHC-E: a putative target for vaccination?. *Trends in immunology*, 43(5), 355–365. https://doi.org/10.1016/j.it.2022.03.002

Vukmanovic-Stejic, M., Vyas, B., Gorak-Stolinska, P., Noble, A., & Kemeny, D. M. (2000). Human Tc1 and Tc2/Tc0 CD8 T-cell clones display distinct cell surface and functional phenotypes. *Blood*, 95(1), 231–240.

Waheed, A. A., & Freed, E. O. (2012). HIV type 1 Gag as a target for antiviral therapy. *AIDS research and human retroviruses*, 28(1), 54–75. https://doi.org/10.1089/AID.2011.0230

Walker, B. D., & Yu, X. G. (2013). Unravelling the mechanisms of durable control of HIV-1. *Nature reviews. Immunology*, 13(7), 487–498. https://doi.org/10.1038/nri3478

Wesley, P. K., Clayberger, C., Lyu, S. C., & Krensky, A. M. (1993). The CD8 co receptor interaction with the alpha 3 domain of HLA class I is critical to the differentiation of human cytotoxic T-lymphocytes specific for HLA-A2 and HLA-Cw4. *Human immunology*, 36(3), 149–155. https://doi.org/10.1016/0198-8859(93)90118-k

Wyatt, R. C., Lanzoni, G., Russell, M. A., Gerling, I., & Richardson, S. J. (2019). What the HLA- I!-Classical and Non-classical HLA Class I and Their Potential Roles in Type 1Diabetes. *Current diabetes reports*, 19(12), 159. https://doi.org/10.1007/s11892-019-1245-z

Yan, Q., Barros, T., Visperas, P. R., Deindl, S., Kadlecek, T. A., Weiss, A., & Kuriyan, J. (2013). Structural basis for activation of ZAP-70 by phosphorylation of the SH2-kinase linker. *Molecular and cellular biology*, 33(11), 2188–2201. https://doi.org/10.1128/MCB.01637-12

Yang, H., Rei, M., Brackenridge, S., Brenna, E., Sun, H., Abdulhaqq, S., Liu, M., Ma, W.,Kurupati, P., Xu, X., Cerundolo, V., Jenkins, E., Davis, S. J., Sacha, J. B., Früh, K., Picker,L. J., Borrow, P., Gillespie, G. M., & McMichael, A. J. (2021). HLA-E-restricted, Gag- specific CD8+ Tcells can suppress HIV-1 infection, offering vaccine opportunities. *Science immunology*, 6(57), eabg1703. https://doi.org/10.1126/sciimmunol.abg17

Yu, F. H., Huang, K. J., & Wang, C. T. (2020). HIV-1 Mutant Assembly, Processing and Infectivity Expresses Pol Independent of Gag. *Viruses*, 12(1), 54. https://doi.org/10.3390/v12010054

Chapter 2.

Identification and evaluation of highly functional HIV Gag KF11-specific T cell receptors restricted by HLA-B*57

Preamble:

The results presented in this chapter are unpublished. I use the terms “we” and “our” to reflect the contributions of other researchers and trainees to this work. I performed a majority of the TCR cloning, DNA sequencing, in vitro functional assessments and data analyses that are reported here. Dr. Anju Bansal and Dr. Paul Goepfert (Univ of Alabama-Birmingham) provided TCR sequences for this study and generated the 721.221 target cell lines used for my studies. Dr. Gisele Umviligihozo and Dr. Francis Mwimanzi provided technical support and advice to optimize the luciferase reporter assay. Cristina Delmaestro and Zerufael Derza assisted with data collection, preparation of peptide stocks and maintenance of cell lines. Finally, Dr. Mark Brockman and Dr. Zabrina Brumme provided supervision and mentorship.

2.1. Introduction

Approximately 39 million people globally live with Human Immunodeficiency virus (HIV), of which 29.8 million were receiving combination antiretroviral therapy (cART) in 2022. The availability of cART has significantly reduced the number of AIDS-related deaths, but there is still no vaccine or cure for HIV. Thus, HIV continues to be one of the most prominent global health issues today (UNAIDS, 2023).

A small proportion of individuals who are living with HIV, approximately 0.2 to 0.5%, exhibit the remarkable ability to maintain an extremely low or “undetectable” level of the virus (i.e. below 50 RNA copies/mL) in their bodies even without the use of cART. These individuals are often referred to as HIV controllers, or in some cases, elite controllers (Borrell et al., 2021). CD8+ cytotoxic T lymphocytes (CTL or CD8), which recognize viral peptides presented by Human Leukocyte Antigen class I (HLA-I) proteins on the surface of infected cells, play an important role in suppressing HIV replication

during early infection (Safrit et al.,1994; Douek et al.,2003). In addition, a high frequency of virus-specific CTL are also associated with the HIV controller phenotype (Walker et al., 2012). HIV controllers typically display strong and enduring CTL responses indicating the critical role of CTLs in regulating HIV infection (Yang et al., 1996; Sacha et al., 2007; Monel et al., 2019). Interestingly, certain HLA-I alleles are associated with slower disease progression and are often able to generate robust CTL responses (Goulder and Walker, 2012). These alleles, often referred to as “protective alleles”, are relatively uncommon in the human population, but they are observed frequently in individuals who control HIV infection. Among these, the HLA-B*57 family has been studied extensively. While B*57 alleles are less than 1% in the global population, approximately 40 to 60% of HIV controllers possess these alleles (Lobos et al., 2022). The B*57 family shows regional and ethnic variability. Specifically, the B*57:01 allele is more prevalent in Asian and Caucasian populations, while the B*57:02, B*57:03, and B*58:01 variants are predominantly found in African populations (Lobas et al., 2022; Petros et al., 2017). Among persons living with HIV, those with B*57:01 exhibited the lowest viral load, while B*57:03 and B*57:02 offered relatively less protective effects (Lobas et al., 2022).

Several immuno-dominant HIV Gag epitopes are associated with more robust CTL responses and better immune control in the context of HLA-B*57 (Kiepiela et al., 2007). Of these, Gag epitopes IW9 (ISPRTLNAW, Gag 138-146), KF11 (KAFSPEVIPMF, Gag 162-172), and TW10 (TSTLQEQIGW, Gag 240-249) are the most notable (Lobas et al., 2022). During the initial stages of infection, the immune system primarily targets IW9 and TW10 epitopes. While in later stages of infection, CTL responses to KF11 become dominant and are often observed in individuals who maintain lower viral loads (Stewart-Jones et al., 2012; Gillespie et al., 2006; Altfeld et al., 2003). Recent studies by the Goepfert lab (Bansal et al., 2021) demonstrated that CTL cell responses against KF11 were mediated not only by HLA-B*57, but also by the non-classical HLA-E. Further investigation is warranted to confirm this new observation and to understand the potential role of HLA-E in control of HIV.

Antigen-specific CD8 T cell responses are typically oligoclonal composed by multiple T cell lineages expressing a distinct T cell receptor (TCR) sequence. This oligoclonal response is referred to as the TCR repertoire. Each TCR clone within the repertoire can exhibit a different capacity to recognize the consensus peptide as well as peptide variants. Intriguingly, the TCR repertoire of HIV-positive individuals carrying

B*57:03 were shown to display higher sequence diversity but lower cross-reactivity to Gag peptide variants compared to those from individuals carrying B*57:01 (Yu et al., 2007). Several studies have indicated that prolonged HIV-1 exposure leads to the expansion of virus-specific CD8 T cells, resulting in a biased TCR repertoire within the cell population (Pantaleo et al., 1997,1994; Gorochov et al., 1998; Dalgleish et al., 1992). For example, two TCR beta Variable (V) genes (TRBV19 and TRBV7) have been shown in elite controllers to predominate the CD8 T cell response to Gag KF11, indicating that TCR encoding these V genes may be superior (Mendoza et al., 2012; Yu et al., 2007).

A prior study by Bansal et al. identified CD8 T cells in chronic HIV-infected individuals that recognized HIV Gag KF11 (KAFSPEVIPMF; Gag 162-172) presented in the context of HLA- B*57:01 as well as HLA-E*01:01, indicating for the first time that an HLA-E restricted response could be elicited against HIV following infection (Bansal et al., 2021). To determine this, the authors expanded antigen-specific T cells by culturing peripheral blood mononuclear cells (PBMC) with KF11 peptide pulsed HLA-E and B*57 cells for 7-12 days. CD8 T cell lines were then re-stimulated with KF11 presented by immortalized human B cells (721.221-derived cell lines) expressing either B*57:01 (721.221- B*57:01 clone) or HLA-E*01:01 (either AEH or 41A3.A2 clone). Activated CD8 T cells were quantified by flow cytometry based on upregulation of surface CD107a and intracellular expression of IFN-γ cytokine; these cells were also isolated by FACS using the Activation-Induced Marker (AIM) method based on upregulation of surface CD137 (4-1BB) and subjected to single-cell RNA sequencing to identify 151 putative KF11-specific TCR alpha/beta gene sequences restricted by B*57 and/or HLA-E (Bansal et al., 2021).

Given these prior observations, we wished to gain a better understanding of diverse TCR clones restricted by HIV Gag KF11. To do this, we examined the panel of TCR sequences described by Bansal et al. that were anticipated to recognized Gag KF11 when presented by B*57:01 and/or HLA-E. The goals of this work were: (1) to confirm the epitope/HLA restriction of these TCR sequences; and (2) to investigate genetic features that may contribute to mechanisms of viral peptide recognition. In this chapter, we present the results of our analysis for KF11-specific TCR in the context of HLA-B*57. In Chapter 3, we will present our efforts to examine this question in the

context of HLA-E. The results of this project provide new evidence to support efforts in designing vaccines and therapeutics to prevent or treat HIV infection.

2.2. Methods

2.2.1. Selection of TCR clones for this study

As a member of the Bansal et al. study team, Dr. Brockman performed pair-wise analyses of all TCR alpha and beta V genes (TRAV and TRBV) using the bioinformatics program, TCRdist, and then constructed a network graph to visualize sequence similarity among these clones (Figure 2.1) (Bansal et al., 2021). Briefly, TCRdist applies the Blossum62 substitution scoring method to calculate a weighted similarity value (or distance) between pairs of TCR based on their amino acid sequences in complementary determining regions (CDR)1, CDR2, CDR2.5, and CDR3 (Dash et al., 2017). These CDR motifs form loops in the TCR structure that contribute as major sites of contact with peptide and/or HLA. TCRdist generates a matrix of pair-wise distances between all TCR clones analyzed, providing a single numerical measure of sequence similarity among diverse clones. TCRdist results were displayed as a network graph, constructed using Cytoscape open-source software, where each TCR clone is depicted as a node and similarity values (referred to as Hamming distances) less than 150 are depicted as edges. Visualization of the data in this way identified “clusters” of TCR alpha/beta clones that displayed higher sequence similarity (and thus were expected to display similar functional characteristics). Notably, sequence-based clusters were consistent with the anticipated HLA restriction of KF11-specific CD8 T cells shown in figure 2.2 (i.e., HLA-E only, B*57 only, and dual HLA-restricted sub-clusters were visible). Based on these results, we selected 67 TCR clones shown in that were expected to be restricted by KF11 in the context of B*57 or HLA-E for in vitro functional analysis (Figure 2.2).

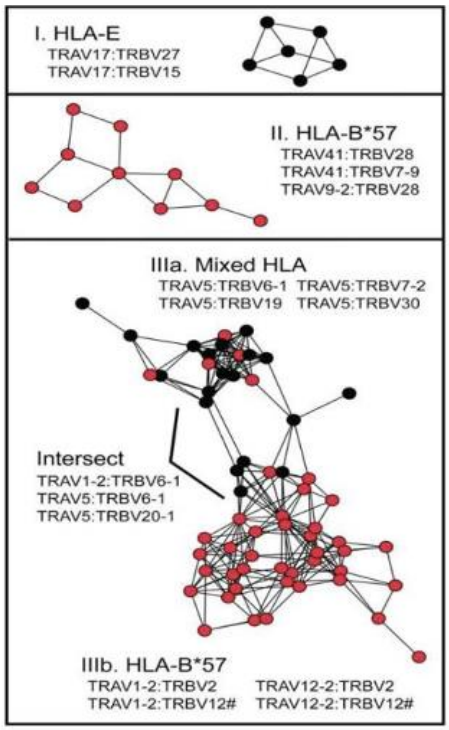

Figure 2.1. Genetic clustering of HLA-E vs. B*57 restricted T cells against Gag KF11

Network graphs depict the results of TCRdist analysis for 77 KF11-specific TCR sequences (displaying 299 edges) using a Hamming distance threshold of 150. TCR clones identified in the context of HLA-E are shown as black nodes; those identified in the context of B*57 are shown as red nodes. Clusters with less than 5 TCR members are not displayed. TRAV, human T cell receptor variable alpha gene; TRBV, human T cell receptor variable beta gene.

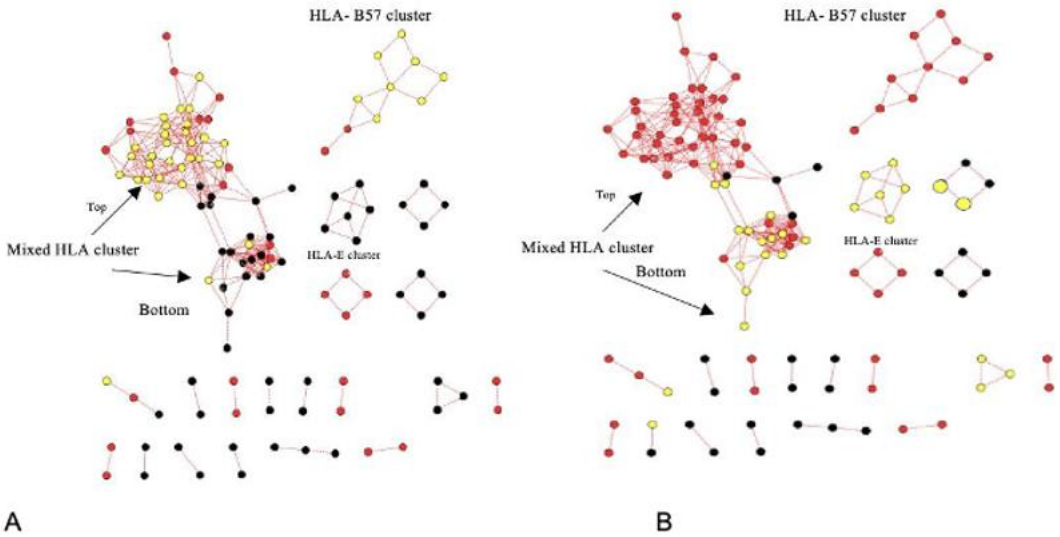

Figure 2.2. Selection of TCR clones for functional analysis of B*57 and HLA-E restricted responses against Gag KF11.

Network graphs showed results of TCRdist analysis for 124 KF11-specific TCR sequences (displaying 670 edges) using a Hamming distance threshold of 150 TCR clones restricted by

HLA-E are shown as black nodes; those restricted by B*57 are shown as red nodes. (A) Yellow highlighted nodes represent 67 TCR clones selected for functional studies in the context of HLA-B*57. A majority of these clones are located in the upper (top) subgroup of the mixed HLA cluster or in the HLA-B*57 cluster. (B) Yellow highlighted nodes represent selected 28 TCR clones selected for functional analyses in the context of HLA-E (presented in Chapter 3). Most of these clones are located in the lower (bottom) subgroup of the Mixed HLA cluster or in the HLA-E cluster.

2.2.2. Molecular cloning of TCR alpha and beta genes

Single-cell RNA sequencing was used to obtain paired TCR gene products spanning the CDR3 alpha and CDR3 beta motifs (Bansal et al., 2021). This information was used to re- construct full-length TCR alpha and beta open reading frames that encoded the appropriate V gene, CDR3 and a Constant domain. Full-length sequences were codon-optimized and synthesized commercially as gBlocks by Integrated DNA Technologies (IDT). Products were digested and ligated into the pSelectGFP plasmid (InvivoGen) using 5' Asc I and 3' Sac II restriction sites. Following ligation, DNA products were transformed into E. cloni Chemically Competent Cells (Lucigen), plated on an LB-agar containing Zeocin antibiotic and grown overnight at 37°C. Zeocin-resistant colonies were selected and grown in LB liquid media containing Zeocin overnight at 37°C. Plasmid DNA products were purified with EZNA DNA mini kit (Omega Bio-tek).

2.2.3. TCR Sequence Validation

TCR plasmids were validated by Sanger DNA sequencing using forward and reverse primers located in the pSelect-GFP plasmid (701 Forward, 710 Forward, 789 Reverse and 791Reverse) synthesized commercially by IDT. Each TCR sequence was aligned to its synthetic template and examined using Geneious Prime software (Biomatters Ltd.).

2.2.4. Eukaryotic cell culture

Jurkat E6.1 cells (ATCC, TIB-152) were provided by Dr. Jonathan Choy and 721.221- derived cell lines were provided by Dr. Paul Geopfert. Jurkat cells were cultured in RPMI-1640 (Lonza or Gibco) supplemented with 10% fetal bovine serum (Sigma or Gibco), 1000 U/mL penicillin, and 1 mg/mL streptomycin (all from Sigma-Aldrich) (referred to as R10+). 721.221 cells were cultured with RPMI-1640 supplemented with 20% fetal bovine serum (Gibco), 1000 U/mL penicillin, 1 mg/mL

streptomycin, and 1% sodium pyruvate (all from Sigma-Aldrich) (referred to as R20+ with pyruvate). After transfection, Jurkat cells were recovered in RPMI- 1640 (Lonza and Gibco) supplemented with 20% fetal bovine serum (Sigma or Gibco), 1000 U/mL penicillin, and 1 mg/mL streptomycin (all from Sigma-Aldrich) (called R20+). During TCR reporter assays, cells were cultured with RPMI-1640 without phenol red (Sigma), supplemented with 20% fetal bovine serum (Sigma), 2mM L-glutamine, 1000 U/mL penicillin, and 1mg/mL streptomycin (all from Sigma-Aldrich) (called R20+ no phenol red). All cell lines were maintained at 37°C with 5% CO2.

2.2.5. Preparation of effector Jurkat T cells (Jurkat cell transfection)

Jurkat cells were transfected by electroporation in 96-well plates using a Bio-Rad GenePulser MXcell electroporation system. For each transfection, 3 million cells were resuspended in 150 uL of Opti-MEM reduced serum medium (Gibco), containing 3 ug of pSelect- TCRalpha, 3 ug of pSelect-TCR beta, 3 µg of pORF9-hCD8α and 8 ug of pNFAT-Luciferase. Following transfection, Jurkat cells were transferred into 2 mL “bullet” tubes (Nunc) containing 700 uL of R20+ media and rested in an incubator for 24 hours at 37°C with 5% CO2.Transfection efficiency was assessed by flow cytometry (Beckman CytoFLEX) by detection of green fluorescence protein (GFP; expressed by TCR plasmids) and surface CD8 alpha (allophycocyanin (APC)-Cy7; clone SK1, BD Pharmingen).

2.2.6. Validation of HLA expression on 721.221 target cells

HLA expression on 721.221 target cell lines (immortalized human B cells) was confirmed by flow cytometry. HLA-E- null 721.221 cells expressing HLA-A2 (41A3.A2 clone) or HLA-B*57:01 (721.221-B*57 clone) were stained with anti-human A2 (allophycocyanin (APC); clone BB7.2, BioLegend), anti-human HLA-E (Phycoerythrin (PE); clone 3D12, Biolegend), and anti-HLA class I BW4 (for B*57) (allophycocyanin (APC); clone REA274, Miltenyi Biotec).

2.2.7. Preparation of 721.221 target cells (Peptide pulsing)

KF11 and FK10 peptides were commercially obtained from JPT Peptide Technologies and stocks were prepared in DMSO at 3 mg/mL. Stock peptides were

diluted in diethyl pyrocarbonoate water (DEPC-H2O) to achieve a working concentration of 120 ng/uL for reporter assays (or 30 ng/uL final concentration after co-culture). For each reaction, 50,000 721.221 cells were pelleted and resuspended in 52.5 uL of R20+ no-phenol red media. Then, 17.5 uL of KF11 or FK10 peptide was added to cells in a white 96-well, round-bottom plate (Corning), to a final volume of 70ul, and incubated at 37°C for 1 hour.

2.2.8. TCR stimulation and luciferase reporter assays

TCR-transfected Jurkat cells were pelleted and resuspended in R20+ no phenol red media at 8.33 x106 cells/mL. For each reaction, 30 uL of Jurkat cells (250,000 cells) was added to 70 uL peptide-pulsed 721.221 target cells in a white 96-well, round bottom plate (Corning), to a final volume of 100 uL. Co-cultures were incubated at 37°C for 6-8 hours to allow TCR to engage peptide/HLA presented by 721.221 cells and to initiate TCR-dependent NFAT signaling to produce luciferase. Luciferase activity was measured as luminescence using the Steady-Glo luciferin assay (Promega) on an Infinite 200 Pro plate reader (Tecan). For this, 100 uL of luciferin solution was added directly to 100 uL of co-cultured cells in a white 96-well, round bottom plate and incubated at room temperature for 10 minutes in dark conditions. Luminescence was measured using a 3000 ms integration time, 100ms settle time (between wells) and no signal attenuation.

2.2.9. TCR structure modeling

The AGA TCR model was downloaded from the Protein Data Bank (PDB: 2YPL) (Stewart-Jones et al,2012). The TCR13/TCR46 model was generated using the TCRmodel2.0 program developed by the Pierce lab at the University of Maryland (Yin et al., 2023) (available online at: https://tcrmodel.ibbr.umd.edu). In brief, sequences for TCR α and β chains, as well as KF11 epitope and HLA-B*57:01, were submitted. TCRmodel 2.0 applies template-based and deep learning methods to predict the structure of TCRs and TCRs in complex with peptide-MHC (pMHC) targets. The program generated five models with confidence scores ranging from 0.87 to 0.78. The model with the highest confidence score was selected for our analyses. The AGA structure and the predicted TCR13/TCR46 model were both visualized using Chimera, an open- source visualization software for molecular structure analysis developed by the University of California, San Francisco. Putative interactions between TCR13/TCR46

and the KF11 peptide at positions 6 and 7 were assessed using the 'find clashes/contact' tool in Chimera. Parameters for clash/contact analysis were set as follows: (1) identifying atoms with van der Waals overlap greater than or equal to -0.6 angstroms, (2) disregarding contacts between pairs separated by four or fewer bonds, (3) including contacts within the same molecule, and (4) adjusting overlap values potentially attributable to hydrogen bonding by subtracting 0 angstroms.

2.3. Results

2.3.1. Selection and cloning of TCR genes

While most T cells express one TCR alpha and one TCR beta transcript (Haque et al., 2017 and Tanno et al., 2019), we observed that multiple alpha and beta transcripts were often associated with each “single” T cell in the RNA sequencing data provided by the Goepfert lab (data not shown). This indicated the unfortunate possibility that more than one cell was isolated and sequenced following by KF11 stimulation in many cases. As a result, the alpha/beta gene pair that contributed to the KF11 response was not clear. To address this issue, we selected 67 putative B*57 or HLA-E/KF11-restricted TCR clones for analysis that reflected the diversity of unique alpha and beta gene combinations that were present in the data. For example, if a selected sample contained more than one potential TCR alpha/beta pair, we aimed to test all possible pairs in our study. Appendix Table A1 displays the genetic details, clonal ID, and well ID of these TCR clones. Notably, the sequences of TCR clones 13 and 46 were identical, but they were identified using target cells expressing HLA-E (TCR 13) or B*57 (TCR 46). This observation suggested that TCR 13/46 might be dual HLA-restricted and capable of recognizing KF11 presented by both HLA-E and HLA-B*57.

Then 67 selected TCR clones were composed by 28 of V alpha genes (Vα) and 26 of V beta genes (Vβ). For gene construction, unique Vα genes were identified using an Alpha clone number, and unique Vβ genes were identified as Beta clone number. All TCR genes were reconstructed as full-length open reading frames, synthesized commercially by IDT, cloned into pSelectGFP and then verified by Sanger sequencing. Figure 2.3 illustrates a phylogenetic tree where each cloned TCR sequence is grouped with its corresponding reference sequence, indicating the successful cloning of all TCR samples with no genetic mutations.

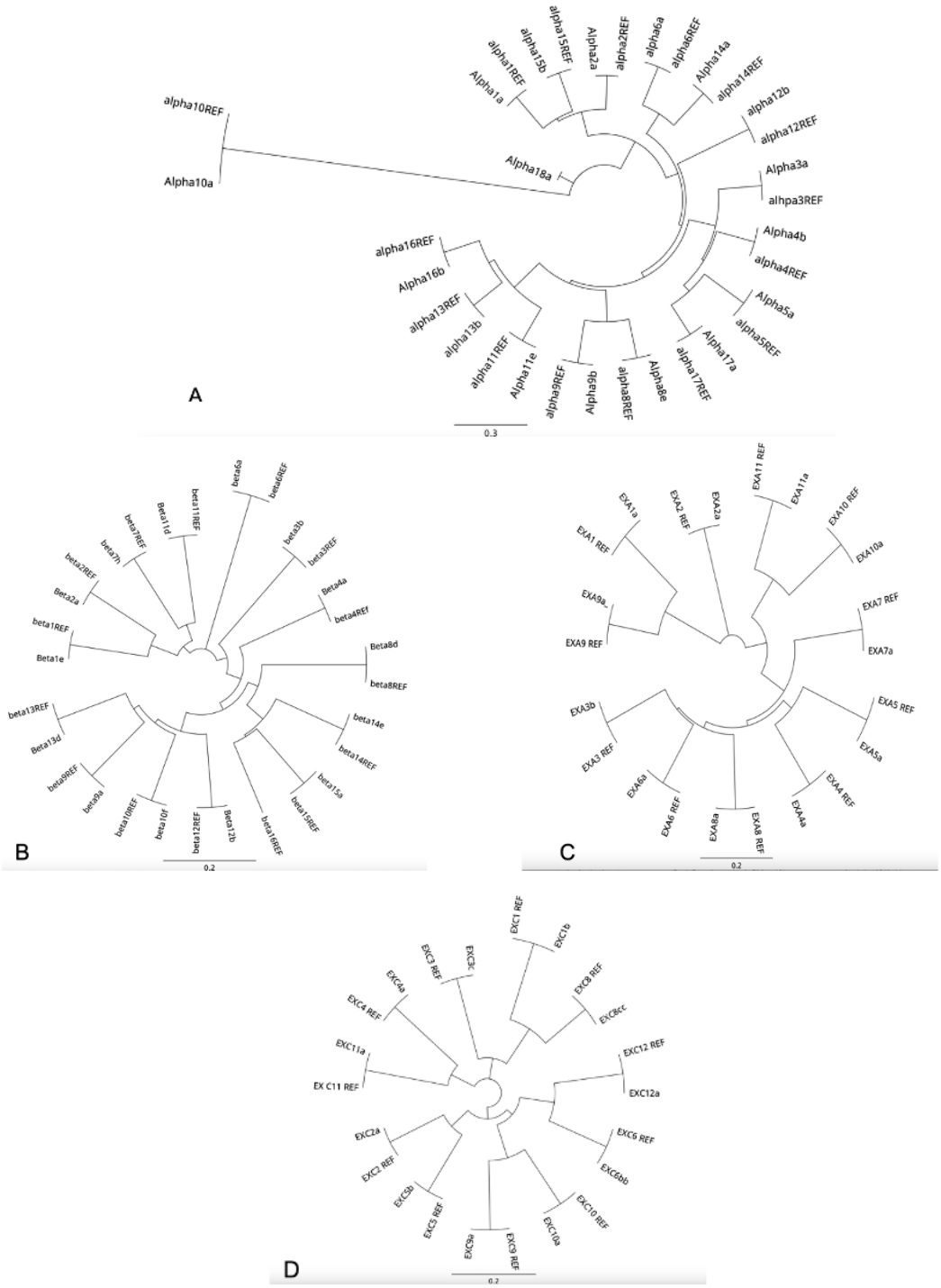

Figure 2.3. Phylogenetic analysis of TCR clonal sequences with references
(A and C) Phylogenetic analysis of alpha clone sequences and corresponding reference genes (ref) are shown for 26 Vα genes. (B and D) Phylogenetic analysis of beta clone sequences and corresponding reference genes are shown for 25 Vβ genes. Trees were built using the Tamura-Nei model and the neighbor-joining method in Geneious software.

2.3.2. Verification of HLA expression on 721.221 target cells

To functionally assess different TCR clones, we have established an in vitro luciferase reporter cell line. For TCR reporter assay, we intended to use 721.221-derived 41A3.A2 cells and 721.221-B*57:01 cells as target cells. 41A3.A2 cells were constructed to express only HLA- A2 whereas 721.221-B*57:01 cell express only B*57:01 (Bansal et al., 2021). To ensure that each cell line expressed appropriate HLA alleles, all 221 derived cell lines were stained with anti-A2 and anti-B*57 antibodies and examined by flow cytometry. As expected, 99.6% of 41A3.A2 cells expressed HLA-A2 (Figure 2.4A). Similarly, 83.1% of 721.221-B*57:01 cells expressed HLA-B*57 (Figure 2.4B). Results indicated that both cell lines express the appropriate HLA of interest and supported their use as target cells in the TCR reporter assay.

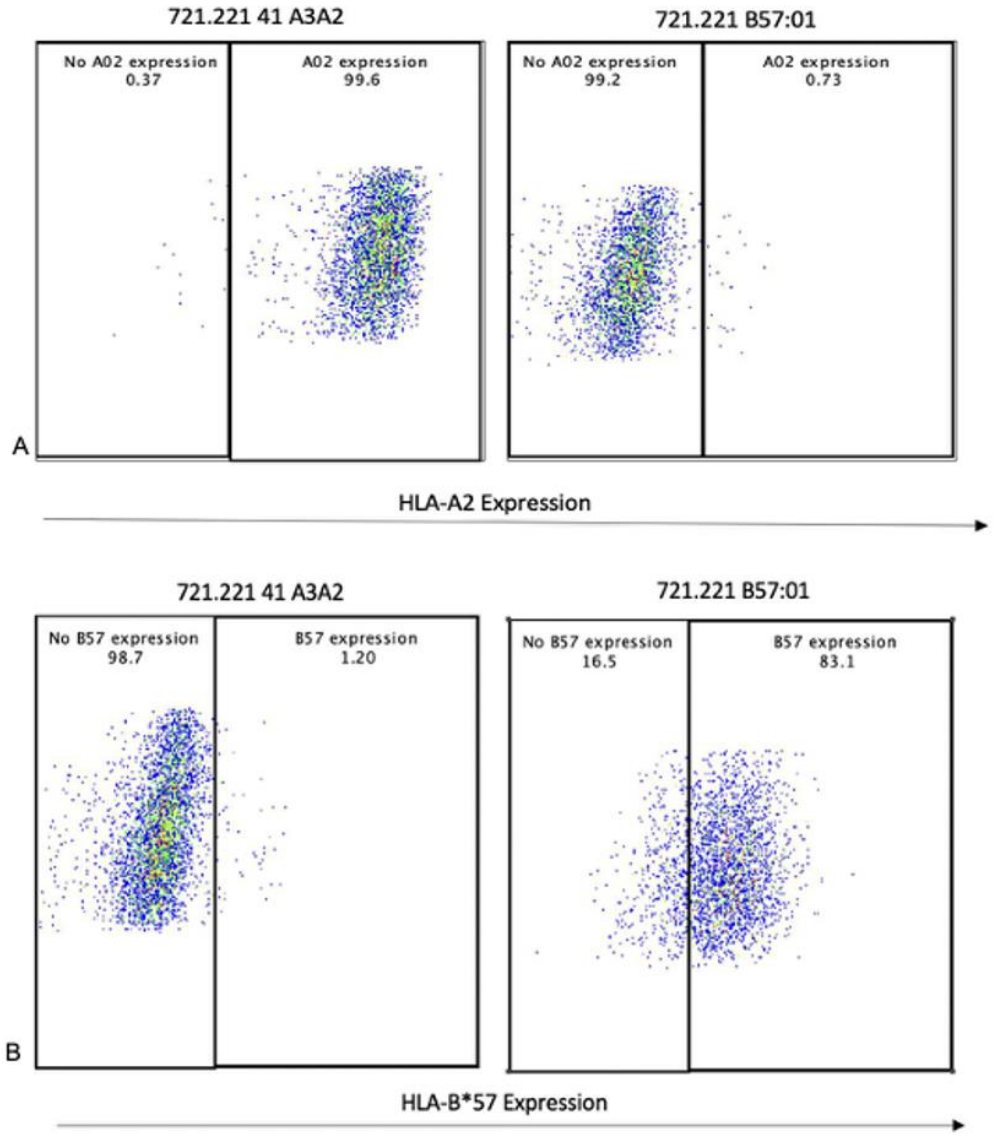

Figure 2.4. Verification of HLA expression in 721.221 41A3.A2 and 721.221 B*57:01 cell lines.

(A)41A3.A2 and 721.221-B*57:01 cells were stained with HLA-A2 antibody (allophycocyanin, APC); clone BB7.2, BioLegend) and examined by flow cytometry. Only 721.221 41A3.A2 cells expressed HLA-A2. (B) 41A3.A2 and 721.221-B*57:01 cells were stained with HLA-B*57 antibody (allophycocyanin, APC); clone REA274, Miltenyi Biotec) and examined by flow cytometry. Only 721.221-B*57:01 cells expressed HLA-B*57.

2.3.3. Verification of jurkat effector cells

For this study, we adapted a TCR reporter assay that was previously developed by the Brockman lab (Anmole et al., 2015). In the initial report, jurkat cells were transfected by electroporation using a 0.4 cm cuvette (Figure 2.5 A). However, to increase assay throughput, we modified the procedure to use a 96-well transfection plate so that multiple TCR samples could be tested simultaneously. The original reporter assay demonstrated that a transfection efficiency of 42% (reflecting the proportion of live CD8+ TCR+ cells) was sufficient to generate robust TCR- mediated recognition of a peptide/HLA complex (Figure 2.5). Our modified plate-based method resulted in a transfection efficiency of 49.2%. Since the modified procedure resulted in a similar or better transfection efficiency and also allowed us to test TCR clones more quickly, we adopted this method for the rest of our studies.

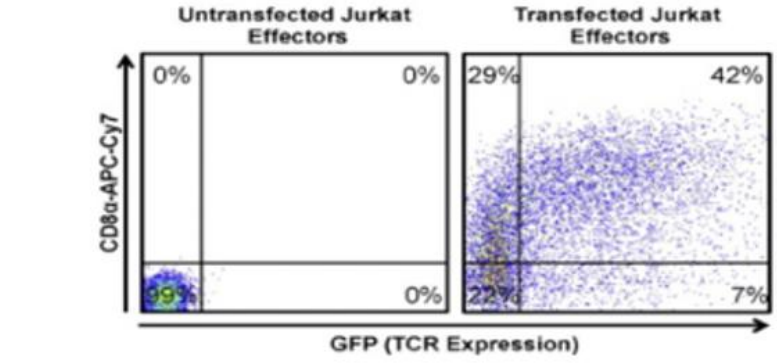

A

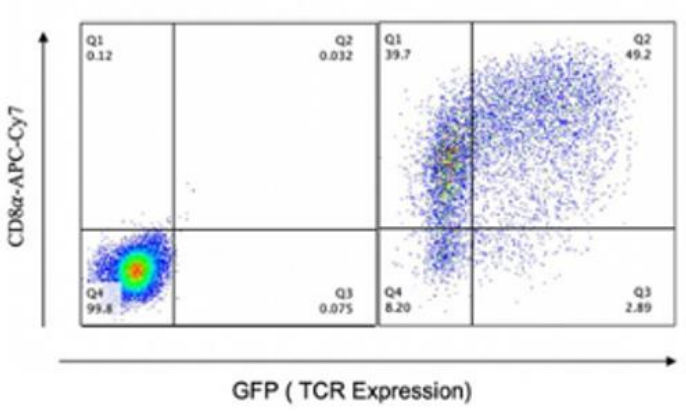

B

Figure 2.5. Comparison of transfection efficiency in Jurkat cells using cuvette and transfection plate method.

(A) Expression of GFP (A2-FK10 restricted 5B2 TCR alpha/beta) and CD8 alpha was detected by flow cytometry. CD8 alpha was stained with antibody (allophycocyanin, APC)-Cy7, SK1, Biolegend). Left panel represents untransfected Jurkat cells and right panel represents transfected Jurkat cells with CD8 alpha and TCR samples. Graph is from Anmole et al., (2015).(B) Expression of GFP (5B2 TCR alpha/beta) and CD8 alpha was detected by flow cytometry. CD8 alpha was stained with antibody (allophycocyanin, APC)-Cy7, SK1, Biolegend). Left panel represents untransfected Jurkat cells and right panel represented transfected Jurkat cells with CD8 alpha and TCR samples. This data is collected with the assistance of Zerufael Derza.

2.3.4. Identifying functional TCRs restricted by B*57:01-KF11

To identify functional TCR clones, we co-cultured TCR-transfected Jurkat cells with 721.221-derived target cells in our reporter assay. Since KF11 can be presented by both B*57 and HLA-E, but not HLA-A2 (Bansal et al., 2021 and Los Alamos National Laboratory, 2023), we tested each TCR clone against 721.221 target cells expressing

either B*57:01 (as the test allele), E*01:01 (as a potential cross-reactive allele) or A*02 (as a negative HLA-mismatch control). In addition, we included a previously characterized TCR clone (5B2), which recognizes the Gag FK10 epitope presented by HLA-A2, as a positive control (Anmole et al., 2015).

The functionality of each TCR clone was assessed based on its ability induce TCR- dependent NFAT signaling following co-culture with KF11 peptide-pulsed target cells, which was detected as luminescence activity. We observed that TCR-transfected jurkat cells generated a wide range of luminescence signal when co-cultured with target cells that were not pulsed with KF11 peptide or when co-cultured with HLA mismatched targets, indicating that non-specific or basal signaling differed among the TCR clones (Appendix Table A2). To overcome this variation, luminescence results were converted into the fold-change of TCR-dependent signal, defined as the quotient of light units produced using peptide-pulsed target cells divided by light units produced using non-peptide-pulsed target cells. We defined TCR clones as functional if they induced more than 1.5-fold change in luminescence signal in the presence of KF11-pulsed 721.221-B*57:01 target cells versus non-KF11-pulsed cells and versus HLA mismatched (A2+) cells.

In initial screening, we observed seven (of 67) TCR clones that met our criteria for being responsive to B*57-KF11. These were clones TCR 1, TCR 9, TCR 16, TCR 13/46, TCR 20, TCR 23, and TCR 39 (Appendix Table A2). To verify the activity of these clones, we re-tested them in independent experiments. The data from three biological replicates demonstrated that all seven clones consistently elicited a B*57-restricted KF11 response in our reporter assay (Figure 2.6 A and B). These clones generated on average a 11.8- to 53.4-fold change in luminescence signal in the presence of B*57-KF11 target cells, whereas signals induced by non-specific target cells (i.e. 41A3.A2) were low (ranging from 1.2 to 3.6 fold). For all seven TCR clones, p-values from the unpaired Students t-test comparing the B*57-specific and non-specific responses were found to be less than 0.05. Together, we identified seven TCR samples were able to generate specific B*57 Gag KF11 CD8 T-cell response. TCR clones will undergo further functional assessment to evaluate their ability to recognize KF11 when presented by HLA target cells. This analysis amid to identify potential dually restricted TCRs.

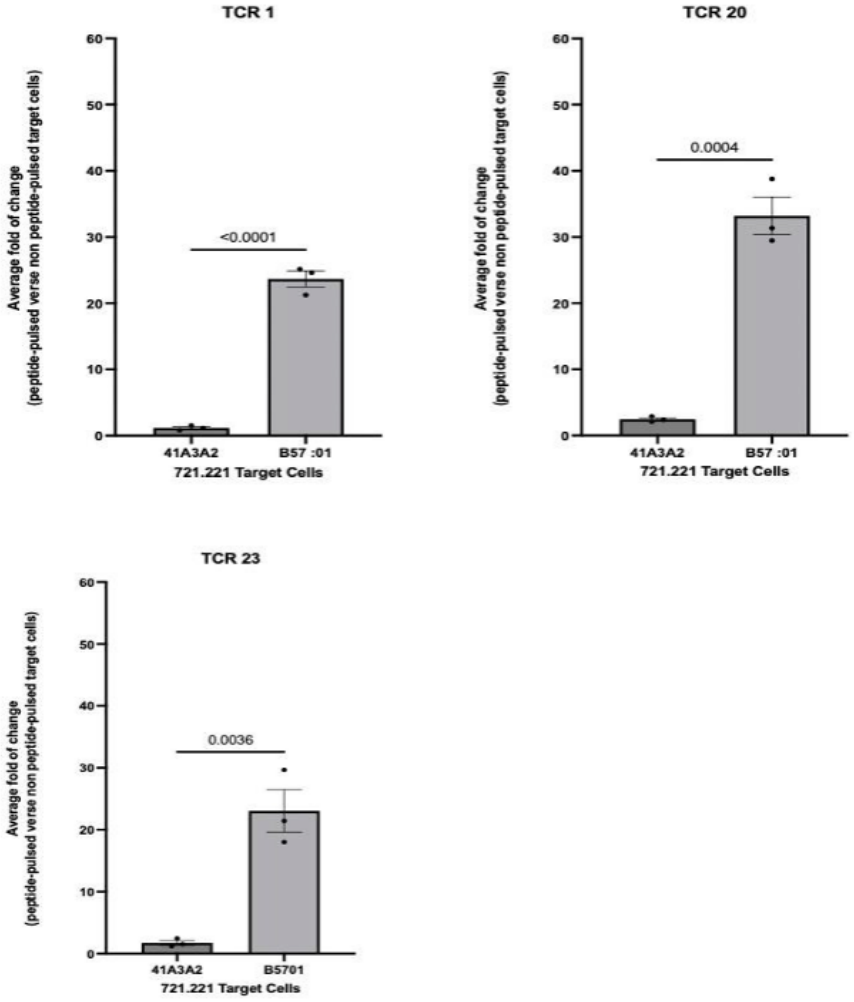
TCR 1
Average fold of change
(peptide-pulsed verse non peptide-pulsed target cells)
60
50
40
30
20
10
0
<0.0001
41A3A2
B57 :01
721.221 Target Cells
TCR 20
Average fold of change
(peptide-pulsed verse non peptide-pulsed target cells)
60
50
40
30
20
10
0
0.0004
41A3A2
B57 :01
721.221 Target Cells
TCR 23
Average fold of change
(peptide-pulsed verse non peptide-pulsed target cells)
60
50
40
30
20
10
0
0.0036
41A3A2
B5701
721.221 Target Cells

A

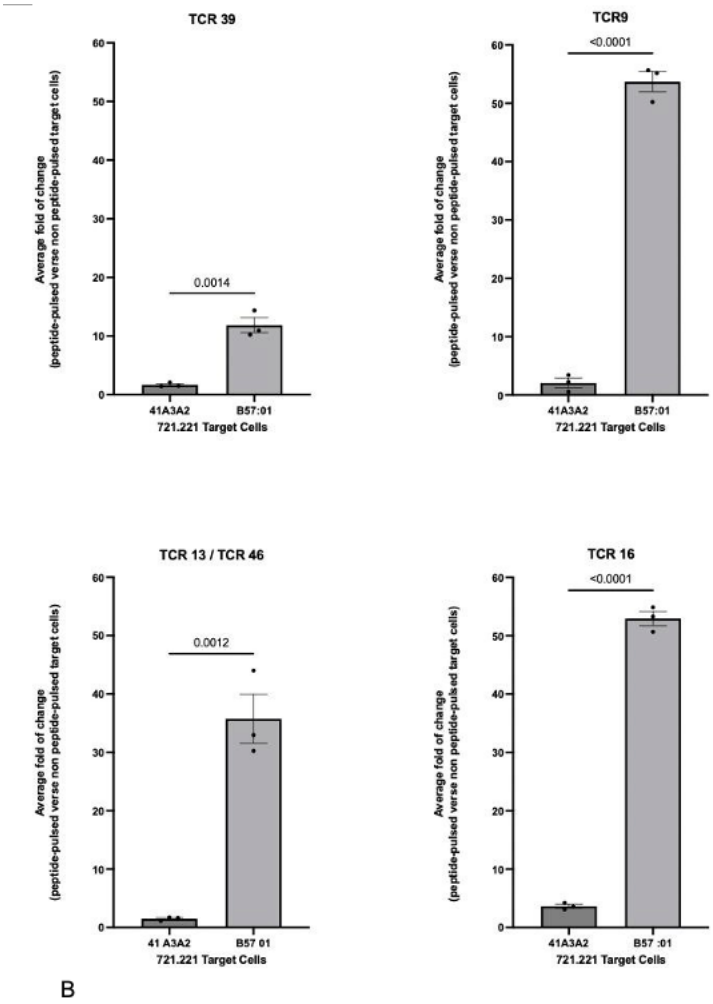

Figure 2.6. Validation of seven TCRs demonstrated their ability to generate robust B*57- KF11 CD8 T cell response via TCR reporter assay

(A and B) Each TCR clone was tested in three independent biological replicates using a luciferase-based TCR reporter assay. Luminescence signal of TCR-transfected Jurkat cells was determined after co-culture with target cells pulsed with KF11 peptide (B*57:01) or target cells without peptide (41A3.A2), and a fold- change calculated. The final peptide concentration was 30 ng/µL in each experiment. The error bars represented standard error mean (SEM). Unpaired t-tests were used to calculate the difference between non-specific and B*57-KF11-specific responses in each sample. P values are shown above each comparison.

2.3.5. Genetic characteristics of functional B*57-KF11 restricted TCR clones

TCR sequences are highly diverse, especially in the hypervariable complementarity determining region 3 (CDR3) (Thakkar and Bailey-Kellogg et al., 2019). Similarity in CDR3 sequences among TCR clones has been used to identify clones with comparable epitope specificity, shared MHC/HLA restrictions, and associated pathologies (Dash et al., 2017 and Thakkar and Bailey-Kellogg et al., 2019). Since

CDR3 motifs are often critical for the interaction between a TCR and its cognate HLA-peptide antigen, it could provide us valuable insights into genetic features that are crucial for initiating a KF11-specific response by analyzing CDR3 regions.

Interestingly, all of identified highly functional TCR clones (7 of them) are located within the 'mixed HLA' cluster initially described by Bansal et al (Figure 2.7A). All of these clones shared the same TCR alpha V gene (TRAV), TRAV5, which encodes the CDR1, CDR2 and CDR2.5 motifs used by TCRdist (Figure 2.7B). Notably, these seven clones displayed only three distinct CDR3 alpha motifs, and those sequences were differed by only one amino acid (at position 3): CA**E**SGGYQKVTF, CA**V**SGGYQKYTF, and CA**G**SGGYQKVTF. Gene usage for the beta chain was also limited within these seven clones. Five of the clones encoding the TCR beta variable gene (TRBV) TRBV6-1 and two clones encoding TRBV19. The five clones encoding TRBV6-1 shared two distinct CDR3 beta motifs that differed by four amino acids: CA**CA**G**TS**YGYTF and CA**ST**G**GT**YGYTF. The two clones encoding TRBV19 displayed distinct CDR3 beta motifs that also differed by four amino acids: CA**IS**G**QT**YGYTF and CA**SS**G**AV**YGYTF. Together, these results suggest that genetic features encoded by TRAV5 and TRBV6-1/TRBV19, as well as CDR3, contribute to a robust B*57-restricted Gag KF11 response.

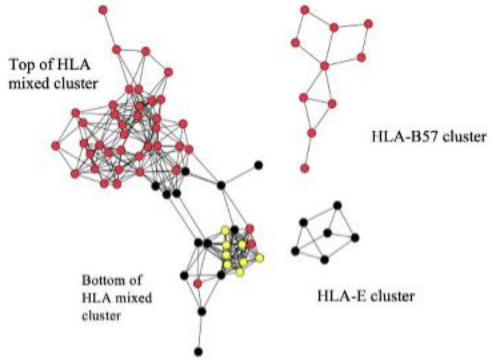

A

Clone_ID	CDR3 Alpha	CDR3 Beta	Variable Alpha Gene	Variable Beta Gene
E-1 (TCR1)	CAESGGYQKVTF	CACAGTSYGYTF	TRAV5	TRBV6-1
E-59 (TCR 16)	CAVSGGYQKVTF	CASTGGTYGYTF	TRAV5	TRBV6-1
E-4 (TCR 9)	CAVSGGYQKVTF	CACAGTSYGYTF	TRAV5	TRBV6-1
B57-65/ E-56 (TCR13/TCR 46)	CAESGGYQKVTF	CASTGGTYGYTF	TRAV5	TRBV6-1
E-11 (TCR 20)	CAESGGYQKVTF	CASAGGEYGYTF	TRAV 5	TRBV6-1
B57-4 (TCR 39)	CAVSGGYQKVTF	CAISGQTYGYTF	TRAV5	TRBV19
E-24 (TCR 23)	CAGSGGYQKVTF	CASSGAVYGYTF	TRAV 5	TRBV19

B

Figure 2.7. Sequence features of highly functional B*57-KF11 restricted TCR clones.

TCR sequence similarity is depicted as a network graph, based on results of TCRdist. HLA-E restricted TCRs are shown as black nodes; those restricted by B*57 are shown as red nodes. Yellow nodes represent TCR clones capable of mounting a robust B*57-KF11 response in our TCR reporter assay. All highly functional TCR clones are located within the lower HLA mixed cluster (bottom). (B) Genetic features of seven highly functional B*57-KF11 restricted TCR clones are shown. Amino acids highlighted in red (E, glutamic acid; V, valine; G, glycine, indicate differences between CDR3 alpha sequences.

2.3.6. Differences in antigen sensitivity among seven highly functional B*57-KF11 restricted TCR clones

We next wanted to explore whether these seven TCR clones displayed different sensitivity toward B*57-KF11 antigen. To do this, we pulsed 721.221-B*57:01 target cells with various concentrations of KF11 peptide (37.5 to 1.48 ng/uL) and co-cultured these cells with TCR-transfected Jurkat cells. Our standard TCR reporter assay uses a pulse of 30 ng/uL peptide and was able to generate robust B*57-restricted Gag KF11 responses. To mitigate potential cytotoxicity associated with high concentrations of dimethyl sulfoxide (DMSO) (Dludla et al., 2018), we used a maximum concentration of 37.5 ng/μL peptide in this study. We observed that TCR clone 16 displayed the highest signaling activity when co-cultured with721.221 B*57:01 target cells at all KF11 peptide

concentrations tested. By contrast, TCR 39 displayed the lowest activity under the same conditions (Figure 2.8). At the highest peptide dose (37.5 ng/uL), TCR 16 showed ~81-fold induction whereas TCR 39 showed ~22-fold induction, indicating that TCR 16 was 3.7 times more sensitive than TCR 39 in recognizing KF11 peptide. Signal intensity for TCR 13/46, TCR 23 and TCR 20 decreased at the highest peptide dose (37.5 ng/uL), possibly due to saturation of the response and/or toxicity due to higher DMSO concentrations resulting in cell death. These results demonstrate that these seven TCR clones exhibited different antigen sensitivities for B*57-KF11, which could contribute to biologically meaningful differences in CD8 T cell function in vivo.

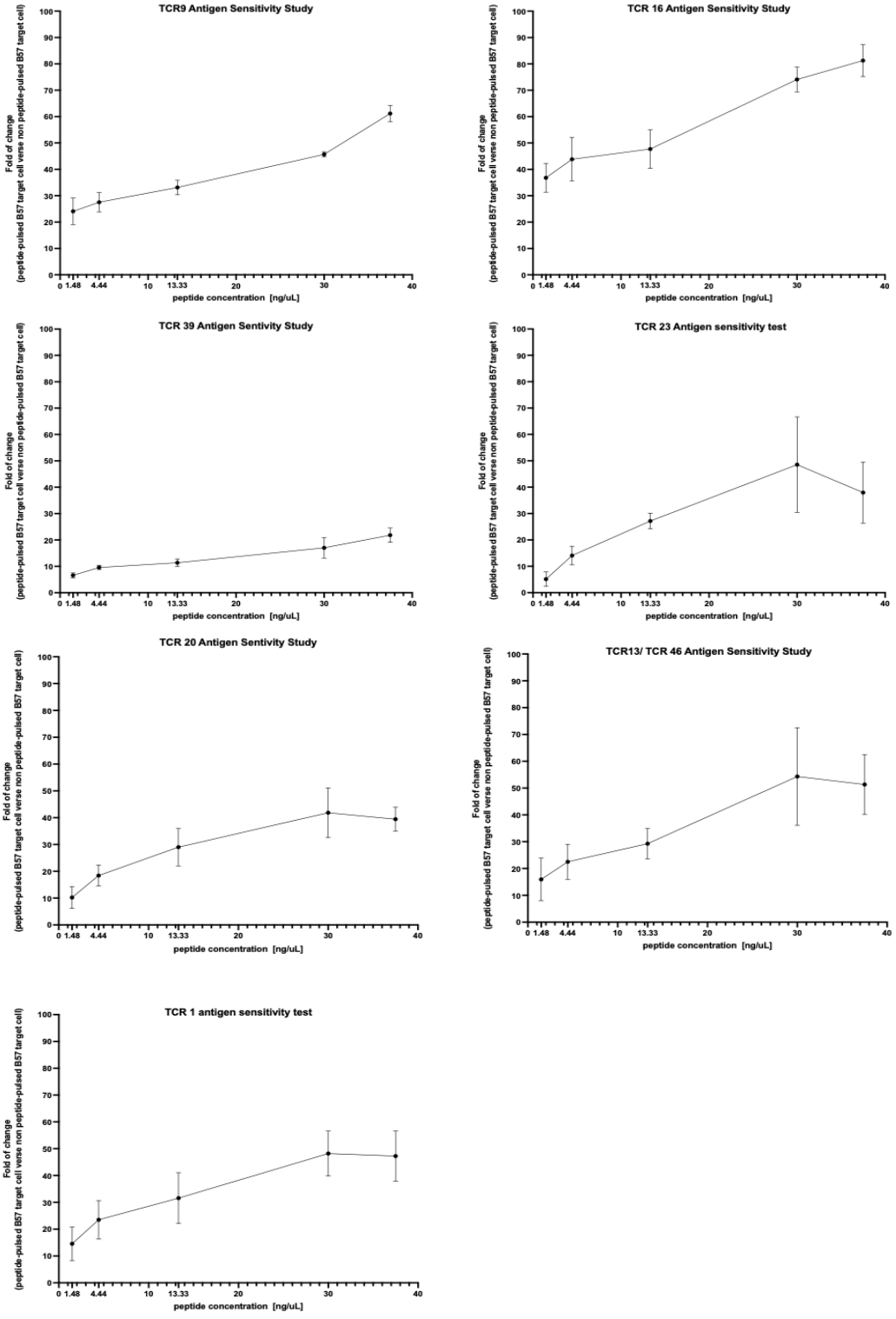

Figure 2.8. KF11 Antigen sensitivity analysis among seven identified functional TCRs in mounting HLA-B*57:01 restricted Gag KF11 response.

721.221 B*57:01 cells were peptide pulsed with five different concentrations(37.5, 30, 13.33, 4.44,1.48 ng/uL) and co-cultured with transfected jurkat cells. The fold of change for each concentrations were based on the difference in signal between peptide-pulsed target verses non

peptide-pulsed target cells. TCR 16 sample showed highest signal in all peptide pulsing concentrations indicating most sensitive to KF11 antigen. All seven samples showed dose dependent signal from 30 to 1.48 ng/uL. Four samples (TCR 1, 20, 23 and 13/46) showed decreased signal in 37.5 ng/uL compared to 30 ng/uL due to cell death caused by high DMSO concentration in peptides. Fold of change in signal were presented as mean from 3 biological replicates and error bars were standard error mean (SEM).

2.3.7. Alanine scanning reveals differential abilities of TCR to recognize KF11 variants

The phenomenon of TCR binding degeneracy allows a single TCR to bind to different peptides presented by the same MHC/HLA complex. While recognition of diverse peptides can be facilitated by the structural flexibility of a TCR's CDR motifs, recognition of single amino acid variants is often due to a TCR's ability to bind strongly to selected residues within the peptides (Sewell, 2012). In the context of B*57-KF11, prior studies suggest that TCR recognition is often focused on position 6 of the peptide, which is a charged glutamic acid (E) in consensus HIV sequences (Stewart-Jones et al., 2005). Given this, we wanted to identify positions in KF11 that have the greatest impact on antigen recognition by the seven highly functional TCR clones described here.

To study the interaction between peptide binding to HLA-B*57 and TCR, we synthesized KF11 peptide variants that substituted each non-alanine position with alanine (A). This resulted in 10 variant peptides, since KF11 already encodes A at position 2. All seven functional TCR clones were tested against 721.221-B*57:01 target cells pulsed with each variant peptide using our jurkat reporter cell assay. The luminescence signal mediated by each variant peptide was normalized to signal mediated by wild-type (WT) KF11 tested in parallel and reported as a relative value. In previous experiments shown in Figure 2.8, TCR 16 exhibited the highest sensitivity to KF11 antigen at a concentration of 30 ng/uL, which resulted in a signal exceeding 80-fold in our reporter assay. By contrast, the other six TCR clones induced changes ranging from 15 to 55-fold. To ensure the accuracy of the alanine screening experiment for TCR 16 and rule out any potential differences in antigen sensitivity, these experiments for TCR 16 were conducted at a lower peptide concentration (13.33 ng/uL) that resulted in a fold change of ~46, which more closely resembled the fold change observed for other TCR at 30 ng/uL.

We observed that alanine substitutions at KF11 positions 3, 5, 6, and 11 disrupted signaling by all TCR clones substantially, often to below 20% of WT KF11

activity (Figure 2.9 A and B). Alanine substitution at position 9 significantly decreased signaling for most clones compared, while the effect of other substitutions was more variable among TCR clones. For example, alanine substitution at position 4 resulted in a decrease of approximately 30 to 40% in signaling for TCR 13/46 and TCR 20, while there was little to no impact on the other five TCR clones (Figure 2.9 A). Alanine substitution at position 7 showed little impact on TCR 13/46, but led to a moderate (40 to 50%) decrease in signal for TCR 16, TCR 9, and TCR 1, and even greater impairment of signal for TCR 20, TCR 23, and TCR 39 (Figure 2.9 B). Alanine substitution at position 8 resulted in TCR 16, TCR 9, TCR 1, TCR 39, and TCR 20 showing a decrease of approximately 20 to 60% in signal, whereas TCR13/46 and TCR23 showed increased signals compared to WT (Figure 2.9 B). Alanine substitution at position 10 led to TCR 16, TCR 9, and TCR 1 experiencing a slight decrease in signal (approximately 10 to 30%), and TCR 39 showed a ~65% decrease compared to wildtype (Figure 2.9 B). Finally, TCR 13/46 and TCR 23 demonstrated a much better ability to recognize the alanine mutant at position 10 compared to WT.

2.3.8. Assessing the impact of alanine mutants on HLA-B*57 binding

Since our TCR reporter assay relies on target cells presenting peptide on HLA, a loss or reduction of signaling might have been due to poor binding of KF11 alanine variants to HLA- B*57:01. To assess the possible impact of alanine substitutions on B*57 binding interactions, we applied a bioinformatics algorithm (NetMHCpan v. 4.1 http://services.healthtech.dtu.dk/services/NetMHCpan-4.1/) to predict peptide binding to HLA (Figure 2.9C). Using this approach, the binding affinity of KF11 alanine variants for HLA-B*57:01 was calculated and compared to WT peptide. Strong peptide binding was identified based on a %Rank score below 0.5; weak binding as %Rank below 2 (see Appendix Table A3). According to NetMHCpan-4.1, all KF11 alanine variants are expected to bind strongly to B*57:01, except variants at position 1 (weak) and 11 (predicted non-binder). Based on this result, we conclude that loss of TCR signaling for the KF11 alanine variant at position 11 is likely due to disruption of peptide binding to B*57, but mutations at other positions 3 to 10 are unlikely to have a large impact on peptide presentation that could affect TCR signaling.

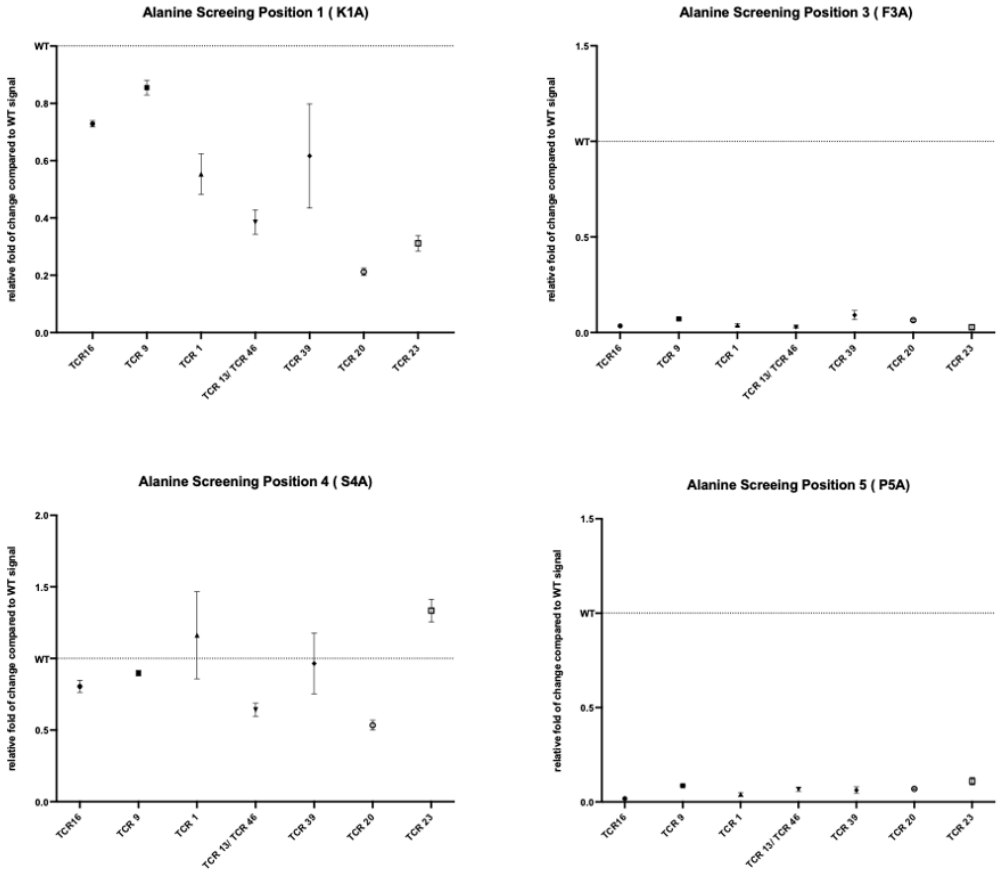
Alanine Screeing Position 1 (K1A)
Alanine Screening Position 3 (F3A)
Alanine Screening Position 4 (S4A)
Alanine Screeing Position 5 (P5A)
relative fold of change compared to WT signal
WT
TCR16
TCR 9
TCR 1
TCR 13/ TCR 46
TCR 39
TCR 20
TCR 23

A

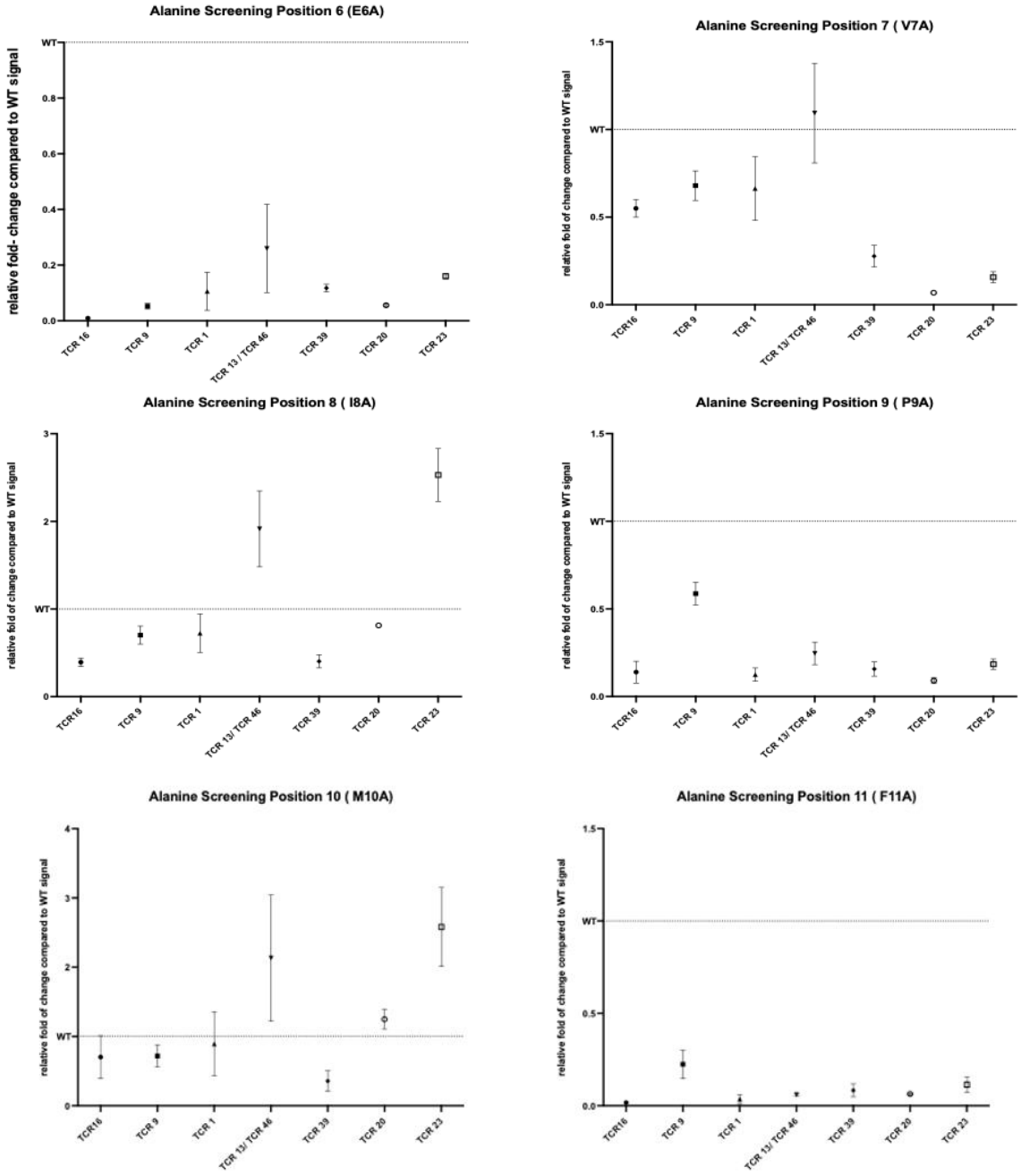
Alanine Screening Position 6 (E6A)
relative fold- change compared to WT signal
WT
0.0
0.2
0.4
0.6
0.8
TCR 16
TCR 9
TCR 1
TCR 13 / TCR 46
TCR 39
TCR 20
TCR 23
Alanine Screening Position 7 (V7A)
relative fold of change compared to WT signal
1.5
WT
0.5
0.0
TCR16
TCR 9
TCR 1
TCR 13/ TCR 46
TCR 39
TCR 20
TCR 23
Alanine Screening Position 8 (I8A)
relative fold of change compared to WT signal
3
2
WT
0
TCR16
TCR 9
TCR 1
TCR 13/ TCR 46
TCR 39
TCR 20
TCR 23
Alanine Screening Position 9 (P9A)
relative fold of change compared to WT signal
1.5
WT
0.5
0.0
TCR16
TCR 9
TCR 1
TCR 13/ TCR 46
TCR 39
TCR 20
TCR 23
Alanine Screening Position 10 (M10A)
relative fold of change compared to WT signal
4
3
2
WT
0
TCR16
TCR 9
TCR 1
TCR 13/ TCR 46
TCR 39
TCR 20
TCR 23
Alanine Screening Position 11 (F11A)
relative fold of change compared to WT signal
1.5
WT
0.5
0.0
TCR16
TCR 9
TCR 1
TCR 13/ TCR 46
TCR 39
TCR 20
TCR 23

B

KF11 and HLA-B57 binding level predictions	
KAFSPEVIPMF	SB
AAFSPEVIPMF	WB
KAASPEVIPMF	SB
KAFAPEVIPMF	SB
KAFSAEVIPMF	SB
KAFSPAVIPMF	SB
KAFSPEAIPMF	SB
KAFSPEVAPMF	SB
KAFSPEVIAMF	SB
KAFSPEVIPAF	SB
KAFSPEVIPMA	Non-binding

C

Figure 2.9. Recognition of KF11 Alanine variants of seven B*57-Gag KF11 functional TCRs

Each panel represented seven different TCRs in recognizing single alanine substitution at specific position. Briefly, each TCR was co-cultured with peptide (alanine variant) pulsed 721.221 B*57:01 target cells resulting TCR signaling measured by luminescence. Then, TCR signaling generated by alanine variants was standardized with its own WT signal reported as relative fold of change compared to WT. If the value was less than one indicating alanine substitution at specific location impacted peptide-HLA binding or TCR recognition. Each alanine mutant was tested with seven different TCR samples in biological replicates and error bars were represented as standard error mean (SEM).

(A) and (B) Recognition of KF11 alanine substitutions at position 1 to 11 of seven B*57 Gag KF11 functional TCRs. (C) NetMHCpan prediction of peptide binding between KF11 alanine variants with HLA-B*57:01. Predicting method was mentioned at Appendix Table A3. SB indicated strong binding, and WB indicated weak binding. Alanine substitutions at position 1 and 11 showed as weak or no binding to HLA- B*57:01. Therefore, indicating poor signaling of seven TCRs at alanine substitutions 1 and 11 were impaired by peptide-MHC interactions. All TCR signaling were diminished at position 3,5,6 and 9 suggesting these positions were crucial during TCR recognition. Alanine substitution at position 4, TCR 13/46 and TCR 20 showed decreased in signaling whereas other TCRs remained little to no impact. Alanine substitution at position 7 showed TCR13/46 had no impact whereas other TCR samples showed decreased signaling. TCR13/TCR46 and TCR 23 had advantage in recognizing alanine variants at position 7 and 10 whereas other TCRs showed decreased signaling.

2.3.9. Structural determinants of KF11-B*57 recognition: comparing the AGA crystal structure to a model of TCR 13/46

Even if KF11 alanine mutations are not predicted to affect binding to HLA-B*57 directly, they are likely to impact the structure of the B*57-bound peptide in other ways. In a previous report describing a crystal structure of the AGA TCR clone bound to B*57:03-KF11 (pdb: 2YPK), Stewart-Jones et al. demonstrated that the proline residues at positions 5 and 9 stabilize the central bulge structure that is present in the HLA-bound KF11 structure (Stewart-Jones et al., 2005). Therefore, it is possible that alanine substitutions at these positions could disrupt this central bulge structure and shift the

KF11 structure without disrupting peptide binding to B*57. In addition, Stewart-Jones et al. observed that isoleucine at position 8 interacted with the side chain of the HLA-B*57 complex, suggesting that alanine at this site might hinder the binding or orientation of KF11 in the HLA peptide binding groove (Stewart-Jones et al., 2005). Perhaps most notably, KF11 positions 6 (E) and 7 (V) are situated at the apex of the bulge, and they were shown to be particularly important points of contact for the AGA TCR clone (Stewart-Jones et al., 2005).

Additional studies are needed to examine the impact of alanine mutations on the B*57- bound KF11 structure to fully assess the mechanisms of reduced TCR function that we observed. Nevertheless, we wanted to begin this process by comparing one highly functional TCR clone to existing structural data. In our alanine screening experiments, we observed a range of TCR recognition for KF11 alanine mutants at various positions. To begin to investigate how variation in a TCR sequence and structure can affect recognition of KF11 variants, we focused on peptide positions 6 and 7 that are expected to have close contact with TCR. We used the published AGA TCR structure to guide our analysis of one highly functional TCR clone 13/46, which was modeled in silico using the bioinformatics tool TCRmodel (https://tcrmodel.ibbr.umd.edu).

Stewart-Jones et al. previously reported a crystal structure for AGA TCR in complex with B*57:03-KF11, however our study looked at the interaction between TCR clones KF11 bound to B*57:01. HLA-B*57:01 and B*57:03 differ by two amino acids, positions 114 and 116 that are located at the C-terminus of the peptide binding pocket. As a result, these differences are unlikely to influence the TCR interaction with KF11 at the central bulge. In the crystal structure of AGA, KF11 position 6 (E) interacts with Y31 and Y33 located in the CDR1α loop, as well as with S92, G93, G94, Y95, and Q96 located in the CDR3α loop (Figure 2.10 B1). Additionally, AGA TCR clone used S96 and Y97 in the CDR3β loop to contact KF11 position 7 (Stewart-Jones et al., 2005, Figure 2.10 C1). In summary, the AGA TCR clone interacts with KF11 position 6 using several features of its α chain, and interacts with position 7 using its β chain CDR3 (Figure 2.10 B3 and C3).

Based on our alanine screening results, the TCR 13/46 exhibited the highest ability to recognize the KF11 alanine mutant at position 7 (Figure 2.9 B). Moreover, both the AGA TCR and the TCR 13/46 shared the TRAV5 gene along with very similar

CDR3α sequences, although they possessed distinct TRBV genes (Figure 2.10 A1). Thus, given their shared genetic features in the TRAV gene, we anticipated that TCR 13/46 would interact with KF11 position 6 in a manner similar to AGA (Figure 2.10 A2). Since AGA and TCR 13/46 did not shared the similar genetic features in the TRBV genes (Figure 2.10 A3), where KF11 position 7 exhibited the highest level of interaction, we anticipated that they would have distinct TCR contact sites. To explore this, we employed an in silico TCR modeling tool (TCRmodel) to generate model structures of TCR 13/46 in complex with HLA-B*57-KF11. The modeling tool produced five options, from which we selected the model that displayed the highest confidence score (provided by AlphaFold-multimer based on overall topology measures). Subsequently, we visualized the top predicted model using Chimera, and employed its feature for detecting contacts and clashes to identify interacting residues. This enabled us to predict TCR contact sites at KF11 positions 6 and 7 for TCR clone 13/46. We observed that TCR13/46 is predicted to contact KF11 position 6 using residues Y33 in CDR1α; S92 and Y95 in CDR3α; as well as G98 and Y99 in CDRβ (Figure 2.10 B2). In addition, TCR13/46 is predicted to contact position 7 using residue T94 in CDR3β (Figure 2.10 C2). Compared to the AGA structure, both TCR clones were seen to rely on Y33, S92, and Y95 in CDRα to bind KF11 residue 6, suggesting that these polar residues are important to engage the charged residue in this peptide (Figure 2.10 B3). However, AGA and TCR13/46 encode different TRBV genes, so it was expected that they might engage with KF11 residue 7 differently. This was indeed the case, though both TCR clones appear to rely solely on their CDR3β motifs for this interaction.

In our analysis of the AGA crystal structure and TCR13/46 model, we observed that both TCR clones primarily engaged KF11 position 6 through their CDRα chain (Figure 2.10 B3), with minimal involvement of the CDRβ chain. Furthermore, it is notable that all of the highly functional B*57-KF11 restricted TCR clones identified by our studies shared the TRAV5 gene and exhibited very similar CDR3α sequences. We anticipated these TCRs use a similar mechanism to bind to KF11 position 6, which is also consistent with the poor activity of all clones for the position 6 alanine variant peptide. When focusing on KF11 position 7, we observed that both AGA and TCR13/46 interacted with this site primarily through their CDRβ chain (Figure 2.10 C3), although they employed different amino acid residues in their CDR3β motifs for this interaction. We found greater sequence variability in the CDR3β motif among our seven highly functional TCR clones,

as well as greater functional variability in their capacity to recognize the position 7 alanine variant. Together, this suggests that different TCR beta chains display distinct mechanisms of engaging KF11 position 7.

	TRAV gene	TRBV gene	CDR3 alpha	CDR3 beta
AGA1	TRAV5	TRBV19	CAVSGGYQKVTF	CASTGSYGYTF
TCR13/TCR46	TRAV5	TRBV6-1	CAESGGYQKVTF	CASTGGTYGYTF

(A1)

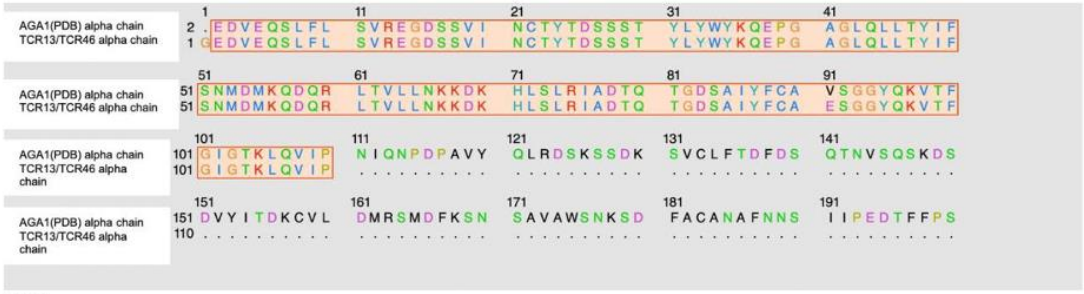

(A2)

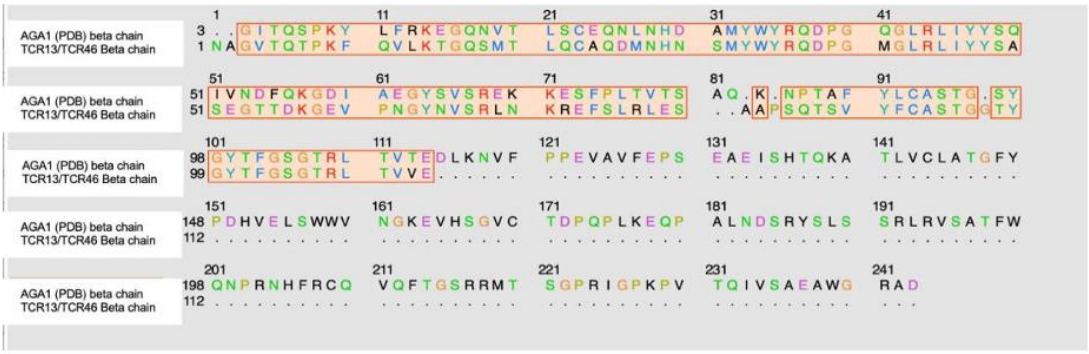

(A3)

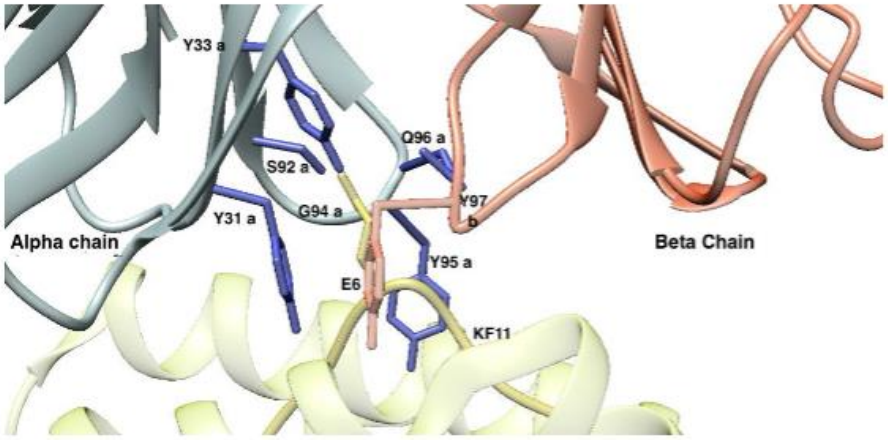

AGA

(B1)

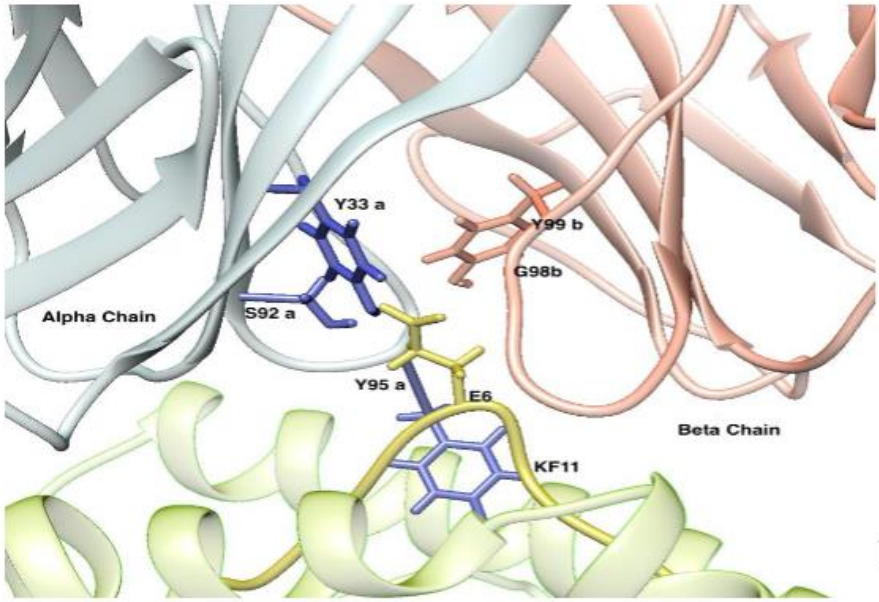

TCR13/TCR46

(B2)

KF11 E6 contacting site							
AGA	Y31 Alpha	Y33 Alpha	S92 Alpha	G94 Alpha	Y95 Alpha	Q96 Alpha	Y97 Beta
TCR 13/ TCR 46		Y33 Alpha	S92 Alpha		Y95 Alpha	G98 Beta	Y99 Beta

(B3)

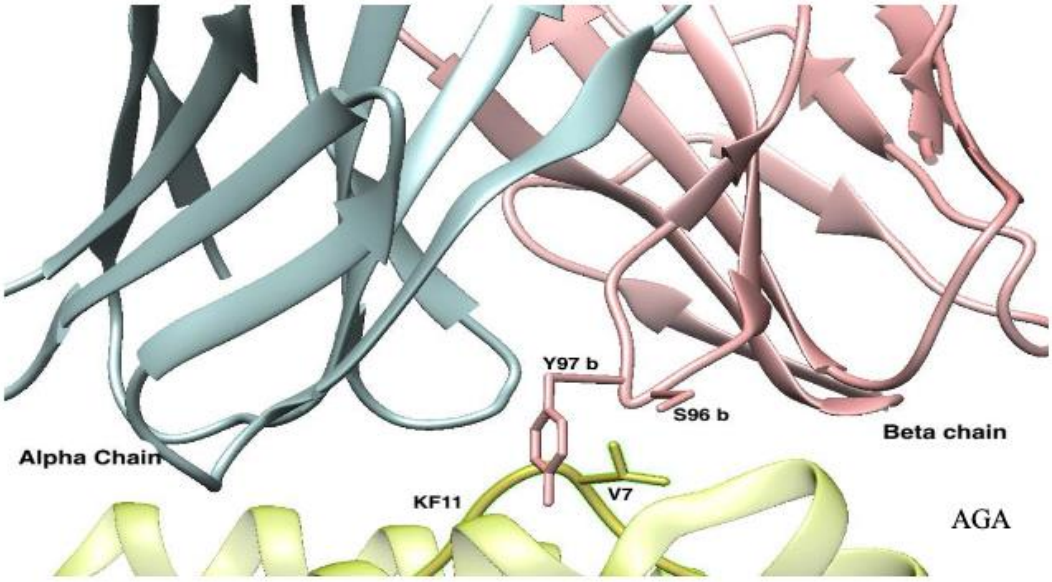

(C1)

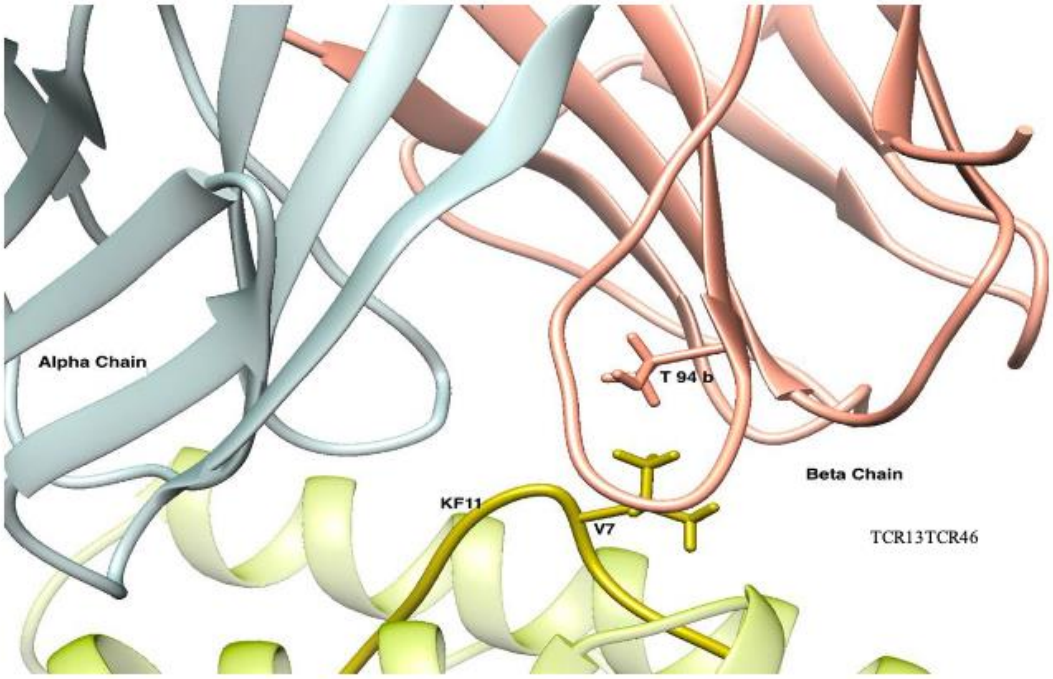

(C2)

KF11 V7 contacting site		
AGA	S96 beta	Y 97 beta
TCR13/TCR46	T 92 beta	

(C3)

Figure 2.10. Structural Analysis of AGA and TCR13/TCR46 interacting with KF11 position 6 and 7

(A1) Genetic feature of AGA and TCR 13/TCR 46: AGA and TCR 13/TCR 46 shared TRAV5 gene with one amino acid difference in CDR3 region. AGA had TRBV19 and TCR13/TCR46 had TRBV6-1 genes with several amino acid difference in CDR3 region. (A2) AGA and TCR13/TCR46 alpha chain alignment: AGA and TCR13/TCR46 alpha chain were aligned utilizing chimera structural comparison tool. AGA and TCR13/TCR46 alpha chain were highly similar with one amino acid difference in CDR3 region. The dot represented gap in sequence. (A3) AGA and TCR13/TCR46 beta chain alignment: AGA and TCR13/TCR46 beta chain were aligned utilizing chimera structural comparison tool. AGA and TCR13/TCR46 beta chain had distinct genetic feature.

(B1) Direct interaction between AGA with KF11 at position 6: AGA made direct contact with E6 of KF11 utilizing Y31a, Y33a, S92a, G94a,Y95a,Q96a and Y97b. A indicated alpha chain, B indicated beta chain. Besides Y31a and Y33a, all other contacted residues located either in CDR3or CDR3regions. (B2) Direct interaction between TCR13/TCR46 with KF11 at position 6: TCR13/TCR46 made direct contact with E^6 of KF11 utilizing Y33a, S92a, Y95a, G98b and Y99b. S92a, Y95a, G98b and Y99b located in CDR3or CDR3regions. Direct interaction were based on the E^6 with van der Waals overlap greater than or equal to -0.6 angstroms. The negative cutoff angstroms can used to identify favorable contacts. Teal color represented alpha chain, orange color represented beta chain. Dark yellow color represented KF11 peptide.(B3) Summary chart of AGA and TCR13/TCR46 direct interaction with KF11 at position 6: Both TCR contacted E^6 with Y33a, S92a,and Y95a.

(C1) Direct interaction between AGA with KF11 at position 7: AGA made direct contact with V7 of KF11 utilizing S96b and Y97 b. Both S96b and Y97 b located in CDR3region. (C2) Direct interaction between TCR13/TCR46 with KF11 at position 7: TCR13/TCR46 made direct contact with V^7 of KF11 utilizing T94b located at CDR3region. B indicated beta chain. Direct interaction were based on the V^7 with van der Waals overlap greater than or equal to -0.6 angstroms. The negative cutoff angstroms can used to identify favorable contacts. Teal color represented alpha chain, orange or pink color represented beta chain. Dark yellow color represented KF11 peptide.(B3) Summary chart of AGA and TCR13/TCR46 direct interaction with KF11 at position 7: Both TCRs contacted V^7 with different amino acids however all of them located at CDR3region.

2.4. Summary and Discussion

In this study, we assessed the function of 67 putative KF11 restricted TCR clones using TCR reporter assay. We successfully identified seven TCR clones that appeared to be highly functional in generating B*57-KF11 T cell responses. Interestingly, these seven TCR displayed similar sequences that featured highly biased V alpha gene usage, namely TRAV5 (for all clones) and either TRBV6-1 (5 out of 7) or TRBV19 (2 out of 7). A further comparison of these TCR revealed extensive genetic similarity among CDR3α motifs, but more diversity among CDR3β motifs. Together, these results suggest that TCR clones encoding TRAV5 are highly functional and may be selected preferentially during a B*57-KF11-driven immune response.

Consistent with our findings, a previous study by Gillespie et al. noted a genetic preference for TRAV5 and TRBV19 in the B*57:01-KF11 response from three HIV-infected participants (Gillespie et al., 2006). CD8 T cell clones isolated from these individuals encoded TRAV5 and closely related CDR3α gene sequences that differed by only one amino acid: CALSGGYQKVTF, CAVSGGYQKVTF, and CAGSGGYQKVTF. Additionally, all three clones encoded TRBV19 and shared similar CDR3β sequences that differed by a single residue: CASTGSYGYTF and CASTGVSYGYTF. Intriguingly, two highly functional clones identified in our study (TCR 39 and TCR 23) shared TRAV5 and TRBV19 genes. Moreover, their CDR3α sequences (CAVSGGYQKVTF and CAGSGGYQKVTF) were identical to two clones from the Gillespie et al report. This observation indicated the genetic features of TCR encoding TRAV5 are important for B*57-KF11 responses. Notably, the functional TCRs identified in our study exhibited distinct CDR3β sequences compared to the clones reported by Gillespie et al., suggesting that beta chain sequences are not as tightly restricted and thus may contribute more to functional variability within the TCR repertoire.

One aspect of KF11 that might contribute to selection of a highly restricted TCR response is its bulged structure in the context of B*57. HLA class I molecules typically present peptides that span a length of 8 to 10 amino acids, where amino acids located at peptide positions 2 and the C-terminus serve as binding sites anchoring the peptide to the HLA complex (van de Sandt et al., 2019). This results in a flat peptide orientation within the HLA binding surface. Longer peptides, including those 11 amino acids or longer, can also interact with HLA class I, but in such cases the central residues of the peptide tend to protrude outward from the HLA binding surface while contact with the anchor residues is maintained (van de Sandt et al., 2019; Josephs et al., 2017; Chan et al., 2018). The altered conformation of longer peptides, characterized by their bulging structure, presents difficulties for TCR recognition. Indeed, the widely accepted consensus is that the CDR3 regions primarily interact with peptide, whereas the CDR1 and CDR2 regions engage with the HLA complex (La Gruta et al., 2018; Feng et al., 2007; Rossjohn et al., 2015). But, prior studies have demonstrated that TCR recognition of an EBV-derived “super-bulged” peptide adopted an atypical structure that was dominated by multiple peptide interactions with non-CDR3 residues (Tynan et al., 2005; Tynan et al., 2007). Related to this question, we investigated how alanine mutations at KF11 positions 6 and 7 (located in the bulge) affected the ability of TCR to recognize

B*57-KF11. We found that all seven functional TCR required the consensus glutamic acid (E) at position 6. Conversely, we observed variable recognition of the position 7 alanine mutant by these TCR clones. In their study, Stewart-Jones et al. reported that the AGA TCR clone's interaction with the KF11 peptide was centered around positions 6 and 7 (Stewart-Jones et al., 2005). They provided further insights, indicating that glutamic acid (E) at position 6 established multiple contacts with the TCR alpha chain, including an atypical interaction with the CDR1α loop (facilitated by Y31α) as well as the CDR3α. Upon examining the crystal structure of AGA and a model for TCR 13/46, it became evident that both TCR clones primarily interact with KF11 position 6 through their CDR3α loops, utilizing similar amino acids. This leads us to anticipate that all seven functional TCR clones have a similar mode of interaction with glutamic acid (E) at position 6 peptide, which could explain why all TCR clones lost their ability to recognize alanine mutants at this position.

By contrast, valine (V) at position 7 of KF11 is engaged primarily by a more conventional interaction with the CDR3β in both the AGA structure and the TCR 13/46 model, though distinct amino acids within the CDR3 were identified as points of contact. This finding suggests that sequence diversity within the TCR beta chain contributes to the variability in recognition observed for the KF11 alanine mutant at position 7. It should be noted that disparities between AGA and TCR 13/46 may be attributed to limitations inherent in TCR modeling. To confirm and further explore the interactions between TCR 13/46 and B*57-KF11, a crystal structure will be needed.

The sensitivity of TCR for antigen may play a role in triggering responses that ultimately lead to enhanced T cell function. Prior studies have linked CD8 T cell responses with higher antigen sensitivity to more effective control of HIV infection (Almeida et al., 2009), and others have demonstrated that HIV elite controllers can elicit potent T cell responses even at lower antigen concentrations (Mothe et al., 2012). In our investigation, we found that antigen sensitivity for KF11 varied among the seven TCR, with TCR 16 exhibiting the highest signaling activity at all concentrations of peptide tested. This suggests that TCR 16 may be more effective in vivo and could serve as a target for future therapeutic studies. A limitation in our assessment of antigen sensitivity among TCRs was the absence of quantitative measurements. Our evaluation of TCR antigen sensitivity relied on NFAT signaling responses to varying antigen dosages in a

reporter assay. However, a more precise and quantitative approach would involve determining dissociation constants (Kd) for each of the TCRs.

In summary, this study identified and examined seven highly functional B*57-KF11 specific TCR clones. Assessments of TCR antigen sensitivity and recognition of KF11 alanine variants highlighted features of these TCR, including TRAV5 gene usage, that may contribute to their function. A better understanding of antiviral T cell responses against the immune-dominant KF11 epitope can help efforts to advance new HIV therapies and to develop an effective HIV vaccine.

2.5. References

Anmole, G., Kuang, X. T., Toyoda, M., Martin, E., Shahid, A., Le, A. Q., Markle, T., Baraki, B., Jones, R. B., Ostrowski, M. A., Ueno, T., Brumme, Z. L., & Brockman, M. A. (2015). A robust and scalable TCR-based reporter cell assay to measure HIV-1 Nef-mediated T cell immune evasion. *Journal of immunological methods*, 426, 104–113. https://doi.org/10.1016/j.jim.2015.08.010

Almeida, J. R., Sauce, D., Price, D. A., Papagno, L., Shin, S. Y., Moris, A., Larsen, M., Pancino, G., Douek, D. C., Autran, B., Sáez-Cirión, A., & Appay, V. (2009). Antigen sensitivity is a major determinant of CD8+ T-cell polyfunctionality and HIV-suppressive activity. *Blood*, 113(25), 6351–6360. https://doi.org/10.1182/blood-2009-02-206557

Altfeld, M., Addo, M. M., Rosenberg, E. S., Hecht, F. M., Lee, P. K., Vogel, M., Yu, X. G.,Draenert, R., Johnston, M. N., Strick, D., Allen, T. M., Feeney, M. E., Kahn, J. O., Sekaly, R. P., Levy, J. A., Rockstroh, J. K., Goulder, P. J., & Walker, B. D. (2003). Influence of HLA-B*57 on clinical presentation and viral control during acute HIV-1 infection. *AIDS* (London,England), 17(18), 2581–2591. https://doi.org/10.1097/00002030-200312050-00005

Bansal, A., Gehre, M. N., Qin, K., Sterrett, S., Ali, A., Dang, Y., Abraham, S., Costanzo, M. C., Venegas, L. A., Tang, J., Manjunath, N., Brockman, M. A., Yang, O. O., Kan-Mitchell, J., & Goepfert, P. A. (2021). HLA-E-restricted HIV-1-specific CD8+ T cell responses in natural infection. *The Journal of clinical investigation*, 131(16), e148979. https://doi.org/10.1172/JCI148979

Borrell, M., Fernández, I., Etcheverrry, F., Ugarte, A., Plana, M., Leal, L., & García, F. (2021). High rates of long-term progression in HIV-1-positive elite controllers. *Journal of the International AIDS Society*, 24(2), e25675. https://doi.org/10.1002/jia2.25675

Chan, K. F., Gully, B. S., Gras, S., Beringer, D. X., Kjer-Nielsen, L., Cebon, J., McCluskey, J., Chen, W., & Rossjohn, J. (2018). Divergent T-cell receptor recognition modes of a HLA-I restricted extended tumour-associated peptide. *Nature communications*, 9(1), 1026. https://doi.org/10.1038/s41467-018-03321-w

Dalgleish, A. G., Wilson, S., Gompels, M., Ludlam, C., Gazzard, B., Coates, A. M., & Habeshaw, J. (1992). T-cell receptor variable gene products and early HIV-1 infection. *Lancet* (London, England), 339(8797), 824–828. https://doi.org/10.1016/0140-6736(92)90277-a

Dash, P., Fiore-Gartland, A. J., Hertz, T., Wang, G. C., Sharma, S., Souquette, A., Crawford, J. C., Clemens, E. B., Nguyen, T. H. O., Kedzierska, K., La Gruta, N. L., Bradley, P., & Thomas, P.G. (2017). Quantifiable predictive features define epitope-specific T cell receptor repertoires. *Nature*, 547(7661), 89–93. https://doi.org/10.1038/nature22383

Dludla, P. V., Jack, B., Viraragavan, A., Pheiffer, C., Johnson, R., Louw, J., & Muller, C. J. F. (2018). A dose-dependent effect of dimethyl sulfoxide on lipid content, cell viability and oxidative stress in 3T3-L1 adipocytes. *Toxicology reports*, 5, 1014–1020. https://doi.org/10.1016/j.toxrep.2018.10.002

Douek, D. C., Picker, L. J., & Koup, R. A. (2003). T cell dynamics in HIV-1 infection. *Annual review of immunology*, 21, 265–304.200https://doi.org/10.1146/annurev.immunol.21.120601.141053

Feng, D., Bond, C. J., Ely, L. K., Maynard, J., & Garcia, K. C. (2007). Structural evidence for a germline-encoded T cell receptor-major histocompatibility complex interaction 'codon'. *Nature immunology*, 8(9), 975–983. https://doi.org/10.1038/ni1502

Gillespie, G. M., Stewart-Jones, G., Rengasamy, J., Beattie, T., Bwayo, J. J., Plummer, F. A., Kaul, R., McMichael, A. J., Easterbrook, P., Dong, T., Jones, E. Y., & Rowland-Jones, S. L. (2006). Strong TCR conservation and altered T cell cross-reactivity characterize a B*57- restricted immune response in HIV-1 infection. *Journal of immunology* (Baltimore, Md. : 1950), 177(6), 3893–3902. https://doi.org/10.4049/jimmunol.177.6.3893

Gorochov, G., Neumann, A. U., Kereveur, A., Parizot, C., Li, T., Katlama, C., Karmochkine, M., Raguin, G., Autran, B., & Debré, P. (1998). Perturbation of CD4+ and CD8+ T-cell repertoires during progression to AIDS and regulation of the CD4+ repertoire during antiviral therapy. *Nature medicine*, 4(2), 215–221. https://doi.org/10.1038/nm0298-215

Goulder, P. J., & Walker, B. D. (2012). HIV and HLA class I: an evolving relationship. *Immunity*, 37(3), 426–440. https://doi.org/10.1016/j.immuni.2012.09.005

Haque, A., Engel, J., Teichmann, S. A., & Lönnberg, T. (2017). A practical guide to single-cell RNA-sequencing for biomedical research and clinical applications. *Genome medicine*, 9(1), 75. https://doi.org/10.1186/s13073-017-0467-4

HIV Molecular Immunology 2022, Editors: Jennifer L. Mamrosh, Elizabeth-Sharon David-Fung, Bette T. M. Korber, Christian Brander, Dan Barouch, Rob de Boer, Barton F. Haynes, P. J. Klasse, Richard Koup, Bjoern Peters, Michael Seaman, and Bruce D. Walker. 2023. Publisher: Los Alamos National Laboratory, *Theoretical Biology and Biophysics*, Los Alamos, New Mexico. LA-UR-23-24823.

Josephs, T. M., Grant, E. J., & Gras, S. (2017). Molecular challenges imposed by MHC-I restricted long epitopes on T cell immunity. *Biological chemistry*, 398(9), 1027–1036. https://doi.org/10.1515/hsz-2016-0305

Kiepiela, P., Ngumbela, K., Thobakgale, C., Ramduth, D., Honeyborne, I., Moodley, E., Reddy, S., de Pierres, C., Mncube, Z., Mkhwanazi, N., Bishop, K., van der Stok, M., Nair, K., Khan, N., Crawford, H., Payne, R., Leslie, A., Prado, J., Prendergast, A., Frater, J., … Goulder, P. (2007).CD8+ T-cell responses to different HIV proteins have discordant associations with viral load. *Nature medicine*, 13(1), 46–53. https://doi.org/10.1038/nm1520

La Gruta, N. L., Gras, S., Daley, S. R., Thomas, P. G., & Rossjohn, J. (2018). Understanding the drivers of MHC restriction of T cell receptors. *Nature reviews. Immunology*, 18(7), 467–478. https://doi.org/10.1038/s41577-018-0007-5

Lobos, C. A., Downing, J., D'Orsogna, L. J., Chatzileontiadou, D. S. M., & Gras, S. (2022). Protective HLA-B*57: T cell and natural killer cell recognition in HIV infection. *Biochemical Society transactions*, 50(5), 1329–1339. https://doi.org/10.1042/BST20220244

Mendoza, D., Royce, C., Ruff, L. E., Ambrozak, D. R., Quigley, M. F., Dang, T., Venturi, V., Price, D. A., Douek, D. C., Migueles, S. A., & Connors, M. (2012). HLA B*5701-positive long- term nonprogressors/elite controllers are not distinguished from progressors by the clonal composition of HIV-specific CD8+ T cells. *Journal of virology*, 86(7), 4014–4018. https://doi.org/10.1128/JVI.06982-11

Monel, B., McKeon, A., Lamothe-Molina, P., Jani, P., Boucau, J., Pacheco, Y., Jones, R. B., Le Gall, S., & Walker, B. D. (2019). HIV Controllers Exhibit Effective CD8+ T Cell Recognition of HIV-1-Infected Non-activated CD4+ T Cells. *Cell reports*, 27(1), 142–153.e4. https://doi.org/10.1016/j.celrep.2019.03.016

Mothe, B., Llano, A., Ibarrondo, J., Zamarreño, J., Schiaulini, M., Miranda, C., Ruiz-Riol, M., Berger, C. T., Herrero, M. J., Palou, E., Plana, M., Rolland, M., Khatri, A., Heckerman, D., Pereyra, F., Walker, B. D., Weiner, D., Paredes, R., Clotet, B., Felber, B. K., … Brander, C. (2012). CTL responses of high functional avidity and broad variant cross-reactivity are associated with HIV control. *PloS one*, 7(1), e29717. https://doi.org/10.1371/journal.pone.0029717

Pantaleo, G., Soudeyns, H., Demarest, J. F., Vaccarezza, M., Graziosi, C., Paolucci, S., Daucher, M. B., Cohen, O. J., Denis, F., Biddison, W. E., Sekaly, R. P., & Fauci, A. S. (1997). Accumulation of human immunodeficiency virus-specific cytotoxic T lymphocytes away from the predominant site of virus replication during primary infection. *European journal of immunology*, 27(12), 3166–3173. https://doi.org/10.1002/eji.1830271213

Pantaleo, G., Demarest, J. F., Soudeyns, H., Graziosi, C., Denis, F., Adelsberger, J. W., Borrow, P., Saag, M. S., Shaw, G. M., & Sekaly, R. P. (1994). Major expansion of CD8+ T cells with a predominant V beta usage during the primary immune response to HIV. *Nature*, 370(6489), 463–467. https://doi.org/10.1038/370463a0

Petros, Z., Kishikawa, J., Makonnen, E., Yimer, G., Habtewold, A., & Aklillu, E. (2017). HLA- B*57 Allele Is Associated with Concomitant Anti-tuberculosis and Antiretroviral Drugs Induced Liver *Toxicity in Ethiopians*. *Frontiers in pharmacology*, 8, 90. https://doi.org/10.3389/fphar.2017.00090

Rossjohn, J., Gras, S., Miles, J. J., Turner, S. J., Godfrey, D. I., & McCluskey, J. (2015). T cell antigen receptor recognition of antigen-presenting molecules. *Annual review of immunology*, 33, 169–200. https://doi.org/10.1146/annurev-immunol-032414-112334

Sacha, J. B., Chung, C., Rakasz, E. G., Spencer, S. P., Jonas, A. K., Bean, A. T., Lee, W.,Burwitz, B. J., Stephany, J. J., Loffredo, J. T., Allison, D. B., Adnan, S., Hoji, A., Wilson, N. A., Friedrich, T. C., Lifson, J. D., Yang, O. O., & Watkins, D. I. (2007). Gag-specific CD8+ T lymphocytes recognize infected cells before AIDS-virus integration and viral protein expression. *Journal of immunology* (Baltimore, Md. : 1950), 178(5), 2746–2754. https://doi.org/10.4049/jimmunol.178.5.2746

Safrit, J. T., Andrews, C. A., Zhu, T., Ho, D. D., & Koup, R. A. (1994). Characterization of human immunodeficiency virus type 1-specific cytotoxic T lymphocyte clones isolated during acute seroconversion: recognition of autologous virus sequences within a conserved immunodominant epitope. *The Journal of experimental medicine*, 179(2), 463–472. https://doi.org/10.1084/jem.179.2.463

Sewell, A. Why must T cells be cross-reactive?. *Nat Rev Immunol* 12, 669–677 (2012). https://doi.org/10.1038/nri3279

Stewart-Jones, G. B., Simpson, P., van der Merwe, P. A., Easterbrook, P., McMichael, A. J., Rowland-Jones, S. L., Jones, E. Y., & Gillespie, G. M. (2012). Structural features underlying T- cell receptor sensitivity to concealed MHC class I micropolymorphisms. *Proceedings of the National Academy of Sciences of the United States of America*, 109(50), E3483–E3492. https://doi.org/10.1073/pnas.1207896109

Stewart-Jones, G. B., Gillespie, G., Overton, I. M., Kaul, R., Roche, P., McMichael, A. J., Rowland-Jones, S., & Jones, E. Y. (2005). Structures of three HIV-1 HLA-B*5703-peptide complexes and identification of related HLAs potentially associated with long-term nonprogression. *Journal of immunology* (Baltimore, Md. : 1950), 175(4), 2459–2468. https://doi.org/10.4049/jimmunol.175.4.2459

Tanno, H., Gould, T. M., McDaniel, J. R., Cao, W., Tanno, Y., Durrett, R. E., Park, D., Cate, S.J., Hildebrand, W. H., Dekker, C. L., Tian, L., Weyand, C. M., Georgiou, G., & Goronzy, J. J. (2020). Determinants governing T cell receptor α/β-chain pairing in repertoire formation of identical twins. *Proceedings of the National Academy of Sciences of the United States of America*, 117(1), 532–540. https://doi.org/10.1073/pnas.1915008117

Thakkar, N., Bailey-Kellogg, C. Balancing sensitivity and specificity in distinguishing TCR groups by CDR sequence similarity. *BMC Bioinformatics* 20, 241 (2019). https://doi.org/10.1186/s12859-019-2864-8

Tynan, F. E., Burrows, S. R., Buckle, A. M., Clements, C. S., Borg, N. A., Miles, J. J., Beddoe,T., Whisstock, J. C., Wilce, M. C., Silins, S. L., Burrows, J. M., Kjer-Nielsen, L., Kostenko, L., Purcell, A. W., McCluskey, J., & Rossjohn, J. (2005). T cell receptor recognition of a 'super- bulged' major histocompatibility complex class I-bound peptide. *Nature immunology*, 6(11), 1114–1122. https://doi.org/10.1038/ni1257

Tynan, F. E., Reid, H. H., Kjer-Nielsen, L., Miles, J. J., Wilce, M. C., Kostenko, L., Borg, N. A., Williamson, N. A., Beddoe, T., Purcell, A. W., Burrows, S. R., McCluskey, J., & Rossjohn, J. (2007). A T cell receptor flattens a bulged antigenic peptide presented by a major histocompatibility complex class I molecule. *Nature immunology*, 8(3), 268–276. https://doi.org/10.1038/ni1432

UNAIDS. (n.d.). Global HIV & AIDS statistics - fact sheet. UNAIDS. Retrieved October16, 2023, from https://www.unaids.org/en/resources/fact-sheet.

van de Sandt, C.E., Clemens, E.B., Grant, E.J. et al. Challenging immunodominance of influenza-specific CD8+ T cell responses restricted by the risk-associated HLA-A*68:01 allomorph. *Nat Commun 10*, 5579 (2019). https://doi.org/10.1038/s41467-019-13346-4.

Walker, B., & McMichael, A. (2012). The T-cell response to HIV. *Cold Spring Harbor perspectives in medicine*, 2(11), a007054. https://doi.org/10.1101/cshperspect.a007054

Yang, O. O., Kalams, S. A., Rosenzweig, M., Trocha, A., Jones, N., Koziel, M., Walker, B. D., & Johnson, R. P. (1996). Efficient lysis of human immunodeficiency virus type 1-infected cells by cytotoxic T lymphocytes. *Journal of virology*, 70(9), 5799–5806. https://doi.org/10.1128/JVI.70.9.5799-5806.1996

Yin, R., Ribeiro-Filho, H. V., Lin, V., Gowthaman, R., Cheung, M., & Pierce, B. G. (2023). TCRmodel2: high-resolution modeling of T cell receptor recognition using deep learning. *Nucleic acids research*, 51(W1), W569–W576. https://doi.org/10.1093/nar/gkad356

Yu, X. G., Lichterfeld, M., Chetty, S., Williams, K. L., Mui, S. K., Miura, T., Frahm, N., Feeney,M. E., Tang, Y., Pereyra, F., Labute, M. X., Pfafferott, K., Leslie, A., Crawford, H., Allgaier, R., Hildebrand, W., Kaslow, R., Brander, C., Allen, T. M., Rosenberg, E. S., … Walker, B. D. (2007). Mutually exclusive T-cell receptor induction and differential susceptibility to human immunodeficiency virus type 1 mutational escape associated with a two-amino-acid difference between HLA class I subtypes. *Journal of virology*, 81(4), 1619–1631. https://doi.org/10.1128/JVI.01580-06

Chapter 3.

Towards a functional assay to assess HIV-specific T cell receptors restricted by HLA-E

Contributions

The results presented in this chapter are unpublished. I use the terms “we” and “our” to reflect the contributions of other researchers and trainees to this work. My role in this study was to perform a majority of the functional assessments reported here. Dr. Anju Bansal and Dr. Paul Goeppert (Univ of Alabama-Birmingham) provided TCR sequences for this study and generated the 721.221 target cell lines. Cristina Delmaestro and Zerufael Derza assisted with data collection, preparation of peptide stocks and maintenance of cell lines. Dr. Mark Brockman and Dr. Zabrina Brumme provided me with supervision and mentorship in this study.

3.1. Introduction

HIV infection primarily targets CD4 T cells, the loss of which progressively weakens the immune system and, in the absence of combination antiretroviral therapy (cART), ultimately leads to death (Vidya Vikayan et al., 2017). Robust cytolytic CD8 T cell responses are evident in HIV controllers who spontaneously suppress HIV viremia in the absence of cART, highlighting the vital role of these cells in inhibiting infection (Collins et al., 2020). The HIV accessory protein Nef evades CD8 T cell mediated immune defenses by downregulating HLA class I molecules on the cell surface, thereby enhancing viral replication and pathogenesis (van Stigt Thans et al., 2019). Initial studies using laboratory-adapted HIV strains suggested that Nef modulated HLA-A and -B alleles, including the protective HLA-B*57 allele, but it had little impact on HLA-C or non-classical proteins like HLA-E (Swann et al., 2001). This implied that CD8 T cells restricted by HLA-C or HLA-E might have an enhanced capacity to suppress HIV infection (Swann et al., 2001). More recent studies have indicated that primary HIV isolates can downregulate HLA-C and HLA-E (van Stigt Thans et al., 2019; Apps et al., 2016), but the extent of downregulation is modest in comparison to that of HLA-A and HLA-B. Consequently, the potential use of HLA-E- restricted CD8 T cells as an

alternative strategy for eliciting cytotoxic T cell responses against HIV has gained attention.

Several SIV epitopes have been identified that are capable of triggering HLA-E specific CD8 T cell responses in non-human primates, but the HLA-E restricted T cell response to HIV appears to be highly constrained in humans. Notably, a Rhesus Cytomegalovirus (RhCMV) based SIV vaccine demonstrated ~50% effectiveness against SIV infection in Rhesus macaques, which was attributed to a remarkably high frequency of unconventional CD8 T cell responses restricted by HLA-E (Hansen et al., 2019). In follow-up studies, the researchers identified two HLA-E restricted “supertopes” located in SIV Gag (RL9: RMYNPTNIL, Gag 276– 284; and EK9: EKQRESREK, Gag 482-490) that were targeted by CD8 T cells in all vaccine- protected RM (Hansen et al., 2013). Subsequently, Yang et al. identified HLA-E restricted T cells in vaccinated RM targeted RL9, and demonstrated that this response correlated with vaccine protection (Yang et al., 2021). Interestingly, a close homolog to SIV RL9 exists in HIV-1 Gag (RL9: RMYSPTSIL, Gag 275-283). While HIV RL9 can be presented by human HLA-E (Walters et al., 2018) and while HLA-E restricted CD8 T cells generated against RL9 de novo using blood cells from HIV-uninfected individuals can suppress HIV infection in vitro (Yang et al., 2021), HLA-E restricted RL9 responses have not been observed in people living with HIV.

The Goepfert lab (Univ of Alabama-Birmingham) has identified CD8 T cell responses in individuals living with HIV that target Gag KF11 (KAFSPEVIPMF, Gag 162-173), which may be restricted by HLA-B*57:01 and/or HLA-E*01:01 (Bansal et al., 2021). To our knowledge, this represents the first evidence that HLA-E restricted CD8 T cells can be elicited in humans during natural HIV infection, complementing studies by Yang et al. (Yang et al., 2021). Based on this dataset, I identified seven highly functional TCR clones that recognize KF11 presented by HLA-B*57:01 using an in vitro TCR reporter assay (Chapter 2). To extend this work, we wanted to establish similar methods to identify TCR clones that can recognize KF11 presented HLA-E, allowing us to study the characteristics of E-restricted, B*57-restricted and potential dual HLA- restricted CD8 T cell responses.

This chapter describes our efforts to modify the TCR reporter assay for studies of HLA- E-restricted clones. While our optimization of these assays is incomplete, we have

identified five TCR clones that may display weak recognition of HLA-E-KF11. Notably, TCR clone 16 displayed the strongest response to HLA-E-KF11, and this clone was also capable of generating a response to B*57-KF11, indicating that this TCR clone is dual-HLA restricted. Among the potential HLA-E restricted TCR clones, three alpha Variable (V) genes (TRAV5, TRAV17, and TRAV1-2), and three beta V genes (TRBV6-1, TRBV15, and TRBV12.4) were observed. Despite our efforts to amplify HLA-E-mediated signals by extending the co-culture period and inducing endogenous expression of the KF11 epitope, we did not observe a notable increase in assay sensitivity. This underscores the inherent challenge of measuring HLA-E restricted responses using our current TCR reporter assay methods, and signifies a need for further exploration and development.

3.2. Materials and Methods

3.2.1. Selection of TCR clones for this study

TCR sequences were obtained from the Goepfert lab as described in Chapter 2 (Section 2.2). For this study, we selected 42 of 67 KF11-specific TCR clones (colored in yellow) that were putatively restricted by HLA-E or B*57 (Figure 3.1) with a goal to identify clones that are able to recognize KF11 when presented by HLA-E. In the process, seven TCR clones that were highly responsive to B*57-KF11 were assessed for their ability to recognize KF11 presented by HLA-E, potentially identifying them as dual HLA-restricted.

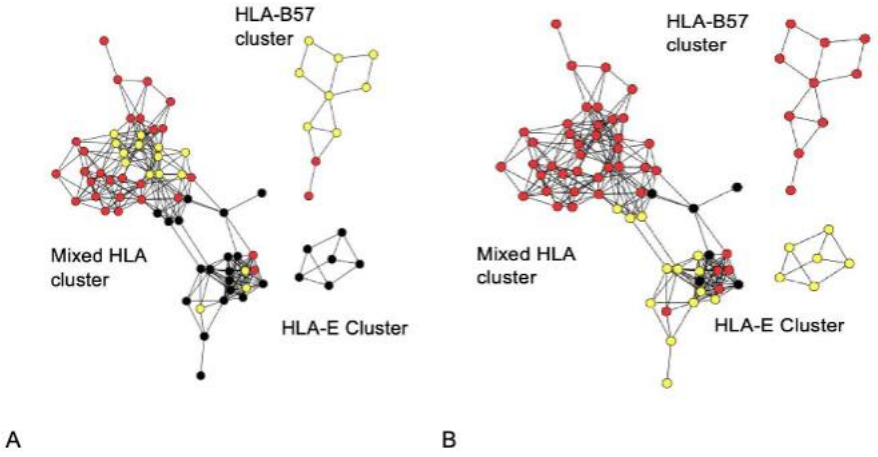

Figure 3.1. 42 selected TCR clones located on genetic clustering of HLA-E vs. B*57 restricted TCR cells against Gag KF11.

Network graphs depict the results of TCRdist analysis for 124 KF11-specific TCR clones (nodes) (displaying 299 edges, a Hamming distance threshold of 150). The putative HLA restriction of each TCR clone (HLA-E or B*57) was determined by the target cell used for KF11 stimulation during AIM assays; HLA-E restricted TCR are shown as black nodes; HLA-B*57 restricted TCR are shown as red nodes. (A) 23 putative B*57-restricted TCR (in yellow) were selected for functional analysis. A majority of these clones were located in the top subgroup of the "mixed" HLA cluster and the HLA-B*57 cluster. (B) 19 putative E-restricted TCR (in yellow) were selected for functional analysis. These clones were mainly located in the bottom subgroup of the "mixed" HLA cluster and HLA-E cluster.

3.2.2. Molecular cloning of TCR alpha and beta genes

Gene synthesis and cloning were performed as described in Chapter 2.

3.2.3. Eukaryotic cell culture

Jurkat cells and 721.221-derived cell lines were maintained as described in Chapter 2. 721.221 derived cell lines expressing HLA-E*01:01 and E*01:03 were provided by Dr. Paul Goepfert (Univ of Alabama-Birmingham).

3.2.4. Preparation of effector Jurkat T cells (Jurkat cells transfection)

Jurkat cells were transfected with TCR alpha/beta, CD8 alpha, and NFAT-luciferase plasmids by electroporation as described in Chapter 2.

3.2.5. Validation of HLA expression on 721.221 target cells

HLA expression on 721.221-43A3A2, 721.221-E*01:01, and 721.221-E*01:03 cells was confirmed by flow cytometry. Each cell line was stained with anti-human A2 antibody (allophycocyanin, APC); clone BB7.2, BioLegend) and anti-human HLA-E antibody (Phycoerythrin, PE;clone 3D12, Biolegend).

3.2.6. Preparation of 721.221 target cells (Peptide pulsing)

KF11, FK10 and RL9 peptides and cell lines were prepared as described in Chapter 2. Prior to the peptide pulsing, 721.221-E*01:01 and 721.221-E*01:03 cells were incubated at 27°C overnight to stabilize surface HLA-E expression. Target cells were pulsed with peptide at 37°C for 1 hour, unless otherwise noted in the text.

3.2.7. TCR stimulation and luciferase reporter assays

TCR-transfected jurkat effector cells and 721.221 target cells were prepared as described in Chapter 2. Cells were co-cultured for 6-8 hours, unless otherwise noted in the text. Luciferase activity was measured as described in Chapter 2.

3.3. Results

3.3.1. Molecular cloning

Genetic information for the 42 selected TCR clones were described in Chapter 2 and Appendix Table A1 and A4. Molecular cloning results were described in Chapter 2.

3.3.2. Verification of HLA expression on 721.221 target cells

721.221-derived cell lines expressing only HLA-A2 (41A3.A2), E*01:01, or E*01:03 were obtained from the Goepfert lab (Univ of Alabama-Birmingham) (Bansal et al., 2021). To confirm their HLA phenotype, each cell line was stained with anti-A2 and anti-HLA-E antibodies and then analyzed by flowcytometry. We observed that 99.6% of 721.221-41A3.A2 and cells expressed HLA-A2, compared to low background staining (<0.5%) on both HLA-E expressing lines (Figure 3.2A). After incubation at 37°C, we found that 29.4% and Mean fluorescence intensity (MFI) 61868 of E*01:01 and

97.8%(MFI:218418) of E*01:03 cells expressed HLA-E, compared to low background staining (0.44%, MFI:NA) on 41A3.A2 cells (Figure 3.2B).Observations from the Goepfert lab (unpublished correspondence) suggest that HLA-E expression is stabilized at lower temperatures. To assess this, we incubated these cell lines overnight at 27°C before staining for flow cytometry. We observed that both E cell lines displayed elevated surface HLA-E expression, with 77.9% of E*01:01 (MFI:143836) and 99.6 % of E*01:03 ($8.88*10^5$) cells demonstrating HLA-E expression (Figure 3.2C). In summary, all three cell lines were verified to express only the HLA of interest and are thus suitable for used as target cells in our TCR reporter assay.

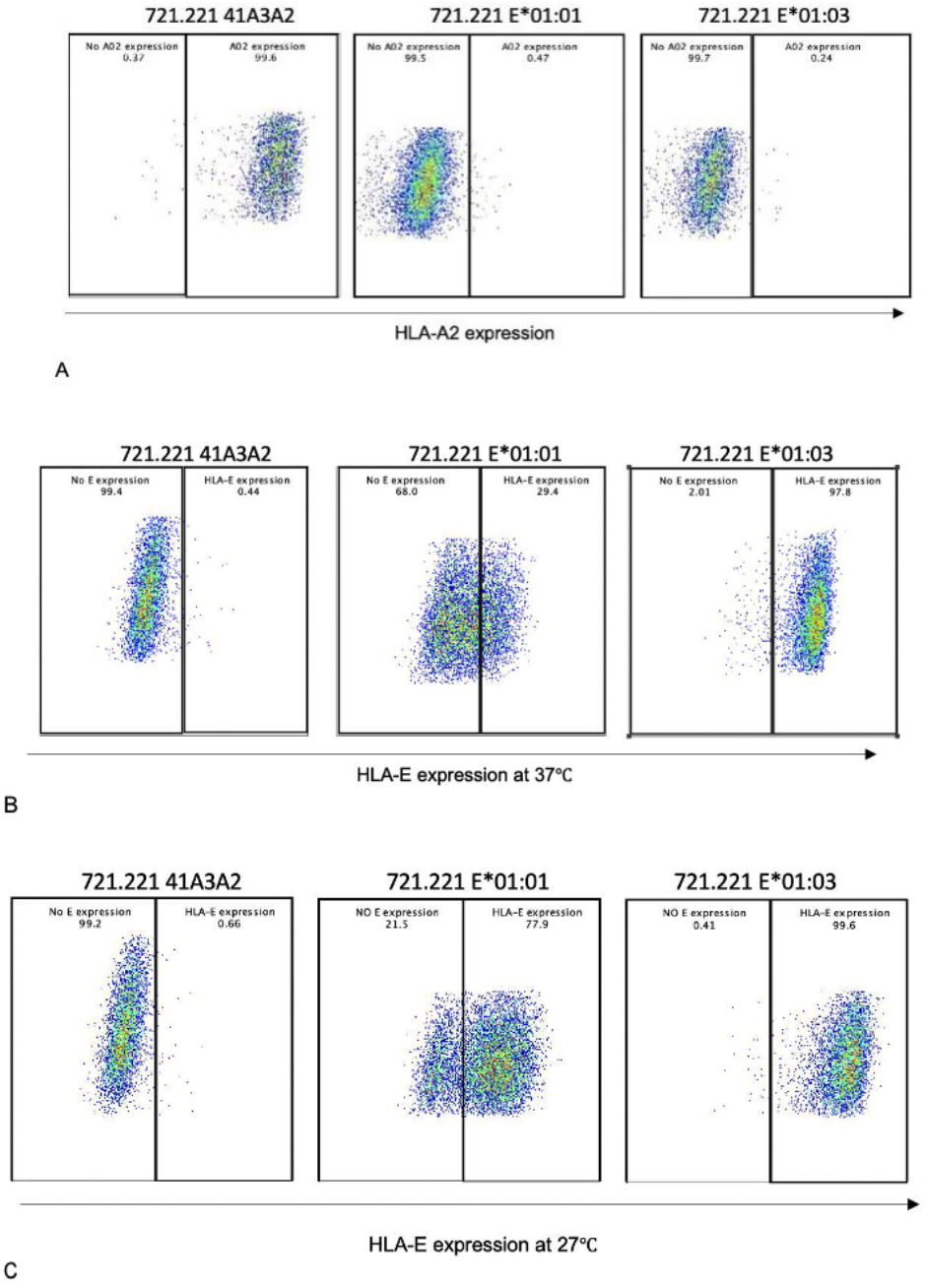

Figure 3.2. Verification of HLA expression in 721.221-derived cell lines.
(A) 721.221- 41A3.A2, E*01:01 and E*01:03 lines were stained with HLA-A2 antibody (allophycocyanin, APC; clone BB7.2, BioLegend) and examined by flow cytometry. Only 721.221-41A3.A2 cells expressed HLA-A2. (B) 721.221-41A3.A2, E*01:01 and E*01:03 cells were incubated at 37°C. All cell lines were stained with HLA-E antibody (phycoerythrin, PE; clone 3D12, Biolegend) and examined by flow cytometry. Only 721.221-E01:01 and E*01:03 cells expressed HLA-E. (C) 721.221-41A3.A2, E*01:01 and E*01:03 cells were incubated overnight at 27°C. All cell lines were stained with HLA-E antibody (phycoerythrin, PE; clone 3D12, Biolegend) and examined by flow cytometry. 721.22-E*01:01 and E*01:03 cells showed an increase in HLA-E expression compared with cells incubated at 37°C.

3.3.3. Identifying functional TCR clones restricted by HLA-E-KF11

The objective of our study was to identify functional TCR clones specific for HIV Gag KF11 that are restricted by HLA-E (either E*01:01 or E*01:03 allele). Previously, we identified seven clones that elicited strong HLA-B*57-KF11 responses. Thus, a secondary aim of this work was to assess these TCR clones for potential recognition of KF11 presented by HLA-E- expressing target cells, which would indicate that the clone displays dual-HLA restriction for KF11 on both HLA-E and B*57. As described in Chapter 2, we used the 721.221 41A3.A2 cell line, which expresses only HLA-A2, as a negative control since any TCR signal resulting from co-culture with this HLA-mismatched cell line is expected to be non-specific. The 5B2 TCR clone (which responds to Gag FK10 presented on HLA-A2) served as a positive control.

Initial screening of selected TCR clones using our standard reporter assay revealed that most clones produced only a weak luminescence signal following co-culture with HLA-E*01:01 and E*01:03 cells pulsed with KF11 that was similar to the background, non-specific signal seen with HLA-A2 expressing target cells (see Appendix Table A4). We evaluated TCR responses for HLA- E-KF11 using the same criteria as outlined in Chapter 2; namely for a clone to be considered functional, it should consistently induce at least a 1.5-fold change in luminescence signal with the appropriate peptide-pulsed target cells compared to non-pulsed target cells as well as non- specific (HLA-A2-expressing) target cells.

While most TCR clones appeared to be non-reactive for HLA-E-KF11 by this criteria, in our initial reporter assays, we observed five clones (TCR 1, 4, 14, 16 and 42) that generated weak KF11 responses with E*01:01 target cells (range: 1.7-fold to 4.5-fold above background). In addition, three clones (TCR 8,16 and17) displayed weak KF11 responses with E*01:03 target cells. Only TCR 16 was able to generate a response on both E*01:01 targets (4.5-fold induction) and E*01:03 targets (2.7-fold induction) in these experiments (Appendix Table A4). Overall, these HLA-E dependent signals appeared to be weaker compared to those observed previously for B*57-KF11 specific clones, which consistently ranged from 15-fold to 55-fold above background (Appendix Table A2).

In a second independent assay, seven TCR clones (TCR 9, 13, 14, 16, 17, 19, and 34) generated weak KF11 responses with E*01:01 expressing target cells (range: 1.8-fold to 3.0- fold above background). In addition, 11 of TCR clones (TCR 3, 9, 13, 14, 15, 16, 17, 18, 19, 34 and 42) generated weak to moderate KF11 responses with E*01:03 targets (range: 1.5-fold to 19.5-fold above background). Of these, the response by TCR 16 on E*01:03 target cells was most striking, at ~19.5-fold above background. Notably, TCR clones 9, 14, 16, 19 and 34 responded to KF11 presented by both E*01:01 and E*01:03 in these experiments (Appendix Table A4). Overall signal strengths in this experiment were higher than those observed in the first assay, which may explain the larger number of TCR clones that displayed weak KF11 responses.

In summary, our experiments indicated that five TCR clones (TCR 14, 16, 17, 19 and 42) displayed the most consistent ability to respond to KF11 presented on HLA-E*01:01 and/or HLA-E*01:03 (Figure 3.3). As a result, we conclude that these TCR clones hold the greatest potential to generate HLA-E-specific responses in vivo. TCR activity on E*01:01 was relatively weaker (range: 1.7-fold to 4.5-fold over background) compared to that on E*01:03 (range: 2.0- fold to 19.5-fold), which may reflect biological differences in the stability and/or peptide binding affinity of these alleles. Notably, TCR clone 16 stood out as the only clone that was able to elicit weak to moderate responses in the context of both E*01:01 (range: 3.0-fold to 4.5-fold induction) and E*01:03 (range: 2.7-fold to 19.5-fold). Interestingly, TCR 16 also exhibited cross- reactivity, since we previously found that it was able to elicit a response to KF11 in the context of HLA-B*57.

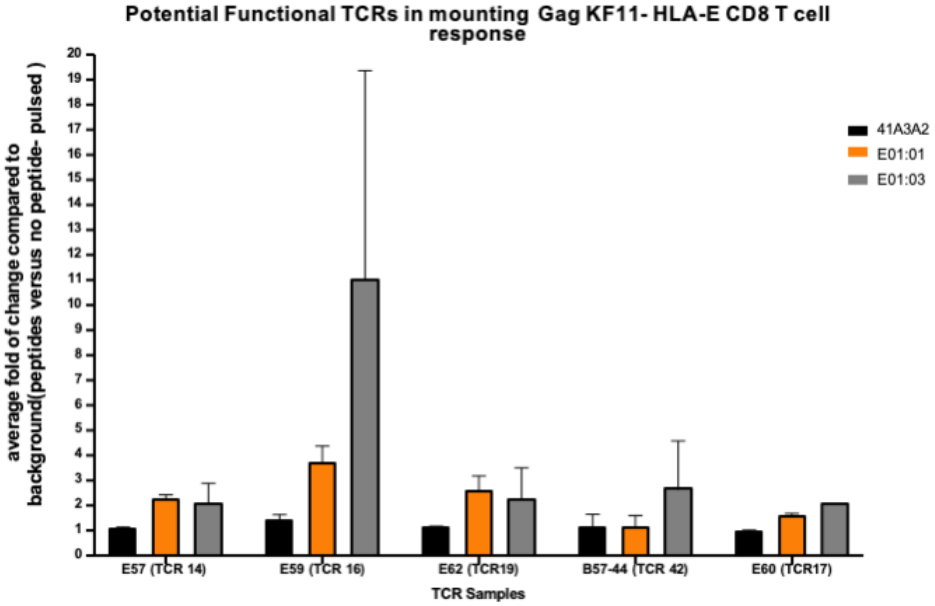

Figure 3.3. Summary analysis of five TCR clones that display potential HLA-E-restricted KF11 responsiveness

Each TCR clone was assessed in two independent experiments (i.e. biological replicates) using a Jurkat reporter cell assay as described in the methods. The fold-change was determined by dividing the TCR-mediated luciferase signal induced by target cells pulsed with KF11 to the signal induced by the same target cells without peptide. Black bars displays TCR responses to an HLA-mismatched target cell line (721.221-41A3.A2) that expresses HLA-A2 and served as a negative control. TCR responses to HLA-E expressing target cells are shown as orange bars (for 721.221-E*01:01 cells) and gray (for 721.221-E*01:03 cells). A peptide concentration of 30 ng/μL was used in each experiment. Error bars represented the standard error mean (SEM).

3.3.4. Genetic characteristics of five TCR clones that display HLA-E-KF11 reactivity

We next investigated the sequences of these five TCR clones to see if they shared any obvious genetic features. Of these five TCR clones, three TRAV genes were used: TRAV5, TRAV17, and TRAV1-2 and each of the clones displayed a unique CDR3α sequence (Figure 3.4A). Gene usage for the beta chain was similarly diverse among the five clones, with two clones encoding TRBV6-1, two clones encoding TRBV15, and one clone encoding TRBV12-4. But, notably, the two TRBV6-1 clones (TCR 14 and 16) displayed an identical CDR3β motif (CASTGGTYGYTF), though their CDR3α motifs were distinct. Additionally, the two TRBV15 clones (TCR 17 and 19) displayed an identical CDR3β motif (CATSDRLAGGETQYF) (Figure 3.4A).

The locations of these five functional TCR clones varied within our initial network graph. TCR 42 was positioned in the top subgroup of the mixed HLA cluster, while TCR

14 and TCR 16 were situated in the bottom subgroup of this extended cluster (Figure 3.4B). By contrast, TCR 17 and TCR 19 were located within the HLA-E cluster (Figure 3.4B).

Samples	Variable Alpha Gene	Variable Beta Gene	CDR3 alpha	CDR3 Beta
E-57 (TCR 14)	TRAV5	TRBV6-1	CAESMGQAGTALIF	CASTGGTYGYTF
E-59 (TCR 16)	TRAV5	TRBV6-1	CAVSGGYQKVTF	CASTGGTYGYTF
E-60 (TCR 17)	TRAV17	TRBV15	CATDAENYGGSQGNLIF	CATSDRLAGGETQYF
E-62 (TCR19)	TRAV17	TRBV15	CATEVGDKLIF	CATSDRLAGGETQYF
B57-44 (TCR 42)	TRAV1-2	TRBV 12-4	CAVNSGYSTLTF	CASSPRGSEQYF

A

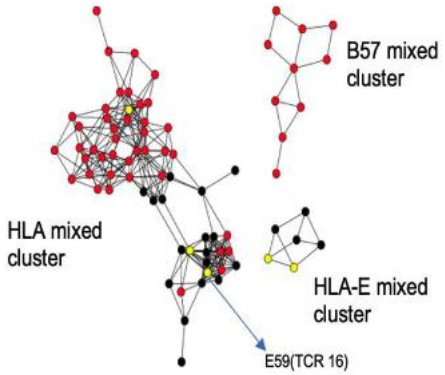

B

Figure 3.4. Genetic features of TCR clones that elicit an HLA-E restricted Gag KF11 T cell response.

(A)TCR alpha and beta Variable gene usage and CDR3 sequences are shown for five TCR clones that mounted weak HLA-E restricted KF11 responses. Some sharing of TRAV and TRBV genes is seen. TCR 14 and TCR 16 encoded the same CDR3β sequence. Similarly, TCR 17 and TCR 19 encoded the same CDR3β sequence.

(B)The location of HLA-E restricted TCR clones relative to non-functional clones is shown in a network graph (as described in Figure 3.2). TCR 16, located in the bottom subgroup of the mixed cluster, elicited the strongest HLA-E*01:01 and HLA-E*01:03 dependent response. Black nodes depict TCR with putative HLA-E restriction; red nodes depict those with putative B*57 restriction. TCR clones that were identified to generate weak to moderate HLA-E KF11 responses are highlighted in yellow nodes.

Optimization of the TCR reporter assay for HLA-E

In light of the relatively weak TCR-mediated signaling that was observed in the context of HLA-E, we wished to further optimize our luciferase reporter cell assay to enhance our ability to detect functional TCR clones. To do this, we examined several variables in the assay design. The results of these tests are described in the following sections, which contain a brief introduction/rationale, a summary of significant changes to the assay protocol and a description of results.

3.4. Promoting endogenous KF11 processing and presentation on HLA-E

3.4.1. Introduction

Previous studies have indicated that HLA-E exhibits lower stability on the cell surface and is expressed at a reduced frequency compared to classical HLA alleles (He et al., 2023). These factors may explain in part the low peptide binding affinity that is observed for some HLA- E restricted epitopes (He et al., 2023; Walters et al., 2022). To circumvent this issue, we introduced an HIV-1 Gag expression plasmid by transfection, thereby facilitating endogenous peptide processing and presentation of KF11 by HLA-E on target cells.

Significant alterations to the reporter assay method

3.4.2. Preparation of 721.221 target cells

pMET7-GAG-EGFP (Addgenes), encoding HIV-1 Gag p55-eGFP fusion protein, was introduced into 721.221 cell lines to promote endogenous expression of Gag and subsequent processing of the KF11 epitope. 721.221-41A3.A2 (HLA-A2) and 721.221-E0101 (HLA-E) cells were transfected by electroporation in 96 plates using a Bio-Rad GenePulser MXcell electroporation system. For each transfection, 3 million cells were resuspend in 150uL of Opti- mem containing 5, 10, 15 or 20ug plasmid. Transfected cells were transferred into 2 mL bullet tubes containing 700uL of R20+ media with pyruvate and rested for 24 hours at 37°C with 5% CO2. Transfection efficiency was assessed by detection of GFP in live cells using flow cytometry (Beckman CytoFLEX).

Results

3.4.3. 721.221 transfection efficiency and co-culture

To enable endogenous expression of the KF11 epitope in HLA-E cell lines, we purchased the pMET7-GAG-EGFP plasmid (Addgene), which encodes the HIV-1 Gag p55 protein fused with GFP. 721.221-derived cells were transfected with 5, 10, 15 or 20ug plasmid by electroporation. To evaluate transfection efficiency, GFP expression was examined by flow cytometry. Our initial results indicated that 5 or 10ug of plasmid yielded low transfection efficiency, with GFP expression observed in less than 15% of cells (Figure 3.5A). Additionally, cell viability was ~50%. Given these results, we increased the plasmid concentration to 10, 15, and 20ug, and we noted enhanced transfection efficiency with the 15 and 20ug doses (Figure 3.5B). The transfection rates achieved with 15ug (23.2%) and 20ug (24.5%) of plasmid were comparable; thus, we chose to proceed with 15ug of plasmid for subsequent assays.

By transfecting Gag expression plasmid into 721.221 cells, we hoped that endogenous antigen processing would allow KF11 to be presented on cell surface in complex with HLA, where it could be recognized by TCR. To test this, we examined TCR clone 16, which we identified as the most probable HLA-E-KF11 restricted TCR in our panel. As a negative control, we selected TCR clone 39, which we identified as an HLA-B*57:01-KF11 restricted TCR that was not likely to recognize HLA-E. As a positive control, we selected TCR clone 5B2, which previous work in the Brockman lab identified as an HLA-A2 restricted TCR specific for the Gag FK10 epitope (Anmole et al.,2015). Therefore, we transfected 721.221-41A3.A2 (HLA-A2) and 721.221-E*0101 cell lines with the Gag expression plasmid and then co-cultured these target cells with Jurkat reporter cells expressing either 5B2, TCR16, or TCR39. We observed that 5B2 generated a 6.3-fold signal above background when co-cultured with Gag-transfected 41A3.A2 cells, whereas it generated a non-specific signal (1.3-fold) when co-cultured with Gag- transfected E01:01 cells. The negative control TCR 39 generated low signal when co-cultured with 41A3.A2 cells (no change over background) or E*01:01 cells (~1.6-fold) (Figure 3.6C).

Unfortunately, the test TCR 16 generated low signal when co-cultured with transfected E*01:01 cells (~1.8-fold over background), but surprisingly generated a

higher signal with 41A3.A2 cells (~2.8 fold induction) (Figure 3.6A). In summary, results from the 5B2 TCR indicated that the TCR reporter assay can be used to detect endogenous Gag antigen when processed and presented by 721.221 cells (Figure 3.6C). However, we did not observe any substantial signal by TCR 16 when co-cultured with transfected E*01:01 target cells, suggesting that detection of endogenous antigen presented on HLA-E may be less efficient.

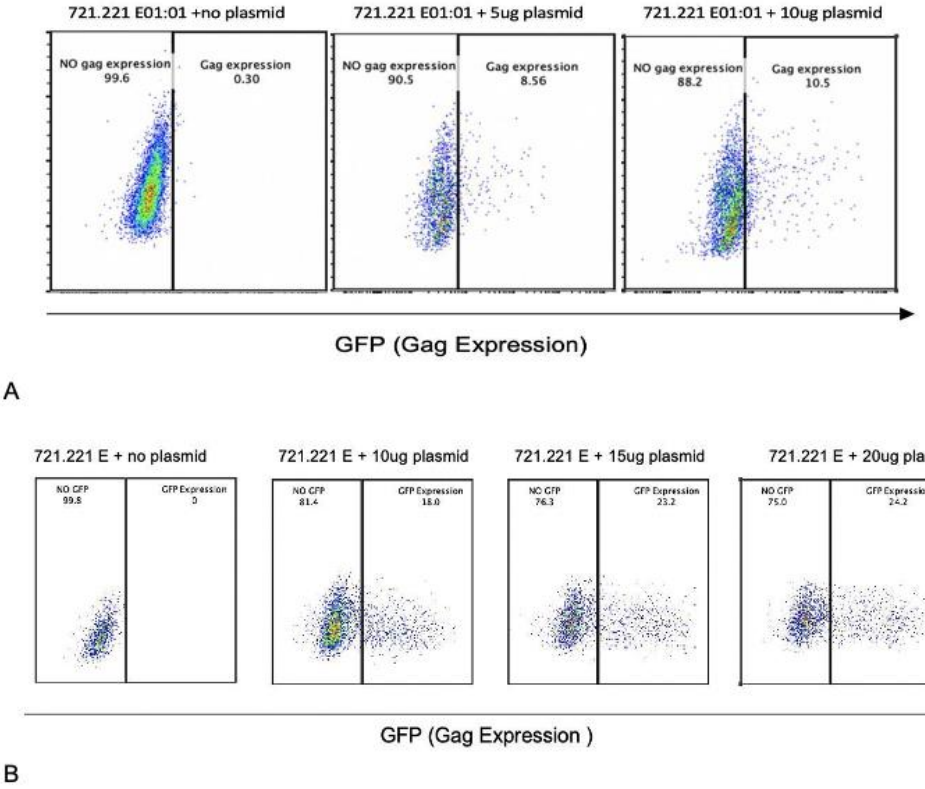

Figure 3.5. Expression HIV-1 Gag by pMET7-GAG-EGFP in 721.221 HLA-E*01:01 cells.

GFP expression (representing HIV Gag) was detected 20 hr after electroporation by flow cytometry. (A) Left panel depicts 721.221 E*01:01 cells transfected with no plasmid, which served as a negative control. Middle panel depicts 721.221 E*01:01 cells transfected with 5ug of plasmid, resulting in a tranfection efficiency of 8.6%. Right panel depicts 721.221 E*01:01 cells transfected with 10 ug of plasmid, resulting in a transfection efficiency of 10.5%. (B) Left to right, panels depict 721.221 E*01:01 cells transfected with no plasmid, 10ug, 15ug and 20ug of plasmid. Transfection efficiencies were 0%, 18%, 23.2% and 24.2%, respectfully

A

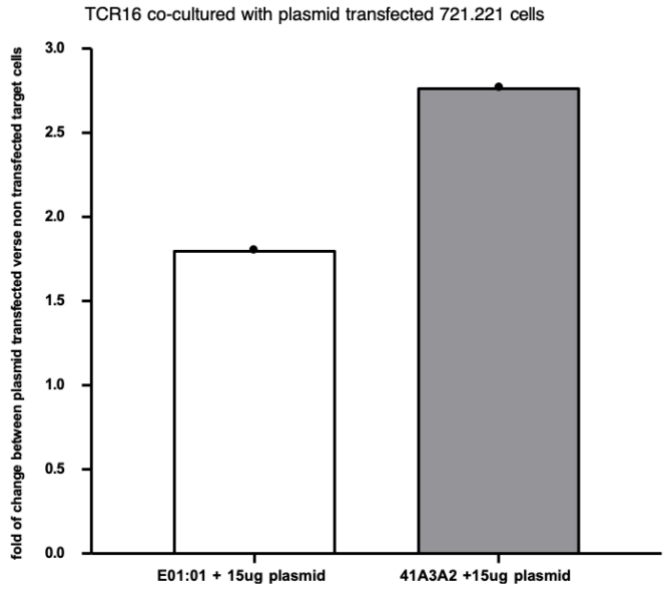
TCR16 co-cultured with plasmid transfected 721.221 cells
fold of change between plasmid transfected verse non transfected target cells
3.0
2.5
2.0
1.5
1.0
0.5
0.0
E01:01 + 15ug plasmid
41A3A2 +15ug plasmid

B

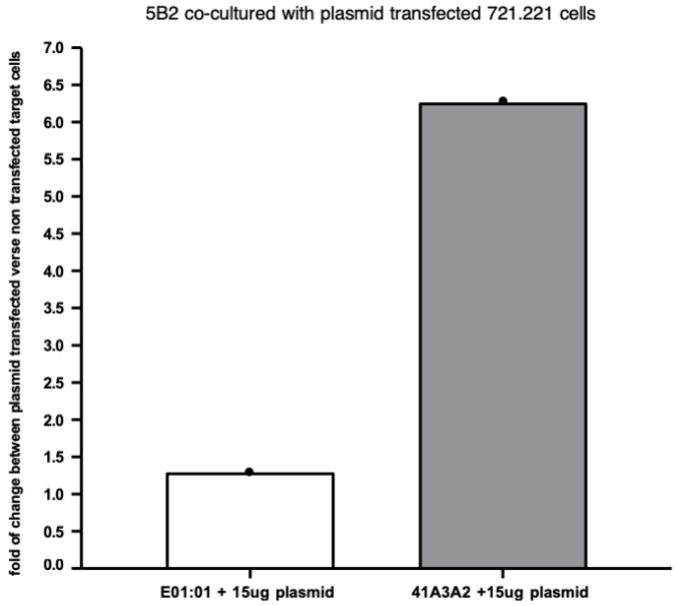
5B2 co-cultured with plasmid transfected 721.221 cells
fold of change between plasmid transfected verse non transfected target cells
7.0
6.5
6.0
5.5
5.0
4.5
4.0
3.5
3.0
2.5
2.0
1.5
1.0
0.5
0.0
E01:01 + 15ug plasmid
41A3A2 +15ug plasmid

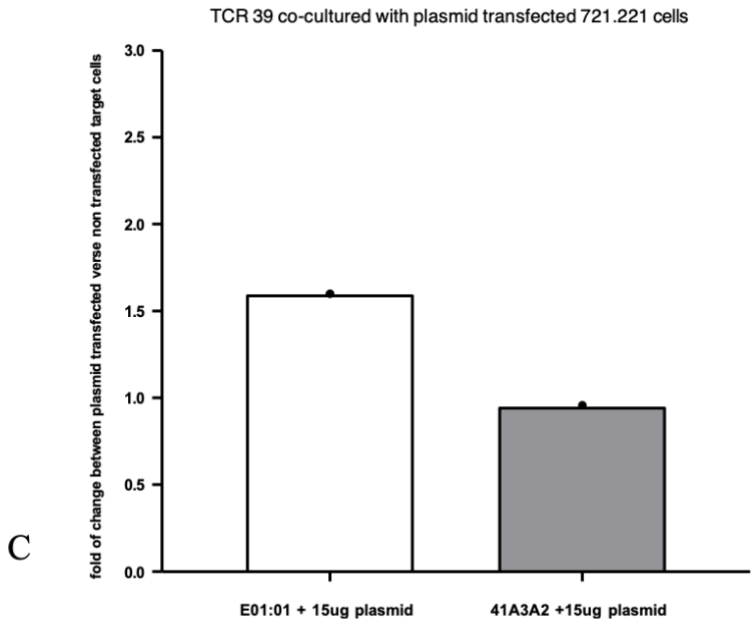

Figure 3.6. TCR recognition of endogenous Gag peptides presented by 721.221 cells.

The y-axis represents fold-change in luminescence between plasmid transfected target cells versus non-transfected cells following co-culture with Jurkat reporter cells. The left bar of each panel displays TCR signaling generated in the context of HLA-E*01:01 whereas the right bar displays TCR signaling generated in the context of HLA-A2 (41A3.A2 cells). For each assay, 15ug of pMET7-GAG-EGFP plasmid was transfected into each 721.221-derived cell line and rested for 20hr prior to co-culture in the reporter assay.(A)TCR 16, previously identified as a potential E-restricted TCR, induced low TCR signaling in both transfected 721.221 cell lines.(B)5B2 TCR, previously identified as an HLA-A2 restricted TCR, induced high signaling in transfected 41A3A2 cells but not in E*01:01 cells.(C)TCR 39, previously identified as a B*57-restricted TCR, induced low TCR signaling in both transfected 721.221 cell lines.

3.5. HLA-E interaction with two well-known HLA-E restricted TCR, KK50.4 and GF4

3.5.1. Introduction

The interaction of TCR binding to peptides presented by classical HLA class I has been well-studied; however, the our understanding of TCR/peptide/HLA-E interactions is limited (Sullivan et al., 2017). Only a few epitopes presented by HLA-E have been identified, such as SL9 from the EBV, RL9 from HIV, and several epitopes from M.tb (Yang et al., 2021; Joosten et al., 2016; Pietra et al., 2010). The most extensively studied TCR interaction with HLA-E involves the VL9 epitope. VL9 is a leader peptide derived from HLA class I molecules and has three different versions:

VMAPRTLVL, VMAPRTLLL, or VMAPRTLFL (McMichael et al., 2017). VL9 binds to HLA-E with higher affinity compared to pathogen-derived epitopes (Walters et al., 2022).

Two VL9-specific TCR clones, KK50.4 and GF4, have been studied extensively and thus could serve as ideal positive controls for our reporter assay. Both KK50.4 and GL9 respond to a VL9 homolog encoded by the CMV UL40 protein (VMAPRTLIL), which the virus uses to modulate the NK cell response. The similarity between UL40-VL9 and the leader sequence VL9 allows KK50.4 and GF4 to recognize the leader sequence VL9 and to activate a CD8 T cell response (Joosten et al., 2016; Sullivan et al., 2017). To explore this further, we aimed to investigate the ability of well-characterized TCR clones KK50.4 and GF4 to elicit HLA-E- restricted TCR signaling in our reporter assay.

Significant alterations to the reporter assay methods

3.5.2. Molecular cloning of TCR alpha and beta genes

KK50.4 and GF4 TCR alpha and beta genes were reconstructed and synthesized (IDT).TCR cloning and sequence validation was performed as described in Chapter 2.

3.5.3. Preparation of 721.221 target cells (peptide pulse)

VL9 (VMAPRTLVL) peptide was purchased from a commercial vendor (Genscript).Stock solutions were prepared as described in Chapter 2.

Results

3.5.4. TCR clones KK50.4 and GF4 generated weak HLA-E01:01-VL9 restricted responses

HLA-E displays lower peptide affinity and surface expression compared to classical HLA class I alleles (Kanevskiy et al., 2019), which could result in a lower capacity to activate T cells . Here, we aimed to see if the well-characterized HLA-E-VL9 restricted TCR clones KK50.4 and GF4 could induce a robust response in our reporter cell assay. We observed that jurkat cells transfected with TCR GF4 displayed approximately a 3-fold increase in luminescence signal over background when co-cultured with VL9-pulsed E*01:01 cells (Figure 3.7). Similarly, jurkat cells transfected

with TCR KK50.4 exhibited about a 3.5-fold increase in signal when co- cultured with VL9-pulsed E*01:01 cells.

While both of these TCR clones demonstrated the ability to recognize HLA-E-VL9, the overall signal strength was relatively low compared to responses mediated by HLA-B*57 or other classical HLA class I alleles. We noted earlier that many of the potential E-restricted TCR clones in our initial panel produced low (3-fold or 4-fold) signals, which is comparable to those that were generated by GF4 and KK50.4. Unfortunately, we did not observe a significant increase in TCR signaling by GF4 and KK50.4 when co-cultured with E*01:01 target cells. This result suggests that this level of response may be the maximum that we can expect to observe for E-restricted TCR clones.

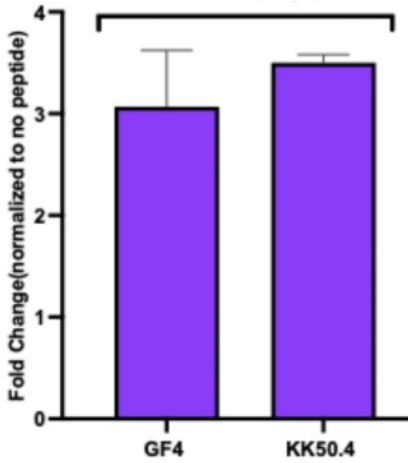

Figure 3.7. KK.50 and GF4 TCR inducing low VL9 HLA-E restricted CD8 T cell response

The data was collected and generated by Zefufael Derza. The fold change at y axis was determined by comparing target cells pulsed with the peptide to those without peptide, while co-cultured with transfected jurkat cells. Target cells were peptide pulsed with VL9 (VMAPRTLVL) 2 hours prior to co-culture assay. Both GF4 and KK50.4 samples generated low 3~4 fold of induction in TCR signaling via TCR reporter assay. This peptide concentration was performed at 30ng /uL for all experiments. Each example were performed with technical replicates and error bar represented standard deviation.

3.6. Extended co-culture for TCR reporter assay

3.6.1. Introduction

In chapter 2, we detected robust TCR signaling when transfected jurkat effector cells co-cultured with peptide pulsed 721.221-B*57 cell lines for 6 hours. In studies with

HLA-E expressing target cells, we have observed consistent low-level TCR signaling when co-cultured for 6 hrs. Prior studies indicate that HLA-E displays a low affinity for most pathogen derived peptides (Strong et al., 2003 and Walter et al., 2022), and loss of peptide could contribute to reduced T cell stimulation in our assay. Earlier work from the Brockman lab suggested that the luminescent signal in the TCR reporter assay was maintained after 16 hours of co-culture (Anmole et al., 2015). More recently, another student in our lab (Zerufael Derza) demonstrated that KF11 restricted responses might be enhanced after co-culture for 18-hours. This led us to hypothesize that TCR signaling in the context of HLA-E might require an extended co-culture period to overcome the challenge posed by lower peptide affinity.

Significant alterations to the reporter assay methods

3.6.2. TCR stimulation and luciferase assays

Co-culture was performed as described in Chapter 2, except that the period of co-culture was extended to 18 hours. Luminescence signal was measured as described previously.

Results

To assess the impact of a longer co-culture on TCR signaling, we tested the same three TCR clones as described in section 3.5: namely, TCR 16, which is expected to show HLA-E- KF11 activity; TCR 39 (negative control), which is not expected to show HLA-E-KF11 activity, and 5B2 (positive control), which is expected to show HLA-A2-FK10 activity. We performed the reporter cell assay as described previously, except the co-culture time was extended to 18 hours. For the positive control TCR 5B2, we observed a strong and specific response when jurkat cells were co-cultured with Gag FK10-pulsed HLA-A2 cells, with a substantial ~30-fold increase in signal over background. Notably, 5B2 did not respond to KF11-pulsed HLA-E target cells even after 18 hours, with signals comparable to background (Figure 3.8). Results for TCR 16 were also encouraging. While this clone exhibited an increase in signaling when effector cells were co-cultured with both peptide-pulsed A2 and HLA-E target cells, the KF11 response on HLA-E elicited a 5- to 6- fold induction compared to background, while the non-specific response on A2 target cells was ~1.5-fold (Figure 3.8). By comparison, TCR

16 elicited a ~2.7 to 19.5-fold response with HLA-E target cells after 6 hours of co-culture (Figure 3.3 and Appendix Table A4). This result suggested that extending the co-culture time to 18 hours allowed for the HLA-E response to develop, even though the absolute signal remained relatively low.

We observed that this clone exhibited a significant increase in signaling when stimulated with KF11-pulsed 721.221 A2 cells (non-specific signals), resulting in a ~60-fold induction over no- peptide controls. Additionally, TCR 39 demonstrated even higher stimulation when co-cultured with KF11-pulsed E*01:01 and E*01:03 cell lines (non-specific signals), achieving ~100-fold increases in signaling activity (Figure 3.8). Unfortunately, our results for TCR 39 are difficult to interpret.

In summary, while we observed an enhancement in the HLA-E restricted response for TCR16 after 18 hours co-culture, this was relatively modest. Unfortunately, we also observed a notable increase in non-specific signal, in particular for TCR 39. As a result, we concluded that prolonging the co-culture period did not significantly amplify the E-specific TCR response, but this could be a viable option if we can identify strategies to reduce non-s

TCR 39 co-culture with 721.221 cell lines for 18hr

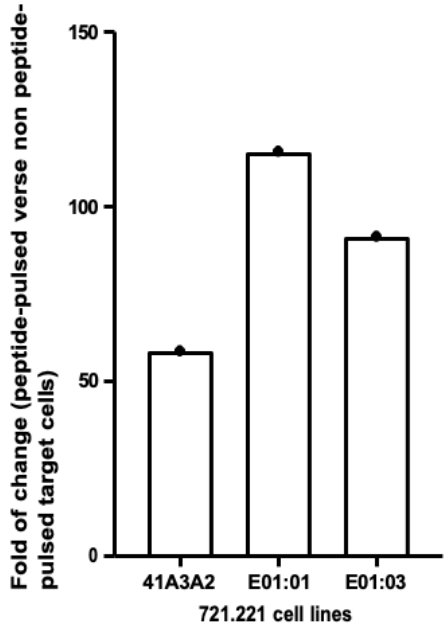

TCR16 co-culture with 721.221 cell lines for 18hr

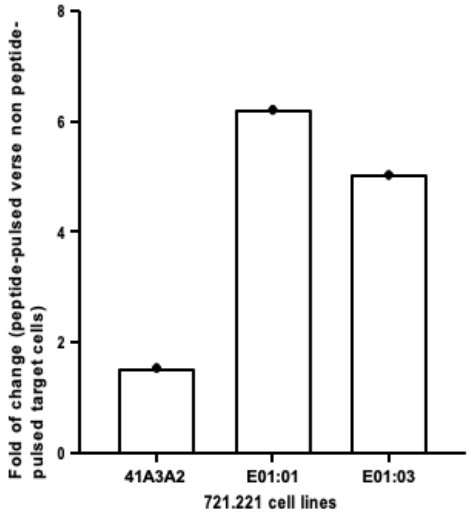

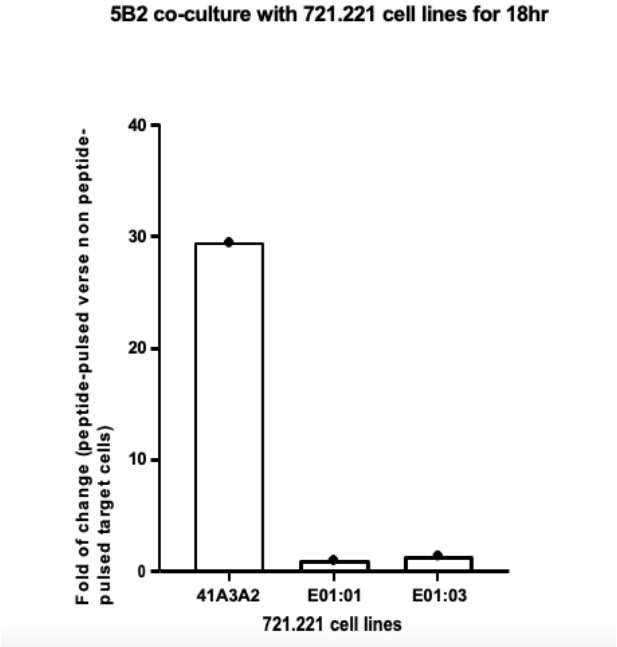

Figure 3.8. Effect of 18-hour co-culture on TCR signal intensity.
The fold change values on the y-axis were determined by comparing target cells that were either pulsed with peptide or not, while being co-cultured with transfected Jurkat cells. For TCR 39, the fold-change was approximately 58-, 115-, and 91- when co-cultured with 721.221 41A3.A2, E*01:01, and E*01:03 cell lines, respectively. For TCR 16, the fold-change was approximately 1.5-, 6.2-, and 5.0- when co-cultured with 721.221 41A3.A2, E*01:01, and E01:03 cell lines, respectively. Lastly, 5B2 induced approximately 29-, 1- and 1.4- fold changes when co-cultured with 721.221 41A3.A2, E*01:01, and E*01:03 cell lines, respectively. All experiments were conducted at a peptide concentration of 30 ng/uL, and were performed as a single trial.

3.7. Discussion

In this chapter, our objective was to employ a reporter cell assay identify KF11-specific TCR clones that exhibit restriction for HLA-E, or potentially dual restriction for both HLA-E and B*57. We noticed consistently low levels of HLA-E signals produced when TCR-transfected jurkat cells were co-cultured with HLA-E target cells pulsed with KF11 peptide. Nevertheless, we were only able to identify five TCR clones: TCR 14,TCR 16,TCR 17, TCR 19, and TCR 42, which demonstrated consistent, but relatively weak activation with HLA-E. Notably, among these, TCR16 exhibited the most robust response in generating E restricted T cell response. Intriguingly, TCR16 was also capable of recognizing Gag KF11 when presented by HLA-B*57, making it the only dually restricted TCR. Previously, Gillespie et al. identified biased TRAV5/ TRBV19 gene usage within HIV individuals generating B*57-KF11 T cell response. To date, there have been no reports addressing TCR gene usage in relation to HLA-E-restricted responses

in the context of HIV. In this study, we observed that TCR 16, which encodes TRAV5 and TRBV6-1, was able to elicit a moderate HLA-E-KF11 response. Additionally, we demonstrated that TCR16 elicited a robust response against Gag KF11 presented by HLA- B*57. The identification of dually restricted TCR that capable to generate robust and broad CD8 T cell response offers potential new therapeutic and vaccine strategies for HIV.

We observed consistently low HLA-E signals with our TCR reporter assay, prompting us to refine the assay to yield a more robust E-restricted response. Several factors could account for the low signal intensity in the context of HLA-E . Previous research indicated that HLA-E has a reduced peptide affinity for pathogen-derived peptides, leading to weaker binding interactions (Walters et al., 2020; Walters et al., 2022). HLA-E is also known for its instability on the cell surface; it is often rapidly internalized after expression, hindering its peptide-binding capabilities (Zheng et al., 2023). Furthermore, in normal tissue, the cell surface level of HLA-E is low.

Moreover, HLA-E possesses a unique peptide binding groove, necessitating a precise conformation, hydrogen bonding capabilities, and hydrophobic properties. As a result, only a limited set of peptides can fulfill these criteria (O'Callaghan et al., 1998). These factors could contribute to the low HLA-E restricted signals that we observed. Despite these challenges, we explored various methods to enhance HLA-E-restricted T cell responses.

In an attempt to allow the development of HLA-E-restricted T cell signals, we conducted co-cultures involving TCR-transfected jurkat cells and peptide-loaded HLA-E targets for an extended duration. While a modest increase in TCR-dependent signal was observed, non- specific activity also increased substantially (particularly for TCR 39). We also hypothesized that the low KF11 peptide binding affinity for HLA-E or weak interactions between the TCR-HLA-E- peptide complexes could contribute to poor TCR signaling. To address potential issues with low KF11 binding to HLA-E, we transfected the HLA-E cell line with a Gag expression plasmid. This allowed for the endogenous presentation of Gag peptides on the cell surface. Following this, we co-cultured them with TCR-transfected jurkat cells, hoping for the development of an E-specific T cell response. While this approach worked for an HLA-A2-restricted TCR clone, we did not observe a significant increase in E-restricted T cell signal.

Several studies have shown HLA-E displays higher affinity for highly conserved VL9 (VMAPRTL/VV/L/FL) leader sequences derived from HLA-A, B, C and G (He et al., 2023 and Walters et al., 2022). The TCR clones KK50.4 and GF4 were found to recognize VL9 peptides: either VMAPRTLIL or VMAPRTLI/VL, respectively (Sullivan et al., 2017 and Hoare et al., 2006). To further examine the sensitivity of our TCR reporter assay, we assessed the ability of KK50.4 and GF4 to signal in response to VL9 presented by HLA-E. Notably, we observed a consistent 3-4 fold induction of signal with these clones. While this level of induction is substantially lower compared to the robust signal that we have observed with TCR clones restricted by HLA-B*57 and other classical HLA alleles, it is similar to the level of response that we found for some putative HLA-E-restricted TCR in our reporter assay. This suggests that HLA-E-restricted TCR may elicit relatively weak signals that will be harder to evaluate using this type of assay. In summary, despite various attempts to enhance E-restricted TCR responses, we were unable to find a strategy that provided an obvious improvement over our existing TCR reporter assay.

The low affinity of HLA-E-specific TCR for VL9 or KF11 may be attributed to a weak interaction between CD8α and HLA-E (Gao et al., 2000; Hoare et al., 2006). CD8α or CD8$\alpha\alpha$ serves as a co-receptor that stabilizes the interaction between the TCR and HLA during CD8 T cell activation. This interaction is crucial for optimal T cell activation (Gao et al., 2000). Notably, HLA-E demonstrates weak binding to the CD8 co-receptors, which might be due to its primary role in interacting with NK cells, where the CD8 co-receptor isn't essential (Gao et al., 2000). In our TCR reporter assay, we used jurkat T cells that naturally lack CD8 expression as effector cells. To allow stimulation by HLA class I (and HLA-E), we transfected the jurkat effectors cells with CD8 alpha, and then co-cultured them with HLA-E cells. It is possible that the transfected CD8 alpha protein may function differently in jurkat cells compared to CD8 T cells, potentially leading to a reduced E-restricted T cell response. Future experiments using alternative cell lines that naturally express CD8 or primary CD8 T cells as effectors might yield better E-restricted responses.

Furthermore, in our TCR reporter assay, we employed NFAT-mediated signaling to assess the ability of TCR to recognize peptides presented by HLA-E. The activity of TCR might also be assessed by measuring the production of activation markers, like CD69 and CD137, that are upregulated on the surface of stimulated T cells (Cibrián et

al., 2017 and Altosole et al., 2023). Alternatively, the production of intracellular markers of T cell stimulation, such as IFN-γ and granzymes, could be measured by flow cytometry (Yang et al., 2021 and Mazzarino et al., 2005). Another potential strategy to evaluate HLA-E restricted T cell responses is through the use of HLA-E-tetramers, though only a few functional studies have implemented these reagents successfully (Joosten et al., 2016 and Allard et al., 2012).

In summary, in an effort to identify KF11-specific TCR that are restricted by HLA-E, we uncovered TCR 16, which may serve as a dually restricted TCR that is able to elicit a weak to moderate E-restricted response as well as a robust B*57-restricted response to Gag KF11.Although TCR 16 generated an approximately 4-fold induction in signal with E01:01 targets, this level of stimulation was comparable of that seen for two well-characterized E-restricted VL9- specific TCR clones, KK50.4 for GF4. While we have tried several strategies to improve the strength of E-restricted TCR signals, we continued to observe moderate to low signals (2-5 fold induction above background), which has been a challenge to this work. Further investigation will be required to optimize the TCR reporter assay to better assess HLA-E restricted responses.

3.8. References

Allard, M., Tonnerre, P., Nedellec, S., Oger, R., Morice, A., Guilloux, Y., Houssaint, E., Charreau, B., & Gervois, N. (2012). HLA-E-restricted cross-recognition of allogeneic endothelial cells by CMV-associated CD8 T cells: a potential risk factor following transplantation. *PloSone*, 7(11), e50951. https://doi.org/10.1371/journal.pone.0050951

Altosole, T., Rotta, G., Uras, C. R. M., Bornheimer, S. J., & Fenoglio, D. (2023). An optimized flow cytometry protocol for simultaneous detection of T cell activation induced markers and intracellular cytokines: Application to SARS-CoV-2 immune individuals. *Journal of immunological methods*, 515, 113443. https://doi.org/10.1016/j.jim.2023.113443

Anmole, G., Kuang, X. T., Toyoda, M., Martin, E., Shahid, A., Le, A. Q., Markle, T., Baraki, B., Jones, R. B., Ostrowski, M. A., Ueno, T., Brumme, Z. L., & Brockman, M. A. (2015). A robust and scalable TCR-based reporter cell assay to measure HIV-1 Nef-mediated T cell immune evasion. *Journal of immunological methods*, 426, 104–113. https://doi.org/10.1016/j.jim.2015.08.010

Apps, R., Del Prete, G. Q., Chatterjee, P., Lara, A., Brumme, Z. L., Brockman, M. A., Neil, S., Pickering, S., Schneider, D. K., Piechocka-Trocha, A., Walker, B. D., Thomas, R., Shaw, G. M., Hahn, B. H., Keele, B. F., Lifson, J. D., & Carrington, M. (2016). HIV-1 Vpu Mediates HLA-C Downregulation. *Cell host & microbe*, 19(5), 686–695. https://doi.org/10.1016/j.chom.2016.04.005

Bansal, A., Gehre, M. N., Qin, K., Sterrett, S., Ali, A., Dang, Y., Abraham, S., Costanzo, M. C., Venegas, L. A., Tang, J., Manjunath, N., Brockman, M. A., Yang, O. O., Kan-Mitchell, J., & Goepfert, P. A. (2021). HLA-E-restricted HIV-1-specific CD8+ T cell responses in natural infection. *The Journal of clinical investigation*, 131(16), e148979. https://doi.org/10.1172/JCI148979

Cibrián, D., & Sánchez-Madrid, F. (2017). CD69: from activation marker to metabolic gatekeeper. European *journal of immunology*, 47(6), 946–953. https://doi.org/10.1002/eji.201646837

Collins, D. R., Gaiha, G. D., & Walker, B. D. (2020). CD8+ T cells in HIV control, cure and prevention. *Nature reviews. Immunology*, 20(8), 471–482. https://doi.org/10.1038/s41577-020- 0274-9

Gao, G. F., Willcox, B. E., Wyer, J. R., Boulter, J. M., O'Callaghan, C. A., Maenaka, K., Stuart,D. I., Jones, E. Y., Van Der Merwe, P. A., Bell, J. I., & Jakobsen, B. K. (2000). Classical and nonclassical class I major histocompatibility complex molecules exhibit subtle conformational differences that affect binding to CD8alphaalpha. *The Journal of biological chemistry*, 275(20), 15232–15238. https://doi.org/10.1074/jbc.275.20.15232

Hansen, S. G., Marshall, E. E., Malouli, D., Ventura, A. B., Hughes, C. M., Ainslie, E., Ford, J. C., Morrow, D., Gilbride, R. M., Bae, J. Y., Legasse, A. W., Oswald, K., Shoemaker, R.,Berkemeier, B., Bosche, W. J., Hull, M., Womack, J., Shao, J., Edlefsen, P. T., Reed, J. S., … Picker, L. J. (2019). A live-attenuated RhCMV/SIV vaccine shows long-term efficacy against heterologous SIV challenge. *Science translational medicine*, 11(501), eaaw2607. https://doi.org/10.1126/scitranslmed.aaw2607

Hansen, S. G., Sacha, J. B., Hughes, C. M., Ford, J. C., Burwitz, B. J., Scholz, I., Gilbride, R.M., Lewis, M. S., Gilliam, A. N., Ventura, A. B., Malouli, D., Xu, G., Richards, R., Whizin, N.,Reed, J. S., Hammond, K. B., Fischer, M., Turner, J. M., Legasse, A. W., Axthelm, M. K., … Picker, L. J. (2013). Cytomegalovirus vectors violate CD8+ T cell epitope recognition paradigms. *Science (New York, N.Y.)*, 340(6135), 1237874. https://doi.org/10.1126/science.1237874

He, W., Gea-Mallorquí, E., Colin-York, H., Fritzsche, M., Gillespie, G. M., Brackenridge, S., Borrow, P., & McMichael, A. J. (2023). Intracellular trafficking of HLA-E and its regulation. *The Journal of experimental medicine*, 220(8), e20221941. https://doi.org/10.1084/jem.20221941

Hoare, H. L., Sullivan, L. C., Pietra, G., Clements, C. S., Lee, E. J., Ely, L. K., Beddoe, T., Falco, M., Kjer-Nielsen, L., Reid, H. H., McCluskey, J., Moretta, L., Rossjohn, J., & Brooks, A. G. (2006). Structural basis for a major histocompatibility complex class Ib-restricted T cell response. *Nature immunology*, 7(3), 256–264. https://doi.org/10.1038/ni1312

Joosten, S. A., Sullivan, L. C., & Ottenhoff, T. H. (2016). Characteristics of HLA-E Restricted T- Cell Responses and Their Role in Infectious Diseases. *Journal of immunology research*, 2016, 2695396. https://doi.org/10.1155/2016/2695396

Kanevskiy, L., Erokhina, S., Kobyzeva, P., Streltsova, M., Sapozhnikov, A., & Kovalenko, E. (2019). Dimorphism of HLA-E and its Disease Association. *International journal of molecular sciences*, 20(21), 5496. https://doi.org/10.3390/ijms20215496

Mazzarino, P., Pietra, G., Vacca, P., Falco, M., Colau, D., Coulie, P., Moretta, L., & Mingari, M.C. (2005). Identification of effector-memory CMV-specific T lymphocytes that kill CMV-infected target cells in an HLA-E-restricted fashion. *European journal of immunology*, 35(11), 3240– 3247. https://doi.org/10.1002/eji.200535343

McMichael, A. J., & Picker, L. J. (2017). Unusual antigen presentation offers new insight into HIV vaccine design. *Current opinion in immunology*, 46, 75–81. https://doi.org/10.1016/j.coi.2017.04.009

O'Callaghan, C. A., Tormo, J., Willcox, B. E., Braud, V. M., Jakobsen, B. K., Stuart, D. I., McMichael, A. J., Bell, J. I., & Jones, E. Y. (1998). Structural features impose tight peptide binding specificity in the nonclassical MHC molecule HLA-E. *Molecular cell*, 1(4), 531–541. https://doi.org/10.1016/s1097-2765(00)80053-2

Pietra, G., Romagnani, C., Manzini, C., Moretta, L., & Mingari, M. C. (2010). The emerging role of HLA-E-restricted CD8+ T lymphocytes in the adaptive immune response to pathogens and tumors. *Journal of biomedicine & biotechnology*, 2010, 907092. https://doi.org/10.1155/2010/907092

Strong, R. K., Holmes, M. A., Li, P., Braun, L., Lee, N., & Geraghty, D. E. (2003). HLA-E allelic variants. Correlating differential expression, peptide affinities, crystal structures, and thermal stabilities. *The Journal of biological chemistry*, 278(7), 5082–5090. https://doi.org/10.1074/jbc.M208268200

Sullivan, L. C., Walpole, N. G., Farenc, C., Pietra, G., Sum, M. J. W., Clements, C. S., Lee, E.J., Beddoe, T., Falco, M., Mingari, M. C., Moretta, L., Gras, S., Rossjohn, J., & Brooks, A. G.(2017). A conserved energetic footprint underpins recognition of human leukocyte antigen-E by two distinct αβ T cell receptors. *The Journal of biological chemistry*, 292(51), 21149–21158. https://doi.org/10.1074/jbc.M117.807719

Swann, S. A., Williams, M., Story, C. M., Bobbitt, K. R., Fleis, R., & Collins, K. L. (2001). HIV-1 Nef blocks transport of MHC class I molecules to the cell surface via a PI 3-kinase-dependent pathway. *Virology*, 282(2), 267–277. https://doi.org/10.1006/viro.2000.0816

van Stigt Thans, T., Akko, J. I., Niehrs, A., Garcia-Beltran, W. F., Richert, L., Stürzel, C. M., Ford, C. T., Li, H., Ochsenbauer, C., Kappes, J. C., Hahn, B. H., Kirchhoff, F., Martrus, G., Sauter, D., Altfeld, M., & Hölzemer, A. (2019). Primary HIV-1 Strains Use Nef To Downmodulate HLA-E Surface Expression. *Journal of virology*, 93(20), e00719-19. https://doi.org/10.1128/JVI.00719-19

Vidya Vijayan, K. K., Karthigeyan, K. P., Tripathi, S. P., & Hanna, L. E. (2017). Pathophysiology of CD4+ T-Cell Depletion in HIV-1 and HIV-2 Infections. *Frontiers in immunology*, 8, 580. https://doi.org/10.3389/fimmu.2017.00580

Walters, L. C., Rozbesky, D., Harlos, K., Quastel, M., Sun, H., Springer, S., Rambo, R. P., Mohammed, F., Jones, E. Y., McMichael, A. J., & Gillespie, G. M. (2022). Primary and secondary functions of HLA-E are determined by stability and conformation of the peptide- bound complexes. *Cell reports*, 39(11), 110959. https://doi.org/10.1016/j.celrep.2022.110959

Walters, L. C., Harlos, K., Brackenridge, S., Rozbesky, D., Barrett, J. R., Jain, V., Walter, T. S., O'Callaghan, C. A., Borrow, P., Toebes, M., Hansen, S. G., Sacha, J. B., Abdulhaqq, S., Greene, J. M., Früh, K., Marshall, E., Picker, L. J., Jones, E. Y., McMichael, A. J., & Gillespie,G. M. (2018). Pathogen-derived HLA-E bound epitopes reveal broad primary anchor pocket tolerability and conformationally malleable peptide binding. *Nature communications*, 9(1), 3137. https://doi.org/10.1038/s41467-018-05459-z

Walters, L. C., McMichael, A. J., & Gillespie, G. M. (2020). Detailed and atypical HLA-E peptide binding motifs revealed by a novel peptide exchange binding assay. *European journal of immunology*, 50(12), 2075–2091. https://doi.org/10.1002/eji.202048719

Yang, H., Rei, M., Brackenridge, S., Brenna, E., Sun, H., Abdulhaqq, S., Liu, M. K. P., Ma, W.,Kurupati, P., Xu, X., Cerundolo, V., Jenkins, E., Davis, S. J., Sacha, J. B., Früh, K., Picker, L. J., Borrow, P., Gillespie, G. M., & McMichael, A. J. (2021). HLA-E-restricted, Gag-specific CD8+ T cells can suppress HIV-1 infection, offering vaccine opportunities. *Science immunology*, 6(57), eabg1703. https://doi.org/10.1126/sciimmunol.abg1703

Zheng, H., Lu, R., Xie, S., Wen, X., Wang, H., Gao, X., & Guo, L. (2015). Human leukocyte antigen-E alleles and expression in patients with serous ovarian cancer. *Cancer science*, 106(5), 522–528. https://doi.org/10.1111/cas.12641

Chapter 4.

Summary and implications of this thesis

Robust Gag-dominant CTL responses correlate with better suppression in HIV viremia and are observed in most HIV elite controllers (Dyer et al., 2008). Some research indicates that genetic characteristics of TCR correlate with a stronger CTL response, but in-depth mechanistic studies are limited (Iglesias et al., 2011; Mendoza et al., 2020). In my thesis, I have examined the sequence and function of Gag KF11-specific TCR clones in the context of the classical HLA- B*57 allele and the non-classical HLA-E allele. HLA-B*57 is known to be a protective allele and is commonly found in HIV elite controllers. B*57-restricted CTL responses are highly effective in killing HIV-infected cells and have been found to persistent throughout HIV-1 infection (Brennan et al., 2012). However, studies have indicated that HIV accessory protein Nef can downregulate HLA-A and -B alleles, but Nef's ability to downregulation HLA-E appears to be modest, suggesting that T cells restricted by HLA-E might maintain a greater ability to suppress HIV infection (Apps et al., 2016; Swann et al., 2001; van Stigt Thans et al., 2019).

In chapter 1, I provided a brief introduction to HIV and the host immune response to infection. I described that T responses are heavily dependent on TCR, and that each unique TCR provides an opportunity to generate a distinct CTL response that may have different impacts on clinical outcomes. I hypothesize that intrinsic features of each TCR contribute to its antigen specificity and potential antiviral function. Specifically, I anticipate that TCR clones capable of generating robust Gag KF11 responses will display similar sequence and/or functional characteristics that can be identified through careful analysis of TCR/peptide/HLA interactions. A better understating of KF11-specific TCR, including the discovery and validation of high affinity HLA-B*57- and HLA-E-restricted TCR clones, may support efforts to design new vaccines or therapeutics to prevent or treat HIV.

In chapter 2, our overall goal was to identify functional B*57-KF11 restricted TCR clones, and to then explore genetic features of these clones to identify characteristics of robust B*57 restricted responses. We successfully identified seven functional TCRs

capable of generating robust B*57 CTL responses. We observed that these seven functional TCRs shared a similar genetic feature as they all consist TRAV5 for their alpha gene and either TRBV19 or TRBV 6-1 for beta genes. In addition, they shared a highly conserved CDR3α, CAG/V/ESGGYQKVTF, with only one amino acid difference in sequence. On the other hand, seven B*57 functional TCRs shared five distinct CDR3β sequences. We further exanimate functional TCR's antigen sensitivity and their ability to recognize alanine mutants via TCR reporter assay. TCR16 appeared to be most sensitive to any given antigen concentration, indicating TCR16 consisted specific genetic feature enabling them to generate robust CTL responses. This result can further be verified with TCR-peptide/HLA crystal structure to show the interaction between TCR16-peptide/HLA complex. The might reveal specific generic features in TCR16 enabling them to highly engage with peptide/ HLA complex, resulting in a superior CTL response.

AGA, a public B*57 restricted TCR clone, is frequently found in HIV elite controllers and is associated with better viral control due to its ability to generate robust CTL response. We observed that our functional B*57 restricted TCRs and AGA shared TRAV5 gene, with only one amino acid difference shared among all samples (Figure 2.8 and 2.11a). We further analyzed B*57 functional TCRs' ability to recognize alanine mutants, and observed that KF11 position 6 (E) are is crucial for TCR recognition. We also examined AGA and one of our identified functional TCRs' interactions between peptide/HLA and TCRs. We observed these TCRs displayed substantial sequence similarity, and all required KF11 position 6 (E) for recognition. My results from chapter 2 highlight features of KF11-specific TCR that can generate robust CTL responses.

In chapter 3, we first observed a broadly low signal generated from HLA-E restricted T cell responses during current TCR reporter assay. Given that HLA-E has a lower peptide affinity, we extended co-culture time during TCR reporter assay to ensure E restricted signals were fully developed (Walters et al., 2022). However, we did not see substantial increase in E restricted signals. To circumvent this issue, we transfected Gag expressing plasmid, allowing the endogenous Gag KF11 to be processed and expressed on to cell surface by HLA-E. Using this method, we did not observe a notable increase in E restricted signals. Finally, we studied KK50.4 and GF4 TCRs interaction with epitope VL9 presented HLA-E. VL9 is known having one of the highest peptide binding affinities among other pathogen-derived peptides. In addition, the interaction TCRs KK50.4 or GF4 with VL9-HLA-E have been studied extensively. Thus, we believed studying those

interaction will provide as insights of HLA-E restricted T cell responses. (Yang et al., 2021; Joosten et al., 2016; Pietra et al., 2010). Unfortunately, we observed consistent low signals generated from KK50.4 and GF4 TCRs when recognizing VL9 presented by HLA-E. While we continue to modify current TCR reporter assay to be suitable in detecting E restricted T cell responses, we observed that TCR16 was able to generate consist weak E restricted T cell response. In addition, TCR16 was previously identified as a B*57 functional TCR in chapter 2, indicating that TCR16 could be a potential E and B*57 dually restricted TCRs.

In my research, I highlight that specific genetic features in TCRs have been associated with generating robust CTL responses. This can provide new evidence to support efforts to design vaccines and therapeutics to prevent or treat HIV infection. In the context of HIV immunotherapy, TCR based gene therapy is a novel approach to generate HIV-specific CTL responses to eliminate HIV. T cell receptor-chimeric antigen receptors (TCR-CARs) are engineered T cells that contain specific TCR targeting epitopes of interest. While traditional CAR T cell therapy only recognize specific antigens on cell surface, TCR-CAR also has additional ability to recognize intracellular targets presented by MHC, leading to a broader cytotoxic effect and resulting a potential better clinical outcome (Poorebrahim et al., 2021). Recent years, immune mobilising monoclonal T-cell receptors Against virus (ImmTAV) has been described as another promising immunotherapy to target HIV. ImmTAV is a soluble bispecific T cell consists of high affinity TCR targeting epitopes of interest and an anti-CD3 antibody that redirects polyclonal T cells to target infected cells. ImmTAV is capable of detecting low level of antigens presented by MHC complex indicating its potential ability to generate CTL response even when MHC downregulated by Nef, resulting in low peptide/MHC presentation (Wallace et al, 2022 ; van Stigt Thans et al., 2019).

While both ImmTAV and TCR-CARs are two promising immunotherapies that could lead to cure for HIV, there has been a major challenge to apply both immunotherapies universally. This is due to HLA restricted barrier; certain HLA-CTL responses are enriched in elite controllers, and those HLAs are rare among most populations. On the other hand, HLA-E is known to be poorly polymorphic, which gives it a greater potential to be designed as a universal therapy (Wallace et al, 2022; Zhou et al., 2021). In chapter 3, my study focuses on adapting current TCR reporter assay to be suitable for identifying E restricted CTL responses. Despite the fact that we did not

observe highly functional E restricted TCRs, we identified TCR16 as a potential dually restricted TCR able to generate both E and B*57 restricted CTL responses.

Finally, our research has enhanced our understating of the TCRs mechanism in generating robust KF11-specific, as well as identifying one potential dually restricted TCR. I believe this information will provide valuable insights to enhance HIV therapeutic development, especially in ImmTAV and TCR-CARs.

4.1. Reference

Apps, R., Del Prete, G. Q., Chatterjee, P., Lara, A., Brumme, Z. L., Brockman, M. A., Neil, S., Pickering, S., Schneider, D. K., Piechocka-Trocha, A., Walker, B. D., Thomas, R., Shaw, G. M., Hahn, B. H., Keele, B. F., Lifson, J. D., & Carrington, M. (2016). HIV-1 Vpu Mediates HLA-C Downregulation. *Cell host & microbe*, 19(5), 686–695. https://doi.org/10.1016/j.chom.2016.04.005

Brennan, C. A., Ibarrondo, F. J., Sugar, C. A., Hausner, M. A., Shih, R., Ng, H. L., Detels, R., Margolick, J. B., Rinaldo, C. R., Phair, J., Jacobson, L. P., Yang, O. O., & Jamieson, B. D. (2012). Early HLA-B*57-restricted CD8+ T lymphocyte responses predict HIV-1 disease progression. *Journal of virology*, 86(19), 10505–10516. https://doi.org/10.1128/JVI.00102-12

Dyer, W. B., Zaunders, J. J., Yuan, F. F., Wang, B., Learmont, J. C., Geczy, A. F., Saksena, N. K., McPhee, D. A., Gorry, P. R., & Sullivan, J. S. (2008). Mechanisms of HIV non-progression; robust and sustained CD4+ T-cell proliferative responses to p24 antigen correlate with control of viraemia and lack of disease progression after long-term transfusion-acquired HIV-1 infection. *Retrovirology*, 5, 112. https://doi.org/10.1186/1742-4690-5-112

Iglesias, M. C., Almeida, J. R., Fastenackels, S., van Bockel, D. J., Hashimoto, M., Venturi, V., Gostick, E., Urrutia, A., Wooldridge, L., Clement, M., Gras, S., Wilmann, P. G., Autran, B., Moris, A., Rossjohn, J., Davenport, M. P., Takiguchi, M., Brander, C., Douek, D. C., Kelleher, A. D., … Appay, V. (2011). Escape from highly effective public CD8+ T-cell clonotypes by HIV. *Blood*, 118(8), 2138–2149. https://doi.org/10.1182/blood-2011-01-328781

Joosten, S. A., Sullivan, L. C., & Ottenhoff, T. H. (2016). Characteristics of HLA-E Restricted T- Cell Responses and Their Role in Infectious Diseases. *Journal of immunology research*, 2016, 2695396. https://doi.org/10.1155/2016/2695396

Mendoza, J. L., Fischer, S., Gee, M. H., Lam, L. H., Brackenridge, S., Powrie, F. M., Birnbaum, M., McMichael, A. J., Garcia, K. C., & Gillespie, G. M. (2020). Interrogating the recognition landscape of a conserved HIV-specific TCR reveals distinct bacterial peptide cross-reactivity. *eLife*, 9, e58128. https://doi.org/10.7554/eLife.58128

Pietra, G., Romagnani, C., Manzini, C., Moretta, L., & Mingari, M. C. (2010). The emerging role of HLA-E-restricted CD8+ T lymphocytes in the adaptive immune response to pathogens and tumors. *Journal of biomedicine & biotechnology*, 2010, 907092. https://doi.org/10.1155/2010/907092

Poorebrahim, M., Mohammadkhani, N., Mahmoudi, R., Gholizadeh, M., Fakhr, E., & Cid-Arregui, A. (2021). Correction: TCR-like CARs and TCR-CARs targeting neoepitopes: an emerging potential. *Cancer gene therapy*, 28(6), 738. https://doi.org/10.1038/s41417-021- 00323-7

Swann, S. A., Williams, M., Story, C. M., Bobbitt, K. R., Fleis, R., & Collins, K. L. (2001). HIV-1 Nef blocks transport of MHC class I molecules to the cell surface via a PI 3-kinase- dependentpathway. *Virology*, 282(2), 267–277. https://doi.org/10.1006/viro.2000.0816

van Stigt Thans, T., Akko, J. I., Niehrs, A., Garcia-Beltran, W. F., Richert, L., Stürzel, C. M., Ford, C. T., Li, H., Ochsenbauer, C., Kappes, J. C., Hahn, B. H., Kirchhoff, F., Martrus, G.,Sauter, D., Altfeld, M., & Hölzemer, A. (2019). Primary HIV-1 Strains Use Nef To Downmodulate HLA-E Surface Expression. *Journal of virology*, 93(20), e00719-19.

Wallace, Z., Singh, P. K., & Dorrell, L. (2022). Combination strategies to durably suppress HIV- 1: Soluble T cell receptors. *Journal of virus eradication*, 8(3), 100082. https://doi.org/10.1016/j.jve.2022.100082

Walters, L. C., Rozbesky, D., Harlos, K., Quastel, M., Sun, H., Springer, S., Rambo, R. P., Mohammed, F., Jones, E. Y., McMichael, A. J., & Gillespie, G. M. (2022). Primary and secondary functions of HLA-E are determined by stability and conformation of the peptide- bound complexes. *Cell reports*, 39(11), 110959. https://doi.org/10.1016/j.celrep.2022.110959

Yang, H., Rei, M., Brackenridge, S., Brenna, E., Sun, H., Abdulhaqq, S., Liu, M. K. P., Ma, W., Kurupati, P., Xu, X., Cerundolo, V., Jenkins, E., Davis, S. J.,Sacha, J. B., Früh, K., Picker, L. J., Borrow, P., Gillespie, G. M., & McMichael, A. J. (2021). HLA-E-restricted, Gag-specific CD8+ T cells can suppress HIV-1 infection, offering vaccine opportunities. *Science immunology*, 6(57), eabg1703. https://doi.org/10.1126/sciimmunol.abg1703

Zhou, Y., Maldini, C. R., Jadlowsky, J., & Riley, J. L. (2021). Challenges and Opportunities of Using Adoptive T-Cell Therapy as Part of an HIV Cure Strategy. *The journal of infectious diseases*, 223(12 Suppl 2), 38–45. https://

Appendix. Additional Data

Table A.1. Genetic information, sample ID, and clone ID of 67 selected study samples.

TCR Samples (Original naming s	TCR Samples (New naming system)	Variable Alpha Gene (Va)	Variable Beta gene (Vb)	Joining Alpha Gene (TRAJ)	Joining Beta Gene (TRBJ)	Constant Alpha Gene (TRAC)	Constant Gene (TRBC)	CDR3 alpha	CDR3 beta	Clone alpha ID	clone Beta ID	well	plate ID
HLA-E_KF11_α_β_1	TCR_1	TRAV5	TRBV6-1	TRAJ13	TRBJ1-2	TRAC*01	TRBC1	CAESGGTQKVTF	CACAGTSYGYTF	alhpa6	beta14	H07	plate 53
HLA-E_KF11_α_β_12	TCR_2	TRAV1-2	TRBV6-1	TRAJ17	TRBJ1-2	TRAC*01	TRBC1	CAPRIKAAGNKLTF	CASAGGETYGYTF	alpha18	beta16	H07	plate 53
HLA-E_KF11_α_β_13	TCR_3	TRAV1-2	TRBV7-2	TRAJ4	TRBJ1-2	TRAC*01	TRBC2	CAVYGGYNKLIF	CASIRGGTGELFF	alpha15	beta11	E04	plate 54
HLA-E_KF11_α_β_17	TCR_4	TRAV5	TRBV7-2	TRAJ15	TRBJ1-2	TRAC*01	TRBC1	CAESMGQAGTALIF	CASSDRRSYGYTF	alpha 10	beta7	D01	plate 54
HLA-E_KF11_α_β_18	TCR_5	TRAV5	TRBV7-2	TRAJ13	TRBJ1-2	TRAC*01	TRBC1	CAVSGGYQKVTF	CASSDRRSYGYTF	alpha14	beta7	D10	plate 54
HLA-E_KF11_α_β_19	TCR_6	TRAV1-2	TRBV7-2	TRAJ4	TRBJ1-2	TRAC*01	TRBC1	CAVYGGYNKLIF	CASSDRRSYGYTF	alpha15	beta7	E04	plate 54
HLA-E_KF11_α_β_2	TCR_7	TRAV5	TRBV6-1	TRAJ15	TRBJ1-2	TRAC*01	TRBC1	CAESMGQAGTALIF	CACAGTSYGYTF	alpha 10	beta14	D07	plate 54
HLA-E_KF11_α_β_3	TCR_8	TRAV1-2	TRBV6-1	TRAJ17	TRBJ1-2	TRAC*01	TRBC1	CAPRIKAAGNKLTF	CACAGTSYGYTF	alpha18	beta14	H07	plate 53
HLA-E_KF11_α_4	TCR_9	ZRAV5	TRBV6-1	TRAJ13	TRBJ1-2	TRAC*01	TRBC1	CAVSGGYQKVTF	CACAGTSYGYTF	alpha14	beta14	D07	plate 54
HLA-E_KF11_α_β_41	TCR_10	TRAV17	TRBV27	TRAJ42	TRBJ2-5	TRAC*01	TRBC2	CATDAENYGQSQQNLIF	CASSPWTGEETQYF	alpha4	beta4	A05	plate 53
HLA-E_KF11_α_β_42	TCR_11	TRAV17	TRBV27	TRAJ47	TRBJ2-5	TRAC*01	TRBC2	CATDMEYGNKLVF	CASSPWTGEETQYF	alpha3	beta4	A05	plate 53
HLA-E_KF11_α_β_43	TCR_12	TRAV17	TRBV27	TRAJ34	TRBJ2-5	TRAC*01	TRBC2	CATEVGDKLIF	CASSPWTGEETQYF	alpha5	beta4	A05	plate 53
HLA-E_KF11_α_β_56	TCR_13	TRAV5	TRBV6-1	TRAJ13	TRBJ1-2	TRAC*01	TRBC1	CAESGGYQKVTF	CASTGGTYGYTF	alhpa6	beta15	H07	plate 53
HLA-E_KF11_α_β_57	TCR_14	TRAV5	TRBV6-1	TRAJ15	TRBJ1-2	TRAC*01	TRBC1	CAESMGQAGTALIF	CASTGGTYGYTF	alpha 10	beta15	D07	plate 54
HLA-E_KF11_α_β_58	TCR_15	TRAV1-2	TRBV6-1	TRAJ17	TRBJ1-2	TRAC*01	TRBC1	CAPRIKAAGNKLTF	CASTGGTYGYTF	alpha18	beta15	H07	plate 53
HLA-E_KF11_α_β_59	TCR_16	ZRAV5	TRBV6-1	TRAJ13	TRBJ1-2	TRAC*01	TRBC1	CAVSGGYQKVTF	CASTGGTYGYTF	alpha14	beta15	D07	plate 54
HLA-E_KF11_α_β_60	TCR_17	TRAV17	TRBV15	TRAJ42	TRBJ2-5	TRAC*01	TRBC2	CATDAENYGQSQQNLIF	CATSDRLAGGETQYF	alpha4	beta3	A04	plate 53
HLA-E_KF11_α_β_61	TCR_18	TRAV17	TRBV15	TRAJ47	TRBJ2-5	TRAC*01	TRBC2	CATDMEYGNKLVF	CATSDRLAGGETQYF	alpha3	beta3	A04	plate 53
HLA-E_KF11_α_β_62	TCR_19	TRAV17	TRBV15	TRAJ34	TRBJ2-5	TRAC*01	TRBC2	CATEVGDKLIF	CATSDRLAGGETQYF	alpha5	beta3	A04	plate 53
HLA-E_KF11_α_β_11	TCR_20	TRAV5	TRBV6-1	TRAJ13	TRBJ2-5	TRAC*01	TRBC1	CAESGGYQKVTF	CASAGGETYGYTF	Alpha 6	Beta16	H07	plate 53
HLA-E_KF11_α_β_21	TCR_21	TRAV12-3	TRBV11-2	TRAJ10	TRBJ1-1	TRAC*01	TRBC1	CAMSFTGGGNKLTF	CASSFHPAGVNTEAEXA4		EXB2	E05	plate 54
HLA-E_KF11_α_β_22	TCR_22	TRAV12-3	TRBV11-2	TRAJ54	TRBJ1-1	TRAC*01	TRBC1	CAMSVIIQGAQKLVF	CASSFHPAGVNTEAEXA5		EXB2	B02	plate 53
HLA-E_KF11_α_β_24	TCR_23	TRAV5	TRBV19	TRAJ13	TRBJ1-2	TRAC*01	TRBC1	CAGSGGTQKVTF	CASSGAIYGYTF	EXA2	EXB3	F11	plate 53
HLA-E_KF11_α_β_29	TCR_24	TRAV12	TRBV5-1	TRAJ20	TRBJ2-7	TRAC*01	TRBC2	CVVNEGSQQNFVF	CASSLGDPSHYEQYEXA7		EXB4	B04	plate 53
HLA-E_KF11_α_β_30	TCR_25	TRAV12-3	TRBV11-2	TRAJ10	TRBJ1-1	TRAC*01	TRBC1	CAMSFTGGGNKLTF	CASSLGGNTEAFF	EXA4	EXB5	B04	plate 53
HLA-E_KF11_α_β_36	TCR_26	TRAV25	TRBV12-3	TRAJ52	TRBJ1-5	TRAC*01	TRBC1	CAGPSNAGGTSYGKLTF	CASSLWGQPQHF	EXA1	EXB7	C02	plate 53
HLA-E_KF11_α_β_5	TCR_27	TRAV12-2	TRBV6-5	TRAJ31	TRBJ1-5	TRAC*01	TRBC1	CAGTPARLMF	CAIGRPEAFF	EXA3	EXB1	F11	plate 53
HLA-E_KF11_α_β_6	TCR_28	TRAV12-2	TRBV6-5	TRAJ10	TRBJ1-1	TRAC*01	TRBC1	CAVNGGGSNKLTF	CAIGRPEAFF	EXA6	EXB1	B12	plate 54

A

B57_KFI1_a_β_1	TCR 29	TRAV9-2	TRBV28	TRAJ57	TRBJ2-7	TRAC*01	TRBC2	CALSPVWGGSEKLVF	CACHSMSSYEQYF	alhpa 12	beta10	D08	plate 56		
B57_KFI1_a_β_10	TCR 30	TRAV41	TRBV28	TRAJ45	TRBJ2-3	TRAC*01	TRBC2	CAVKDLWRSGGGADGL	CASRYMVSDTQYF	alhpha16	beta12	G09	plate 55		
B57_KFI1_a_β_12	TCR 31	TRAV5	TRBV7-2	TRAJ15	TRBJ1-2	TRAC*01	TRBC1	CAESMGQAGTALIF	CASSDRRSYGYTF	alpha 10	beta7	E06	plate 55		
B57_KFI1_a_β_19	TCR 32	TRAV12-2	TRBV 12-4	TRAJ20	TRBJ2-3	TRAC*01	TRBC2	CAGAREGDYKLSF	CASSGGDTQYF	alpha 9	beta1	C06	plate 55		
B57_KFI1_a_β_2	TCR 33	TRAV41	TRBV28	TRAJ45	TRBJ2-7	TRAC*01	TRBC2	CAVPYSGGGADGLTF	CACHSMSSYEQYF	alpha13	beta10	D08	plate 56		
B57_KFI1_a_β_21	TCR 34	TRAV1-2	TRBV 12-4	TRAJ17	TRBJ2-3	TRAC*01	TRBC2	CAPRIKAAGNKLTF	CASSGGDTQYF	alpha18	beta1	A03	plate 55		
B57_KFI1_a_β_23	TCR 35	TRAV1-2	TRBV12-4	TRAJ11	TRBJ2-3	TRAC*01	TRBC2	CAVNSGGDTQYF	CASSGGDTQYF	alpha2	beta1	A03	plate 55		
B57_KFI1_a_β_24	TCR 36	TRAV1-2	TRBV12-4	TRAJ5	TRBJ2-3	TRAC*01	TRBC2	CAVRDTGRRALTF	CASSGGDTQYF	alpha 1	beta1	A03	plate 55		
B57_KFI1_a_β_25	TCR 37	TRAV12-2	TRBV12-4	TRAJ31	TRBJ2-3	TRAC*01	TRBC2	CAVRGNNARLMF	CASSGGDTQYF	alpha8	beta1	C06	plate 55		
B57_KFI1_a_β_3	TCR 38	TRAV41	TRBV28	TRAJ42	TRBJ2-7	TRAC*01	TRBC2	CAVSKHYGGSQGNLIF	CASSGGDTQYF	alpha11	beta10	D08	plate 56		
B57_KFI1_a_β_4	TCR 39	TRAV38	TRBV19*	TRAJ13	TRBJ2-2	TRAC*01	TRBC1	CAYSGGYQKVTF	CASSQDTGGQYF	alpha14	beta8	D01	plate 55		
B57_KFI1_a_β_40	TCR 40	TRAV12-2	TRBV12-4	TRAJ20	TRBJ2-2	TRAC*01	TRBC2	CAGAREGDYKLSF	CASSPRGSEQYF	alpha 9	beta2	C06	plate 55		
B57_KFI1_a_β_42	TCR 41	TRAV1-2	TRBV 12-4	TRAJ17	TRBJ2-7	TRAC*01	TRBC2	CAPRIKAAGNKLTF	CASSPRGSEQYF	alpha18	beta2	A03	plate 55		
B57_KFI1_a_β_44	TCR 42	TRAV1-2	TRBV 12-4	TRAJ11	TRBJ2-7	TRAC*01	TRBC2	CAVNSGYSTLTF	CASSPRGSEQYF	alpha2	beta2	A03	plate 55		
B57_KFI1_a_β_45	TCR 43	TRAV1-2	TRBV 12-4	TRAJ5	TRBJ2-7	TRAC*01	TRBC2	CAVRDTGRRALTF	CASSPRGSEQYF	alpha 1	beta2	A03	plate 55		
B57_KFI1_a_β_46	TCR 44	TRAV12-2	TRBV 12-4	TRAJ31	TRBJ2-7	TRAC*01	TRBC2	CAVRGNNARLMF	CASSPRGSEQYF	alpha8	beta2	C06	plate 55		
B57_KFI1_a_β_6	TCR 45	TRAV41	TRBV28	TRAJ45	TRBJ2-1	TRAC*01	TRBC2	CAVKDLWRSGGGADGL	CASRADPSYNEQFF	alpha16	beta13	G09	plate 55		
B57_KFI1_a_β_65	TCR 46	TRAV5	TRBV6-1	TRAJ13	TRBJ1-2	TRAC*01	TRBC1	CAESGGYQKVTF	CASTGGTYGYTF	alhpa6	beta15	A07 and F06	plate 56 and plate		
B57_KFI1_a_β_7	TCR 47	TRAV9-2	TRBV28	TRAJ57	TRBJ1-2	TRAC*01	TRBC1	CALSPVWGGSEKLVF	CASRDTPYGYTF	alhpa 12	beta9	D08	plate 56		
B57_KFI1_a_β_75	TCR 48	TRAV1-2	TRBV20-1	TRAJ17	TRBJ2-7	TRAC*01	TRBC2	CAPRIKAAGNKLTF	CSAESPSGEEQYF	alpha18	beta6	B05	plate 55		
B57_KFI1_a_β_77	TCR 49	TRAV1-2	TRBV20-1	TRAJ5	TRBJ2-7	TRAC*01	TRBC2	CAVRDTGRRALTF	CSAESPSGEEQYF	alpha 1	beta6	A03 and B05	plate 55 and plate		
B57_KFI1_a_β_8	TCR 50	TRAV41	TRBV28	TRAJ45	TRBJ1-2	TRAC*01	TRBC1	CAVPYSGGGADGLTF	CASRDTPYGYTF	alpha13	beta9	D08	plate 56		
B57_KFI1_a_β_9	TCR 51	TRAV41	TRBV28	TRAJ42	TRBJ1-2	TRAC*01	TRBC1	CAVSKHYGGSQGNLIF	CASRDTPYGYTF	alpha11	beta9	D08	plate 56		
B57_KFI1_a_β_13	TCR 52	TRAV12-2	TRBV2	TRAJ17	TRBJ1-4	TRAC*01	TRBC1	CAGAREGDYKLSF	CASSEYSLNEKLFF	Alpha9	EXB9	H03	plate 55		
B57_KFI1_a_β_14	TCR 53	TRAV12-2	TRBV2	TRAJ35	TRBJ1-4	TRAC*01	TRBC1	CAGTGFGNVLHC	CASSEYSLNEKLFF	EXA8	EXB9	H03	plate 55		
B57_KFI1_a_β_16	TCR 54	TRAV12-2	TRBV2	TRAJ31	TRBJ1-4	TRAC*01	TRBC1	CAVRGNNARLMF	CASSEYSLNEKLFF	alhpa8	EXB9	H03	plate 55		
B57_KFI1_a_β_22	TCR 55	TRAV25	TRBV12-3	TRAJ22	TRBJ2-3	TRAC*01	TRBC2	CASDSGSARQLTF	CASSGGDTQYF	EXA9	B1	B04	plate 55		
B57_KFI1_a_β_27	TCR 56	TRAV12-1	TRBV2	TRAJ20	TRBJ2-7	TRAC*01	TRBC2	CVVSGGSQGNVIF	CASSGGDTQYF	EXA7	B1, B4	B11	plate 55		
B57_KFI1_a_β_28	TCR 57	TRAV12-2	TRBV5-1	TRAJ17	TRBJ1-4	TRAC*01	TRBC1	CAGAREGDYKLSF	CASSLGTNEKLFF	A9	EXB10	H03	plate 55		
B57_KFI1_a_β_29	TCR 58	TRAV12-2	TRBV2	TRAJ35	TRBJ1-4	TRAC*01	TRBC1	CAGTGFGNVLHC	CASSLGTNEKLFF	EXA8	EXB10	H03	plate 55		
B57_KFI1_a_β_33	TCR 59	TRAV12-2	TRBV2	TRAJ31	TRBJ1-4	TRAC*01	TRBC1	CAVRGNNARLMF	CASSLGTNEKLFF	A8	EXB10	H03	plate 55		
B57_KFI1_a_β_43	TCR 60	TRAV25	TRBV12-3	TRAJ22	TRBJ2-7	TRAC*01	TRBC2	CASDSGSARQLTF	CASSPRGSEQYF	EXA9	B2	E04	plate 55		
B57_KFI1_a_β_64	TCR 61	TRAV25	TRBV12-3	TRAJ22	TRBJ2-3	TRAC*01	TRBC2	CASDSGSARQLTF	CASSWRQGRYFQY	EXA9	EXB12	E04	plate 55		
B57_KFI1_a_β_15	TCR 62	TRAV1-2	TRBV2	TRAJ17	TRBJ1-4	TRAC*01	TRBC1	CAPRIKAAGNKLTF	CASSEYSLNEKLFF	A18	EXB9	G06	plate 55		
B57_KFI1_a_β_17	TCR 63	TRAV1-2	TRBV2	TRAJ43	TRBJ1-4	TRAC*01	TRBC1	CAVRSYNNNDMRF	CASSEYSLNEKLFF	EXA10	EXB9	G06	plate 55		
B57_KFI1_a_β_30	TCR 64	TRAV1-2	TRBV2	TRAJ17	TRBJ1-4	TRAC*01	TRBC1	CAPRIKAAGNKLTF	CASSLGTNEKLFF	A18	EXB10	G06	plate 55		
B57_KFI1_a_β_31	TCR 65	TRAV1-2	TRBV2	TRAJ11	TRBJ1-4	TRAC*01	TRBC1	CAVNSGYSTLTF	CASSLGTNEKLFF	A2	EXB10	B04	plate 55		
B57_KFI1_a_β_32	TCR 66	TRAV1-2	TRBV2	TRAJ5	TRBJ1-4	TRAC*01	TRBC1	CAVRDTGRRALTF	CASSLGTNEKLFF	A1	EXB10	B04	plate 55		
B57_KFI1_a_β_34	TCR 67	TRAV1-2	TRBV2	TRAJ43	TRBJ1-4	TRAC*01	TRBC1	CAVRSYNNNDMRF	CASSLGTNEKLFF	EXA10	EXB10	G06	plate 55		

B

67 selected TCR clones were originally named as HLA-E_KF11αβ_(number) or HLA- B*57_KF11αβ_(number) based on whether CD8 T cells were identified in AIM assays using HLA-E or HLA-B*57 target cells. Each clone was assigned a new TCR ID for this study. (A) 28 out of 67 selected TCR (from figure 2.2) were initially identified as E-restricted TCR. This data included its genetic information, well and plate ID obtained from single cell sequencing. (B) 39 out of 67 selected TCR (from figure 2.2) were initially identified as B*57-restricted TCR. This data included its genetic information, well and plate ID obtained from single cell sequencing.

Table A.2. Functional Assessment table of 67 TCR samples in generating B*57-KF11 CD8 T cell response via TCR reporter assay

TCR Samples (Oirginal naming system)	TCR Samples (New naming system)	721.221 41A3A2 target cell #1	721.221 41A3A2 target cell #2	721.221 B57:01 target cell #1	721.221 B57:01 Target cell #2
HLA-E_KF11_α_β_1	TCR 1	1.539	1.595	14.973	92.213
HLA-E_KF11_α_β_12	TCR 2	1.177	1.285	0.615	1.131
HLA-E_KF11_α_β_13	TCR 3	1.455	1.514	0.907	1.235
HLA-E_KF11_α_β_17	TCR 4	1.351	1.234	0.858	1.325
HLA-E_KF11_α_β_18	TCR 5	1.646	1.915	1.475	6.313
HLA-E_KF11_α_β_19	TCR 6	1.631	1.624	0.847	2.299
HLA-E_KF11_α_β_2	TCR 7	1.251	1.356	0.693	1.080
HLA-E_KF11_α_β_3	TCR 8	0.946	1.749	0.332	1.627
HLA-E_KF11_α_β_4	TCR 9	0.566	2.250	55.158	55.666
HLA-E_KF11_α_β_41	TCR 10	1.954	1.283	2.293	2.373
HLA-E_KF11_α_β_42	TCR 11	1.649	1.803	1.812	1.510
HLA-E_KF11_α_β_43	TCR 12	1.248	1.643	1.595	1.556
HLA-E_KF11_α_β_56	TCR 13	1.337	1.686	27.173	56.927
HLA-E_KF11_α_β_57	TCR 14	0.986	1.519	1.746	2.640
HLA-E_KF11_α_β_58	TCR 15	1.254	2.058	2.989	1.496
HLA-E_KF11_α_β_59	TCR 16	1.732	2.955	53.293	100.235
HLA-E_KF11_α_β_60	TCR 17	2.723	1.110	3.059	1.948
HLA-E_KF11_α_β_61	TCR 18	1.261	1.388	2.618	1.378
HLA-E_KF11_α_β_62	TCR 19	1.268	2.453	3.995	1.651
HLA-E_KF11_α_β_11	TCR 20	2.370	2.224	29.193	27.765
HLA-E_KF11_α_β_21	TCR 21	2.353	1.950	3.088	3.084
HLA-E_KF11_α_β_22	TCR 22	2.941	1.568	1.630	1.667
HLA-E_KF11_α_β_24	TCR 23	1.537	1.165	100.776	63.616
HLA-E_KF11_α_β_29	TCR 24	2.028	1.793	1.777	1.587
HLA-E_KF11_α_β_30	TCR 25	3.061	3.201	2.532	3.031
HLA-E_KF11_α_β_36	TCR 26	2.792	2.877	2.082	0.458
HLA-E_KF11_α_β_5	TCR 27	2.285	1.954	1.367	1.631
HLA-E_KF11_α_β_6	TCR 28	4.470	4.475	4.626	5.659
B57_KF11_α_β_1	TCR 29	1.348	0.001	1.385	0.722
B57_KF11_α_β_10	TCR 30	2.276	2.112	1.700	1.397
B57_KF11_α_β_12	TCR 31	1.527	2.457	1.060	0.782
B57_KF11_α_β_19	TCR 32	1.391	3.782	1.368	1.388
B57_KF11_α_β_2	TCR 33	1.965	2.875	1.351	0.899
B57_KF11_α_β_21	TCR 34	1.733	0.693	1.219	0.742
B57_KF11_α_β_23	TCR 35	1.111	2.728	1.029	1.720
B57_KF11_α_β_24	TCR 36	1.423	1.586	1.066	1.459
B57_KF11_α_β_25	TCR 37	1.324	1.888	1.057	0.796
B57_KF11_α_β_3	TCR 38	2.155	6.974	1.482	1.900
B57_KF11_α_β_4	TCR 39	1.438	3.168	3.433	10.917
B57_KF11_α_β_40	TCR 40	0.981	1.992	0.845	1.059
B57_KF11_α_β_42	TCR 41	0.848	2.319	1.438	1.278
B57_KF11_α_β_44	TCR 42	0.640	1.742	1.121	1.804
B57_KF11_α_β_45	TCR 43	0.547	1.598	1.073	1.633
B57_KF11_α_β_46	TCR 44	1.012	2.432	1.567	1.939
B57_KF11_α_β_6	TCR 45	1.149	1.800	1.624	1.469
B57_KF11_α_β_65	TCR 46	0.597	1.921	16.133	36.227
B57_KF11_α_β_7	TCR 47	0.871	2.072	1.317	1.551
B57_KF11_α_β_75	TCR 48	0.809	2.129	1.641	1.698
B57_KF11_α_β_77	TCR 49	0.789	2.417	1.568	2.203
B57_KF11_α_β_8	TCR 50	0.740	2.511	1.397	1.261
B57_KF11_α_β_9	TCR 51	2.253	5.895	2.159	1.701
B57_KF11_α_β_13	TCR 52	2.570	2.533	2.341	2.535
B57_KF11_α_β_14	TCR 53	2.007	2.552	2.117	2.248
B57_KF11_α_β_16	TCR 54	2.122	2.143	1.778	2.393
B57_KF11_α_β_22	TCR 55	2.147	2.076	1.823	2.501
B57_KF11_α_β_27	TCR 56	2.322	2.139	1.807	1.908
B57_KF11_α_β_28	TCR 57	2.543	1.990	1.522	2.078
B57_KF11_α_β_29	TCR 58	2.648	1.927	1.618	2.053
B57_KF11_α_β_33	TCR 59	3.716	3.319	2.732	3.525
B57_KF11_α_β_43	TCR 60	2.394	2.476	1.803	2.549
B57_KF11_α_β_64	TCR 61	4.219	3.331	2.217	2.793
B57_KF11_α_β_15	TCR 62	2.597	1.701	1.861	1.734
B57_KF11_α_β_17	TCR 63	2.255	1.680	1.539	1.797
B57_KF11_α_β_30	TCR 64	2.802	2.334	2.011	1.940
B57_KF11_α_β_31	TCR 65	3.368	1.483	1.669	1.669
B57_KF11_α_β_32	TCR 66	2.075	1.946	1.774	2.292
B57_KF11_α_β_34	TCR 67	2.329	1.686	1.728	1.722
HLA-A02 5B2 (positive control)		22.233	21.177	N/A	N/A

Every TCR sample was analyzed with biological duplicates, and the results were presented as the fold change between peptide-pulsed targets verses non-peptide pulsed target cells. 721.221 41A3A2 (non-specific signal) was used as negative control and 5B2 TCR sample was used as positive control in this experiment. N/A indicated non-available. TCR13 and TCR 46 shared identical genetic feature but captured by different target cells during single cell sequencing. Samples colored in yellow indicated TCRs that were able to generate HLA-B*57 restricted T cell response.

Table A.3. NetMHCpan-4.1 prediction of binding affinity of KF11 alanine

```
# Method: NetMHCcons

# Input is in PEPTIDE format

# Peptide length 11

# Threshold for Strong binding peptides (IC50)     50.000 nM
# Threshold for Weak binding peptides (IC50)       500.000 nM

# Threshold for Strong binding peptides (%Rank)    0.5%
# Threshold for Weak binding peptides (%Rank)      2%

# Allele: HLA-B57:01

# Distance to the nearest neighbour ( HLA-B57:01 ) in the training set: 0.000

# NetMHCcons = NetMHC+NetMHCpan

-----------------------------------------------------------------------------------------------------------
   pos       Allele         peptide         Identity 1-log50k(aff) Affinity(nM)  %Rank   BindingLevel
-----------------------------------------------------------------------------------------------------------
     0   HLA-B57:01     KAFSPEVIPMF          PEPLIST         0.615        64.43   0.25  <=SB
     1   HLA-B57:01     AAFSPEVIPMF          PEPLIST         0.427       489.96   1.00  <=WB
     3   HLA-B57:01     KAASPEVIPMF          PEPLIST         0.536       152.29   0.50  <=SB
     4   HLA-B57:01     KAFAPEVIPMF          PEPLIST         0.627        56.59   0.25  <=SB
     5   HLA-B57:01     KAFSAEVIPMF          PEPLIST         0.626        57.20   0.25  <=SB
     6   HLA-B57:01     KAFSPAVIPMF          PEPLIST         0.621        60.71   0.25  <=SB
     7   HLA-B57:01     KAFSPEAIPMF          PEPLIST         0.616        63.74   0.25  <=SB
     8   HLA-B57:01     KAFSPEVAPMF          PEPLIST         0.595        79.57   0.30  <=SB
     9   HLA-B57:01     KAFSPEVIAMF          PEPLIST         0.609        68.75   0.30  <=SB
    10   HLA-B57:01     KAFSPEVIPAF          PEPLIST         0.563       113.10   0.40  <=SB
    11   HLA-B57:01     KAFSPEVIPMA          PEPLIST         0.182      6940.78   5.00
-----------------------------------------------------------------------------------------------------------
Number of strong binders: 9 Number of weak binders: 1
-----------------------------------------------------------------------------------------------------------
```

NetMHCpan-4.1 prediction of binding affinity of KF11 alanine variants with HLA-B*57:01.NetMHCPan-4.1, a bioinformatic tool developed by Technical University of Denmark, can predict peptides binding to most known MHC class I molecules. Binding level of any given peptides-MHC were predicted by peptide affinity (IC50) or % Rank resulting strong binding or weak binding toward MHC I molecules. SB stands for strong binder and WB stands for weak binder. Substituting alanine at positions 1 and 11 led to either weak binding or no binding between the peptides and HLA-B*57:01, respectively. Whereas substituting alanine at positions 3 to 10 maintained a strong binding interaction between the peptides and HLA-B*57:01.

Table A.4. Functional Assessment table of 42 TCR samples in generating HLA-E*01:01 or HLA-E*01:03 - Gag KF11- E restricted CD8 T cells response via TCR reporter assay.

TCR Samples (Orginal naming system)	TCR Samples (New naming system)	721.221 41A3A2 target cell #1	721.221 E01:01 target cell #1	721.221 E01:03 target cell #1	721.221 41A3A2 target cell #2	721.221 E01:01 target cell #2	721.221 E01:03 target cell #2
HLA-E_KF11_α_β_1	TCR 1	1.5393	2.133	1.819	1.368	1.983	1.439
HLA-E_KF11_α_β_12	TCR 2	1.1765	1.579	1.332	1.465	1.190	1.642
HLA-E_KF11_α_β_13	TCR 3	1.4550	1.456	1.622	0.643	1.356	2.290
HLA-E_KF11_α_β_17	TCR 4	1.3506	1.396	1.893	1.564	2.040	1.740
HLA-E_KF11_α_β_18	TCR 5	1.6460	1.969	2.141	1.143	1.619	1.922
HLA-E_KF11_α_β_19	TCR 6	1.6310	1.650	2.047	1.911	1.301	1.798
HLA-E_KF11_α_β_2	TCR 7	1.2515	0.887	1.719	1.652	1.076	1.340
HLA-E_KF11_α_β_3	TCR 8	0.9458	1.318	1.854	1.187	1.517	1.265
HLA-E_KF11_α_β_4	TCR 9	2.0703	2.637	2.820	1.300	2.970	2.587
HLA-E_KF11_α_β_41	TCR 10	1.9539	1.509	1.705	1.989	2.133	1.978
HLA-E_KF11_α_β_42	TCR 11	1.8032	1.637	1.981	1.760	1.960	1.638
HLA-E_KF11_α_β_43	TCR 12	1.6434	2.139	1.240	1.297	1.910	1.885
HLA-E_KF11_α_β_56	TCR 13	1.3372	1.003	1.516	0.970	1.844	1.437
HLA-E_KF11_α_β_57	TCR 14	0.9855	2.517	1.270	1.229	2.076	2.984
HLA-E_KF11_α_β_58	TCR 15	1.2543	1.804	1.629	1.563	1.560	4.339
HLA-E_KF11_α_β_59	TCR 16	1.7324	4.463	2.716	1.211	3.011	19.450
HLA-E_KF11_α_β_60	TCR 17	1.1101	1.493	2.177	0.926	1.775	2.065
HLA-E_KF11_α_β_61	TCR 18	1.2607	1.061	1.713	0.889	1.265	4.390
HLA-E_KF11_α_β_62	TCR 19	1.2678	3.276	0.992	1.031	1.984	3.596
B57_KF11_α_β_1	TCR 29	1.3479	0.798	0.820	NA	1.568	1.146
B57_KF11_α_β_10	TCR 30	2.2760	0.961	0.944	2.112	1.174	1.269
B57_KF11_α_β_12	TCR 31	1.5273	0.731	0.654	2.457	0.760	0.609
B57_KF11_α_β_19	TCR 32	1.3911	1.264	1.168	3.782	1.287	1.171
B57_KF11_α_β_2	TCR 33	1.9652	0.594	0.915	2.875	2.623	0.852
B57_KF11_α_β_21	TCR 34	1.7334	0.464	0.971	0.693	2.306	1.520
B57_KF11_α_β_23	TCR 35	1.1105	0.704	1.101	2.728	1.318	1.034
B57_KF11_α_β_24	TCR 36	1.4226	0.255	1.067	1.586	1.506	1.652
B57_KF11_α_β_25	TCR 37	1.3236	0.116	0.657	1.888	1.063	1.181
B57_KF11_α_β_3	TCR 38	2.1545	0.271	1.142	6.974	1.322	0.917
B57_KF11_α_β_4	TCR 39	1.4381	0.202	0.988	3.168	2.097	1.147
B57_KF11_α_β_40	TCR 40	0.9810	0.590	1.015	1.992	1.701	0.689
B57_KF11_α_β_42	TCR 41	0.8477	3.643	0.856	2.319	0.980	1.036
B57_KF11_α_β_44	TCR 42	0.6403	1.694	0.745	1.742	0.688	4.671
B57_KF11_α_β_45	TCR 43	0.5471	1.185	1.034	1.598	1.350	2.264
B57_KF11_α_β_46	TCR 44	1.0117	1.447	1.133	2.432	1.994	1.520
B57_KF11_α_β_6	TCR 45	1.1492	1.502	0.897	1.800	1.618	1.559
B57_KF11_α_β_65	TCR 46	0.5970	1.038	0.628	1.921	1.600	1.495
B57_KF11_α_β_7	TCR 47	0.8710	0.859	0.412	2.072	1.370	1.723
B57_KF11_α_β_75	TCR 48	0.8091	0.790	0.597	2.129	1.763	0.832
B57_KF11_α_β_77	TCR 49	0.7890	1.375	0.497	2.417	1.953	2.435
B57_KF11_α_β_8	TCR 50	0.7398	0.766	0.887	2.511	1.670	1.434
B57_KF11_α_β_9	TCR 51	2.2526	1.649	0.498	5.895	2.527	1.731
HLA-A02 5B2 (positive control)		9.095	21.177				

Every TCR sample was analyzed with biological duplicates, and the results were presented as the fold change between peptide-pulsed targets verses non-peptide pulsed target cells. 721.221 41A3.A2 (non-specific signal) was used as negative control and 5B2 TCR (A2 restricted FK10 epitope) sample was used as positive control in this experiment. N/A indicated non-available. TCR13 and TCR 46 shared identical genetic feature but captured by different target cells during single cell sequencing. Green colored samples represented potential functional TCRs in generating Gag KF11- E restricted CD8 T cell. Cells highlighted in yellow exhibited inductions greater than 1.5-fold when co-cultured with peptide-pulsed E target cells. Additionally, these signals surpassed non-specific signals (41A3.A2) by at least 1.5-